

Optimal Investments in Africa's Road Network

Sebastian Krantz*

July 23, 2024

Abstract

This paper characterizes economically optimal investments in Africa's road network in partial and general equilibrium - based on a detailed topography of the network, road construction costs, frictions in cross-border trading, and economic geography. Drawing from data on 144 million trans-continental routes, it first assesses local and global network efficiency and market access. It then derives a large network connecting 447 cities and 52 ports along the fastest routes, devises an algorithm to propose new links, analyzes the quality of existing links, and estimates link-level construction/upgrading costs. Subsequently, it computes market-access-maximizing investments in partial equilibrium and conducts cost-benefit analysis for individual links and several investment packages. Using a spatial economic model and global optimization over the space of networks, it finally elicits welfare-maximizing investments in spatial equilibrium. Findings imply that cross-border frictions and trade elasticities significantly shape optimal road investments. Reducing frictions yields the greatest benefits, followed by road upgrades and new construction. Sequencing matters, as reduced frictions generally increase investment returns. Returns to upgrading key links are large, even under frictions.

Keywords: African roads, spatially optimal investments, big data, PE and GE analysis

JEL Classification: O18; R42; R10; O10

1 Introduction

For several decades, development economists and policymakers have highlighted insufficient or inefficient transport infrastructure, coupled with border frictions and high trading costs, as a major obstacle to African economic development and regional integration. A World Bank report from 2010 states that Sub-Saharan Africa (SSA) has 31 paved roads km per $100km^2$ of land, compared to $134km^2$ in other low-income countries, estimates the annual infrastructure gap at \$93 billion, and urges SSA countries to spend one percent of GDP on roads (Foster & Briceño-Garmendia, 2010). This is echoed by the African Development Report 2010, attesting a financing gap at 5 percent of GDP to overhaul the infrastructure sector (ADB, 2010). More extensive and detailed work by Teravanithorn & Raballand (2009) and Lamarque & Nugent (2022) unveils the nature of transportation and trucking in Africa, the determinants of transport costs and frictions, and discusses the potential and policy options for development along specific transport corridors. However, little remains known about the economic optimality of such investments. Most academic and policy literature analyzes a single country or corridor in isolation and relies on heuristic calculations or strongly reduced road network graphs. Equilibrium concepts and implications for optimal routing and traffic flow, including along non-targeted roads, are often neglected.

This paper instead presents a comprehensive, data-driven, and quantitatively rigorous assessment of Africa's road network and optimal investments into it at the trans-African scale. It (1) conducts a detailed empirical stocktake of Africa's present road network; (2) characterizes global economic optimality in network investments from a market access and welfare perspective; (3) investigates the effects of cross-border frictions on optimal spatial allocations; and (4) presents cost-benefit analyses and evidence on the macroeconomic feasibility of large scale (optimal) investments. This agenda mirrors questions of international policymakers who, in theory, can invest in roads anywhere on the continent and may ask: (1) is it still important to invest in African roads?; (2) where exactly should we invest in African roads?; (3) are investments sensible with/without regulatory reforms?; and (4) are they macroeconomically feasible? The paper engages this ambitious

*Kiel Institute for the World Economy
Address: Haus Welt-Club, Duesternbrooker Weg 148, D-24105 Kiel
E-mail: sebastian.krantz@ifw-kiel.de
Latest version available at <https://sebastiankrantz.com/research>

agenda by building realistic economic topographies informed by routing engines, geospatial big data, and surveys, and analyzing them with tools from optimal transport and spatial economic modeling. It satisfactorily answers these questions in light of present empirical possibilities.¹

Several significant contributions have already been made in economic literature. [Atkin & Donaldson \(2015\)](#) show that the effect of log distance on trade costs within Ethiopia or Nigeria is 4-5 times larger than in the US and $\leq 30\%$ of this effect is explained by the availability and quality of roads. Using ten years of disaggregated monthly price data, [Porteous \(2019\)](#) estimates a dynamic model of agricultural storage and trade comprising 6 grains traded across 230 regional markets in all 42 SSA countries, which are connected in a network with 413 overland links to 30 international ports. He finds median trade costs five times higher than elsewhere in the world. Reducing trade costs to the world average would yield a 46% reduction in grain prices and a welfare gain equivalent to 2.17% of GDP. He further shows that 88% of the welfare gain can be achieved by lowering trade costs through ports and links representing just 18% of the trade network, supporting transport-corridor-based approaches to network improvement.

[Graff \(2024\)](#) studies spatial inefficiency in African national road networks using a regular 0.5° grid-network parameterized with Open Street Map (OSM) routes between adjacent cells. Employing data on population, nightlights (productivity) and ruggedness ([Nunn & Puga, 2012](#)), and the quantitative framework of [Fajgelbaum & Schaal \(2020\)](#), he generates ideal national networks, and estimates that Africa would gain 1.3% of total welfare from better organizing its national road systems (with national welfare gains ranging between 6.6% for Somalia and 0.5% for South Africa), and 0.8% from a 10% optimal expansion. He also documents that colonial infrastructure projects skewed trade networks towards a sub-optimal equilibrium and that regional favoritism and inefficient aid provision hinder optimal network investments ([Graff, 2024](#)). The latter is consistent with findings by [Jedwab & Moradi \(2016\)](#); [Jedwab et al. \(2017\)](#), [Burgess et al. \(2015\)](#), and [Bonfatti et al. \(2019\)](#). Similarly, [Gorton & Ianchovichina \(2021\)](#) analyze trade network inefficiencies and optimal expansions for Latin America closely following [Fajgelbaum & Schaal \(2020\)](#). They find average welfare gains of 1.6% from optimal reallocation and 1.6%/1% from a 50%/10% optimal expansion of national road networks. They also consider transnational networks in the MERCOSUR and Andean Community trade blocs. Disregarding borders, they find that optimal expansions better connect major cities across countries at welfare gains of 1.5-1.9%. Throughout, they find that optimal network investments reduce spatial wealth disparities.

Many further works such as [Jedwab & Storeygard \(2022\)](#), [Peng & Chen \(2021\)](#), [Abbasi et al. \(2022\)](#), [Fiorini et al. \(2021\)](#), and [Moneke \(2020\)](#) study the economic effects of road interventions in Africa. The latter two find that road network expansion in Ethiopia enhanced the impact of trade liberalization/electrification on local firm productivity/industrialization, respectively. A vast further literature studies the effects of road interventions in other world regions, particularly in China ([Faber, 2014](#); [Baum-Snow et al., 2020](#)) and India ([Asher & Novosad, 2020](#); [Alder, 2016](#)).

Apart from the partial equilibrium simulations by [Porteous \(2019\)](#) on a heuristic agricultural trade network, and the work by [Graff \(2024\)](#) examining hypothetically optimal reshuffling and 10% expansion of national road networks on a regular 0.5° grid parameterized in a way that has limited resemblance of optimal routing through real road networks (see Section 4), the literature has not yet (to my knowledge) seen a detailed quantitative attempt to estimate what should be done to improve or extend Africa's continental road network. This paper attempts to fill this void.

Starting from a precise continental grid of 12,016 cells with centroids exactly 50.28km apart, I obtain 144 million OSM routes connecting all points and compute distance-weighted local measures of network quality and continental market access (MA). Using data on trading across borders, which I translate into road distance/travel time, I characterize how cross-border trade frictions impede cell-MA. A trade across the median African border is equivalent to ~ 1000 km of national roads or 3.2 road days. My results imply that particularly cells across the border from major markets such as Nigeria suffer $\leq 80\%$ MA losses due to frictions. Deriving an optimal graph representation of the network where links connecting adjacent cells are weighted to minimize the

¹Nearly all African countries lack subnational trade and (disaggregated) productivity data. General equilibrium simulations also impose a tight computational tradeoff between network size and number of traded products.

routing error through the entire network, I simulate global MA returns from improvements in local connectivity around individual cells. Better connecting cells surrounding urban centers or between major agglomerations along existing transport routes yields sizeable marginal MA gains.

In the second part of the paper, I identify 447 large cities with populations above 100,000 and 52 international ports with a quarterly outflow above 100,000 TEU and obtain routes between them. I process these routes into a realistic representation of the African transport network comprising 1379 nodes and 2344 edges representing 315,000km of road segments. The network connects 444 million people, or 86% of the African urban population. I parameterize the network with fresh routing information along all links and develop an algorithm to find 481 new links (104,000km), yielding route efficiency gains of $\geq 50\%$ (verified with OSM). Using this network graph, I simulate partial equilibrium MA returns from extending and/or upgrading the entire network or individual links. I find that continental MA, denominated in travel time, can be improved by $\leq 78\%$ through eliminating cross-border frictions. Upgrading the entire network to allow travel speeds of 100km/h yields a 42% frictionless MA gain and a 27% MA gain under current frictions. MA gains from new roads are lower and also decrease under frictions. Spatially, including frictions favors investments in national links, significantly reducing the value of transnational and remote links. I also find sizeable differences in the marginal values and cost-benefit ratios of links and propose three investment packages containing high-return links with and without border frictions. These packages cost between 17 and 61 billion 2015 USD, and generate MA gains between 20% and 38%. They are macroeconomically feasible if they can raise the aggregate economic growth rate by $\leq 0.54\%$.

The final part of the paper moves this to a general equilibrium setting following [Fajgelbaum & Schaal \(2020\)](#) and [Graff \(2024\)](#). I first let cities of different sizes trade with each other and with port cities, resembling optimal regional investments at a continental scale. To simulate optimal investments in trans-African roads, I then reduce the network to links connecting the 47 largest (port-)cities and let 17 megacities produce differentiated products traded across the continent. On both networks, I let welfare maximizing social planners spend budgets covering $<1/3$ of all work - 10 and 50 billion USD'15, respectively. I simulate cases with/without frictions, imports, increasing returns to infrastructure, and inequality aversion in the planner's objective. The regional \$50B planner optimally connects large cities with ports and surrounding cities. Investments are redistributional as in [Gorton & Ianchovichina \(2021\)](#). Under increasing returns to infrastructure, this planner upgrades many more roads and expands into remote regions, yielding higher and more equitable welfare gains. Similarly, the trans-African \$10B planner primarily upgrades road segments within different populated regions, enhancing connectivity between major cities and with ports. An inequality-averse planner also upgrades an entire corridor crossing southern central Africa from Luanda/Kinshasa to Mombasa/Dar es Salaam. Lowering the elasticity of substitution between different goods to a value of 2 creates incentives to also build corridors spanning northern central Africa, better connecting Rwanda/Bukavu and Khartoum to western Africa. Under border frictions, investments in connections through Congo and into Nigeria are reduced. Prioritizing the central African infrastructure gap thus requires inequality aversion, optimism about trans-African trade elasticities, and/or efforts to reduce border frictions. The results overall demonstrate that optimal \$10B investments in trans-African roads are non-trivial and differ significantly from AU Trans-African Highways, Chinese BRI investments, or EU Global Gateway corridors.

Methodologically, in this paper, I advance a rigorous quantitative approach to characterizing optimal road network investments. I demonstrate the use of geospatial big data and routing engines to algorithmically create large and accurate network graphs, including potential new roads, and simulate investments on them via established quantitative frameworks. I am also the first to account for cross-border frictions and trade through ports and study their implications on optimal spatial allocations. Detailed estimation of road construction/upgrading costs facilitates interpretation and enables link-level cost-benefit analysis. A corollary of the work is an open-source Julia translation of [Fajgelbaum & Schaal \(2020\)](#)'s MATLAB toolbox presently available on [GitHub](#).²

The paper begins with a high-resolution examination of Africa's road network (Section 2) and cross-border frictions (Section 3). It then proceeds via optimal network representations (Section 4) towards partial equilibrium analysis (Section 5) (including cost-benefit analyses) and culminates with general equilibrium analysis (Section 6) (including trans-African network trade simulations).

²<https://github.com/SebKrantz/OptimalTransportNetworks.jl>

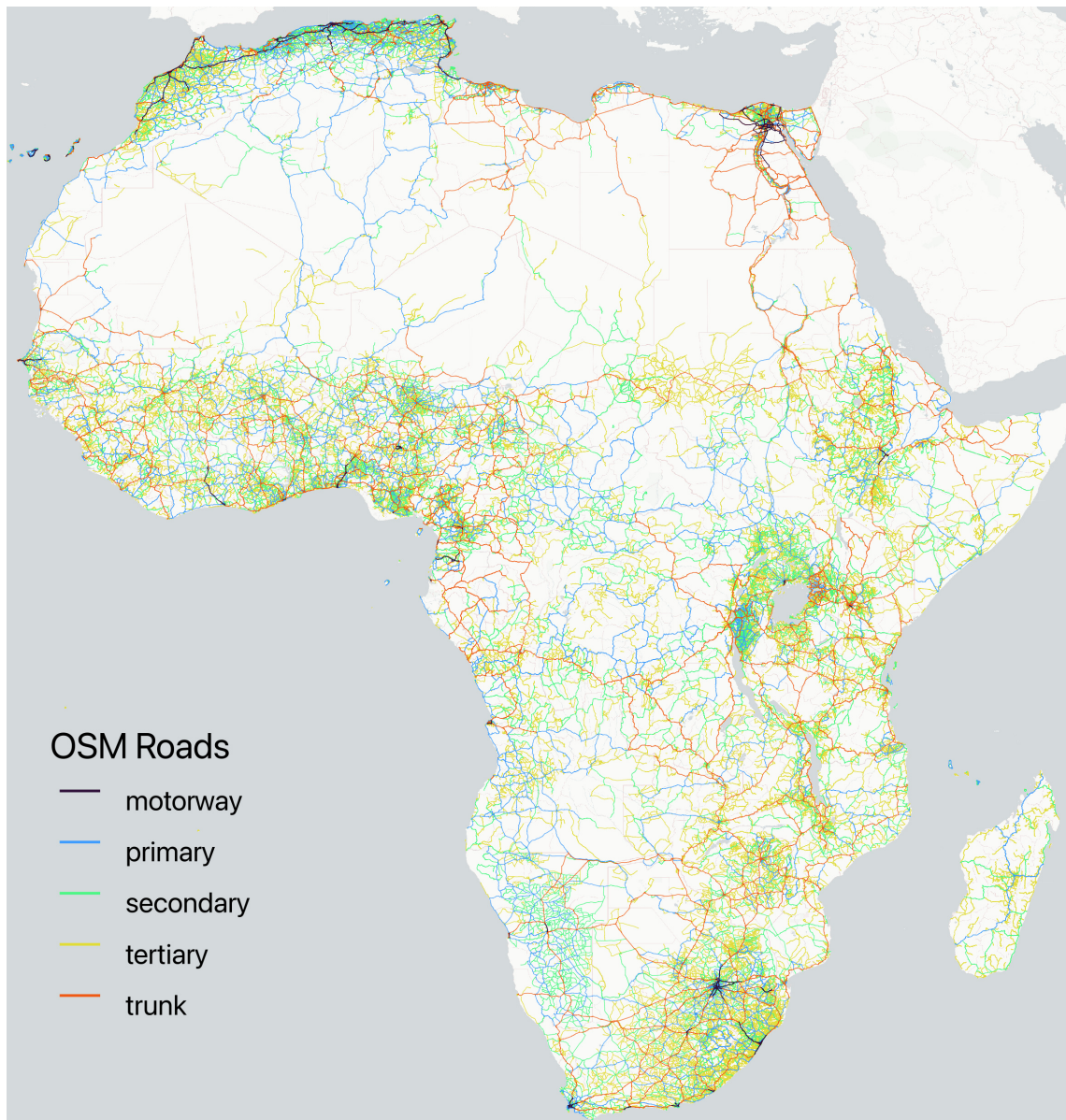
2 Africa's Present Road Network

Africa's road network, like any road network, is multi-layered, consisting of major transport routes between cities across countries, smaller roads connecting villages and towns, inner-city roads, and residential roads. Open Street Map (OSM) has an established hierarchy of tags to classify roads comprising motorway > trunk > primary > secondary > tertiary > residential roads. Table 1 shows a summary of all non-residential roads (excluding short links connecting these roads), and Figure 1 a corresponding map. Combined there are 673,045 roads with a total length of 1,611,912km.

Table 1: African Roads (OSM April 2024)

Highway Tag	N	Length in km	Paved Length in km
motorway	14,986	22,400	17,744 (79.2%)
trunk	75,265	181,459	128,978 (71.1%)
primary	124,547	252,047	136,452 (54.1%)
secondary	158,674	365,939	97,904 (26.8%)
tertiary	299,573	790,067	94,373 (12.0%)
Total	673,045	1,611,912	475,450 (29.5%)

Figure 1: African Roads (OSM April 2024)



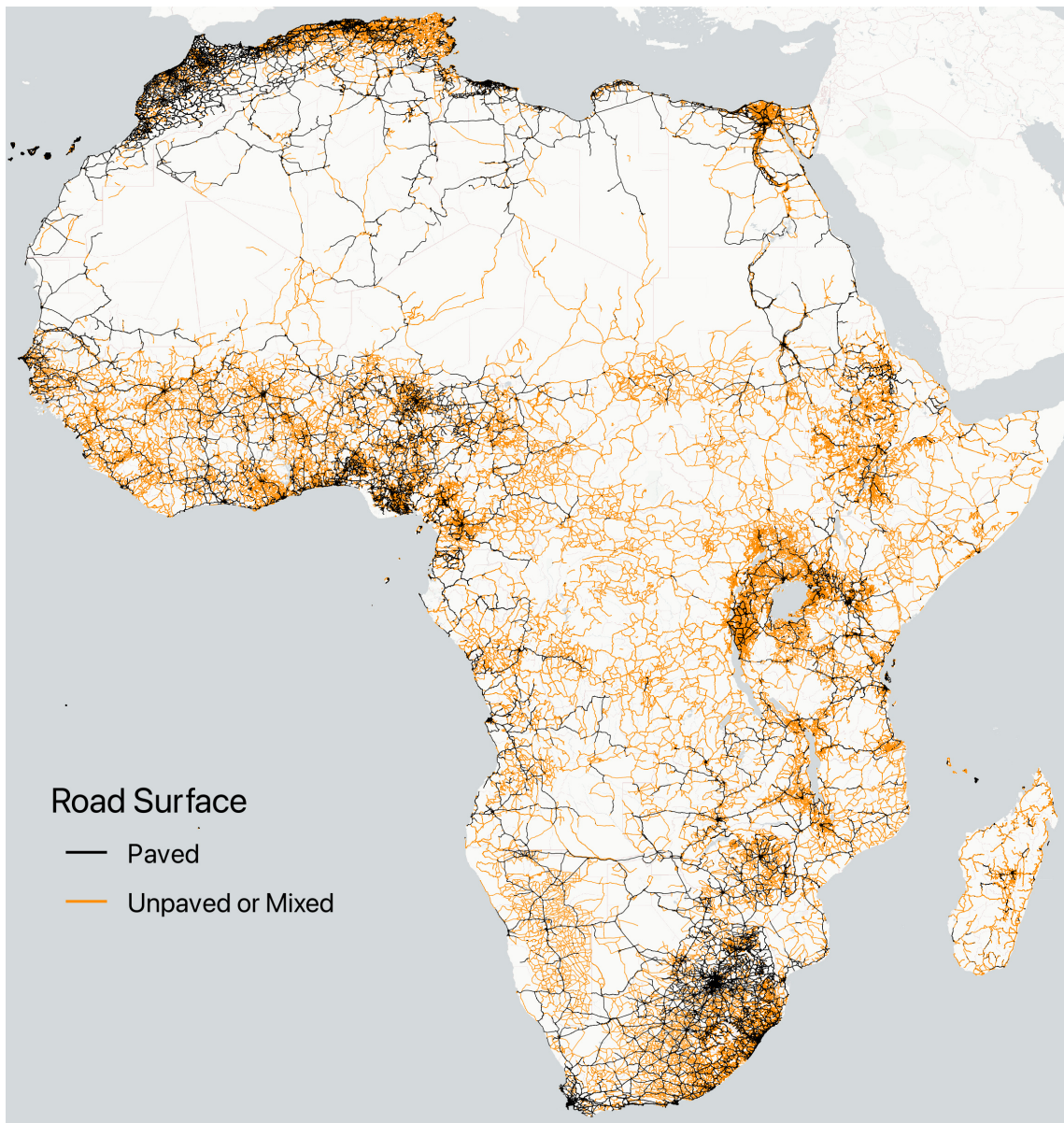
Notes: Figure shows all non-residential roads in the Africa OSM (April 2024) colored by type (OSM 'highway' tag).

Is this a comprehensive account of the network? There is reason to believe so: in 2022, Microsoft Research released a [global dataset of segmented roads](#) indicating that globally, 2.3% of roads are missing from OSM, and in Africa around 2.6%. Presumably, most of these are tertiary roads.

Apart from the sheer extent of the network, the surface material and quality of roads determine their efficacy. OSM has a detailed tagging system for roads, including tags such as 'surface,' 'smoothness,' 'tracktype,' 'lanes,' 'lit,' 'maxspeed,' etc. To keep things simple, I develop a binary classification based on whether the 'surface' tag unambiguously indicates that a road is paved, which I summarize on the right hand side (RHS) of Table 1, and plot in Figure 2.

In early 2024, 29.6% of African transport roads are paved, amounting to 475,450km. The actual fraction is presumably a few percentage points higher due to missing 'surface' tags for 38% of roads, all of which are classified as unpaved. But it may also be that a few roads labeled as 'paved' are actually mixed. It is probably relatively safe to assume that at least 1/3 of the network is paved. Among motorways $\geq 79\%$, trunk roads $\geq 71\%$, and primary roads $\geq 54\%$ are paved. Significantly lower shares of secondary and tertiary roads are paved; $\leq 88\%$ of tertiary roads are dirt roads. Paved roads are also concentrated in northern, southern, and western Africa, and are largely missing in central Africa, the Horn of Africa, and Madagascar.

Figure 2: Surface of African Roads (OSM April 2024) | Paved: 475,450km (29.6%)



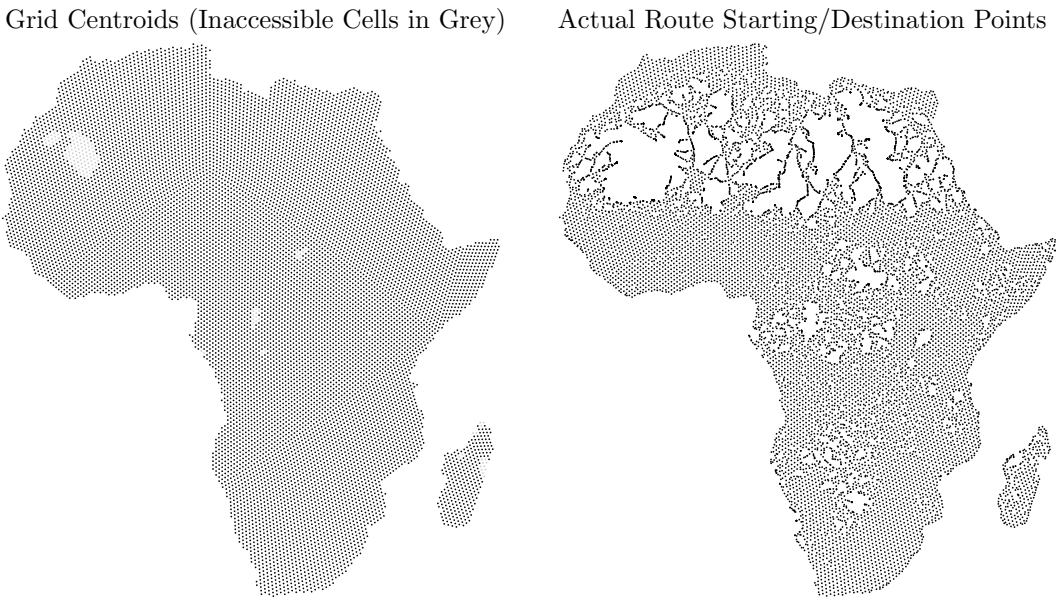
Notes: Figure shows all non-residential roads in the Africa OSM (April 2024) colored by the 'surface' tag.

2.1 Routing Data

Plotting the road network, while informative about its extent, does not permit a rigorous assessment of its efficiency. Routing engines³ provide more precise information on how cars can use the network to get from A to B. In my case, A and B could be anywhere on the continent. Two approaches invite themselves to choose points: (1) using a uniform spatial grid and taking the cell centroids, or (2) selecting the centers of important cities/places. In this paper, I employ both approaches, but for spatial analysis, the grid approach is more suitable. Hence, I begin with it.

Accurate spatial analysis at the continental scale warrants using an equally spaced grid. Discrete Global Grid Systems (DGGS) provide these via hierarchical tessellation of cells partitioning the globe. Sahr et al. (2003) propose the Icosahedral Snyder Equal Area Aperture 3 Hexagon (ISEA3H) as a good general-purpose Geodesic DGGS.⁴ The grid is implemented as part of the DGGRID C++ library (Sahr, 2022), accessed via the 'dggridR' R package (Barnes, 2020). To limit complexity, I choose a resolution 9 ISEA3H grid, with a cell area of 2591.4km^2 and a centroid spacing of 50.28km. Partitioning the African mainland and Madagascar with this grid yields 12,016 cells.

Figure 3: Grid Cell Centroids and OSRM Route Starting and End Points



Notes: Figure shows centroids of 50.28km ISEA3H grid (LHS) and the nearest road segment to each centroid (RHS).

To compute a large number of routes, I configure a server with the Open Source Routing Machine (OSRM)⁵ and a copy of the Africa OSM from the 5th of June 2023, and compute fastest car routes between all cell centroids. This amounts to $12,016^2 - 12,016 = 144,372,240$ routes, for which I obtain both the road distance in m and the estimated travel time in minutes. OSRM 'snaps' cell centroids to the nearest road, yielding divergent route start/endpoints. Figure 3 shows the outcome of this process. For some cells in the Sahara, the Congo Basin, and Madagascar, colored in light grey on the left-hand side (LHS), OSRM cannot find the nearest road and returns 'NA'. For many further cells, the nearest road snapped to is outside of the cell, as shown on the RHS.

I clean the data by first mapping inaccessible cells to the nearest route start/endpoints. I then follow Graff (2024) in adding the spherical centroid-start/end distance to all routes. This increases the length of routes by 0.53% on average. I also adjust travel time estimates by assuming a travel speed of 10km/h on these straight passages, increasing travel time by 3.4% on average.⁶

³Large computer programs used for navigating (routing) through digitized transport networks.

⁴Sahr et al. (2003) vindicate ISEA3H as: "... due to its lower distortion characteristics we choose the icosahedron for our base platonic solid. We orient it with the north and south poles lying on edge midpoints, such that the resulting DGGS will be symmetrical about the equator. Next, we select a suitable partition. The hexagon has numerous advantages, and we choose aperture 3, the smallest possible aligned hexagon aperture. Because equal-area cells are advantageous, we choose the inverse ISEA projection to transform the hexagon grid to the sphere..."

⁵A high-performance open routing engine in C++ optimized for OSM. Website: <https://project-osrm.org/>.

⁶In this regard I differ from Graff (2024), which assumes walking speed of 4km/h. My main reason is that the

2.2 Efficiency of Africa's Road Network

With realistic road distance and travel time estimates for 144 million trans-African routes, I measure the African network's local and global efficiency. Following Wolfram (2021), I first compute two metrics to assess the efficiency of individual routes: (1) route efficiency (RE), which divides the geodesic distance s_{ij} between two locations i and j by the road distance r_{ij} , resulting in an index between 0 and 1 with 1 implying a direct straight road; and (2) time efficiency (TE), which divides s_{ij} by the travel time along the fastest route t_{ij} , and thus measures the average travel speed in the direction of the destination. Formally, for any route between two cells i and j ,

$$\delta_{ij}^r = s_{ij}/r_{ij} \quad (\text{Route Efficiency}) \quad (1)$$

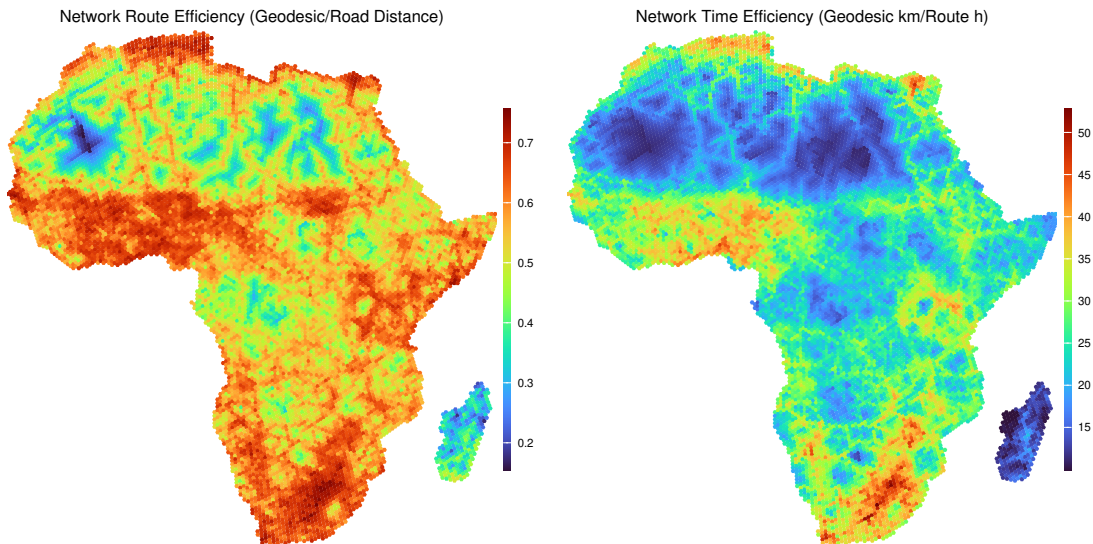
$$\delta_{ij}^t = s_{ij}/t_{ij} \quad (\text{Time Efficiency}). \quad (2)$$

To visualize these metrics, I compute a weighted average across all routes starting in cell i , using the inverse area of an expanding circle around the cell as weight.⁷ For each cell i , I obtain

$$\kappa_i^m = \sum_{j \neq i} \frac{\delta_{ij}^m}{s_{ij}^2} / \sum_{j \neq i} \frac{1}{s_{ij}^2} \quad m \in r, t. \quad (3)$$

Figure 4 reports the cell-level route and time efficiency estimates. Appendix Figure A1 additionally shows the average network speed (NS), computed as r_{ij}/t_{ij} .

Figure 4: Local Route and Time Efficiency of Africa's Road Network



Notes: Figure shows local route efficiency (Eq. 1) and time efficiency (Eq. 2) for each cell i , computed as an inverse-squared spherical distance weighted average across all routes starting in i (Eq. 3).

All three metrics are higher in cities or close to major transport routes. RE is less concentrated than TE and NS, indicating larger heterogeneity in road quality. Particularly outside of major cities, the difference between route and time efficiency is significant. For example, the Southern part of Sudan has, according to Figure 2, a quite dense network of mostly dirt roads, permitting, as Figure 4 suggests, route-efficient navigation at slow driving speeds. Since OSRM does not take into account traffic volumes, TE estimates inside cities and populated areas are too high.

A simple average of these cell-level estimates (κ_i) yields a NS of 40.3km/h (maximum 69.7km/h), RE of 0.534 (maximum 0.756), and TE of 24.9km/h (maximum 52.8km/h). As κ_i is low in

centroid of such cells is unlikely of economic significance, and assuming a travel speed of 4km/h increases travel time by 8.5% on average, whereas assuming 10km/h only increases travel time by 3.4% on average. Furthermore, since most cells where the distance between the cell centroid and the route starting/endpoints is large are in the Sahara, I believe that motorized transport with specialized vehicles (4x4) is possible, and thus a travel speed of 10km/h might be more realistic.

⁷The reason for considering the area (πs_{ij}^2 , π cancels out) as a weight on individual routes is that with increasing distance from i there are more cells j , and each of these cells is a less important destination for cell i dwellers.

uninhabited areas, I also compute a population-weighted average using 2020 total population counts from [WorldPop](#), shown in Appendix Figure A1. This yields a NS of 53.2km/h, RE of 0.625, and TE of 34.4km/h. [Wolfram \(2021\)](#) computes global efficiency directly by probabilistically sampling route start/end points using population weights.⁸ To approximate this strategy, I compute a global weighted average across routes using Newton's Law of Gravity to weight each route by the product of the start/end cell populations divided by their squared spherical distance. This yields NS of 56.7, RE of 0.668, and TE of 38.8. Since research on inter-city migration gravity models such as [Zipf \(1946\)](#) or [Poot et al. \(2016\)](#) suggests that migration varies according to the distance rather than the squared distance, I also consider weights denominated by the simple distance. This yields even higher NS of 64.2, RE of 0.68, and TE of 43.9, indicating that efficiency is higher on longer routes - as [Wolfram \(2021\)](#) finds in the US and Europe. But even the most favorable RE estimate of 0.68 is far below [Wolfram \(2021\)](#)'s estimates of 0.843/0.767 for US/European road networks.

2.3 Market Access

Whereas route and time efficiency are important from a transportation standpoint, the spatial economics literature such as [Donaldson & Hornbeck \(2016\)](#), [Jedwab & Storeygard \(2022\)](#) or [Peng & Chen \(2021\)](#) has used market access (MA), typically defined as an inverse-distance weighted sum of population, or a proxy therefore such as built-up in the case of [Peng & Chen \(2021\)](#), to evaluate economic gains from transport investments. The MA measure for cell i is

$$\text{MA}_i = \sum_{j \neq i} L_j \tau_{ij}^{-\theta}, \quad (4)$$

where L_j is a measure of population and τ a measure of distance, travel time, or transport cost, weighted by an elasticity θ measuring how trade volumes fall as distance/time/costs increase. The value of θ is contentious, for example [Jedwab & Storeygard \(2022\)](#) use $\theta = 3.8$ whereas [Peng & Chen \(2021\)](#) use $\theta = 1$. In both cases, τ_{ij} measures travel time.

To appropriately measure continental MA implied by the road network, I incorporate spatial differences in purchasing power into L_j . [Kummu et al. \(2018\)](#) provide a spatial estimate of GDP in 2015 USD PPP terms by distributing national GDP estimates from the World Development Indicators at 5 arc-min (0.0833 degrees or 9.3km at the equator) resolution using subnational value-added estimates from [Gennaioli et al. \(2013\)](#) and population from the HYDE 3.2 database. For robustness, I also consider a predicted International Wealth Index (IWI) by [Lee & Braithwaite \(2022\)](#), which employ day- and nighttime satellite imagery and OSM features to predict the IWI - a comparable asset-based wealth index calculated from DHS Surveys for 25 countries in SSA conducted since 2017. Appendix Figure A2 shows the raw estimates from [Kummu et al. \(2018\)](#) and [Lee & Braithwaite \(2022\)](#).⁹ To map these estimates into the grid, I sum GDP and average the IWI in each cell. I multiply the IWI with the WorldPop cell-population to estimate total wealth.

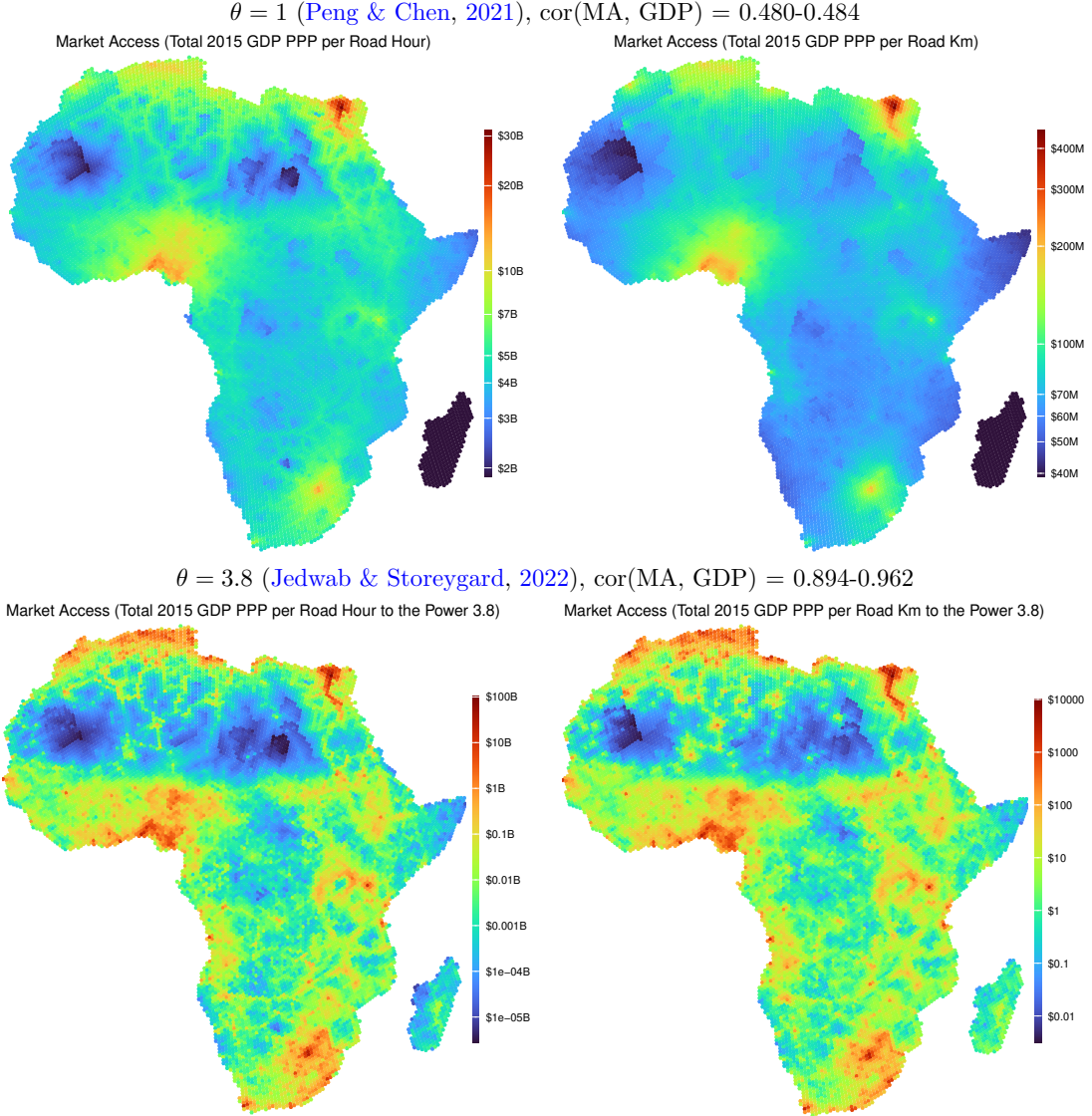
Using Eq. 4, I compute MA maps using both measures of economic mass (L_j), and trade elasticities of $\theta = 1$ ([Peng & Chen, 2021](#)) or $\theta = 3.8$ ([Jedwab & Storeygard, 2022](#)). As Eq. 4 excludes cell i itself, the centers of several large cities have a lower MA measure than adjacent cells. To remedy this, I add i 's GDP/wealth to the MA measure using a distance $\delta_{ij} = 25\text{km}/\kappa_i$, where κ_i is cell i 's RE/TE measure from Figure 4. Figure 5 shows the resulting maps with GDP and Appendix Figure A4 with total IWI-based wealth.

Evidently, $\theta = 3.8$ yields a much stronger concentration of MA around major cities and a high correlation of the MA measure with cell GDP. Both θ values elicit northern Egypt, Nigeria, and, to a lesser extent, greater Johannesburg as high MA areas. Cairo has the greatest MA. The $\theta = 1$ estimates imply that $>\$30\text{B}$ of GDP can be reached within one road hour from Cairo. Wealth-based estimates in Appendix Figure A4 are very similar.

⁸Concretely, [Wolfram \(2021\)](#) computes the route efficiency of the US road network using OSRM-generated routes between 2000 population-weighted random points in the US and finds a median route efficiency of 0.843 with a standard deviation of 0.045 across 4 million routes.

⁹Since the IWI is not available for North Africa, I predict it at 96km² resolution using a rich gridded infrastructure database developed in [Krantz \(2023\)](#) with OSM as principal data source. Imputation using the *MissForest* algorithm ([Stekhoven & Bühlmann, 2012](#)) via the *missRanger* R package ([Mayer, 2023](#)) reaches an R^2 of 97%, as shown in Appendix Figure A3.

Figure 5: Market Access Maps using GDP in 2015 USD PPP



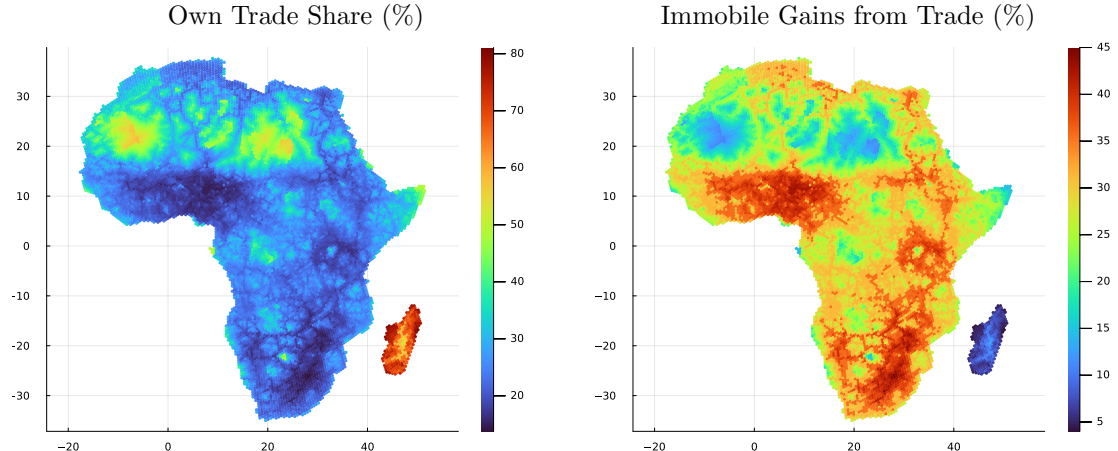
Notes: Figure shows local market access using Eq. 4 where L_j is cell-GDP in 2015 USD PPP from [Kummu et al. \(2018\)](#).

2.4 Gravity Implied Trade and Welfare Gains

A yet more elaborate way to synthesize the data is through the lens of a quantitative spatial model. I take the canonical model of [Redding \(2016\)](#) with fixed labor and calibrate it with iceberg trade costs $d_{ij} = 1 + 0.1 \times \sqrt{\text{travel time in minutes}}_{ij}$, population from WorldPop, the imputed IWI as productivity measure, and residential land area from the [Overture Maps Buildings Dataset](#). Using the parameterization of [Redding \(2016\)](#), I solve the model and compute trade flows between all locations, consumer and land prices, output, consumption, and welfare. Of particular interest are the trade share of a location with itself and the welfare gains from trade vis-a-vis autarky. Figure 6 visualizes these two, indicating that populated, productive, and well-connected locations have higher trade shares with other locations and experience greater gains from trade. In contrast to MA maps, the model emphasizes the large connected economic areas in western, southern, and, to a lesser extent, eastern Africa as exhibiting the greatest potential gains from inner-African trade.

All of these maps, indicative of Africa's potential to trade and benefit from a single market, assume that transport is the only obstacle to accessing distant markets and that there is no congestion. To add some realism, I proceed to examine barriers to cross-border trading in Africa. Section 6 additionally introduces congestion forces through a general equilibrium framework.

Figure 6: Own Trade Share and Welfare Gains from Trade Following Redding (2016)



Notes: Figure shows cell-own trade share and immobile gains from trade in equilibrium of a quantitative spatial model introduced by Redding (2016) (CRS version) using OSRM travel time estimates to inform iceberg trade cost parameters.

3 Barriers to Cross-Border Trade

Africa has 'thick borders,' and any evaluation of continental roads should at least be mindful of them. Trade barriers can broadly be distinguished into three categories: (1) traditional trade tariffs, (2) traditional non-tariff measures such as quantity or quality restrictions (e.g., sanitary and phytosanitary measures), and (3) regulatory obstacles and frictions at the border. This paper will concentrate on type (3) barriers as types (1) and (2) tend to be product- and quantity-specific. But, for the sake of completeness, I begin with a brief overview type (1) and (2) barriers.

3.1 Trade Tariffs

The World Development Indicators provide aggregate estimates of the extensive and intensive margins of trade tariffs applied by each country.¹⁰ Table 2 summarizes these indicators for different country groups. While SSA countries only apply specific (non-ad-valorem) rates on 0.1% of tariff lines, 33.9% of African tariffs exceed 15%. When weighted by the product import shares corresponding to each partner country, the average SSA country applies an 8.2% import tariff and a 7.5% tariff on manufactured products. This is comparatively high and only exceeded by South Asia and the low income country (LIC) average. Averaging across all African countries using 2020 GDP in PPP terms as weights yields very similar outcomes, at an average tariff rate of 8.7%.

The African Continental Free Trade Agreement (AfCFTA), concluded in 2019 and ratified by 47 African states by the end of 2023, aims to facilitate trade by eliminating 97% of tariff lines between members alongside most NTBs. Yet, trading under the agreement has started sluggishly; at present, only 8 countries trade 96 products under the Guided Trade Initiative¹¹. With LDCs given 10+ years to remove tariff lines and the sluggish start of trade under the agreement, it is expected that the full benefits of the agreement will only accrue by the middle of the century.

3.2 Non-Tariff Measures

Non-tariff measures (NTMs) are still difficult to quantify comprehensively, particularly in terms of their depth and effects. A simple database that just counts the incidence of NTMs is the WIIW NTM Database by Ghodsi et al. (2017). According to it, the average African country in 2019 had 101 general NTMs (with all WTO members), whereas the median African country only had 18. Countries with the most NTMs were Uganda (1268), Kenya (492), and South Africa (418). In comparison, the average non-African country had 316 NTMs, and the median non-African country had 86. The country with the most NTMs is the USA (5471), followed by Brazil

¹⁰Based on the World Integrated Trade Solution system with data from United Nations Conference on Trade and Development's Trade Analysis and Information System (TRAINS) database and the World Trade Organization's (WTO) Integrated Data Base (IDB) and Consolidated Tariff Schedules (CTS) database.

¹¹<https://au-afcfta.org/>, <https://www.macmap.org/en/learn/afcfta>

Table 2: World Development Indicators: Tariffs Applied in 2020

Region/Income Status	All Products				Manufactured Products			
	SSR	SIP	TR	WTR	SSR	SIP	TR	WTR
OECD	5.7	2.7	2.0	1.6	0.3	0.6	1.5	1.5
Non-OECD	0.5	19.1	8.0	6.3	0.2	17.8	7.5	6.0
High income	4.3	4.7	3.0	2.6	0.2	3.0	2.6	2.4
Low income	0.0	34.3	11.1	9.3	0.0	32.4	10.6	8.4
Europe & Central Asia	5.0	2.4	2.5	1.9	0.3	0.6	2.2	1.9
Latin America & Caribbean	0.0	19.2	8.0	6.7	0.0	17.7	7.5	6.6
South Asia	0.6	28.6	10.6	8.8	0.6	27.8	10.2	9.9
Middle East & North Africa	0.8	9.3	6.4	5.1	0.1	8.8	5.6	4.8
Sub-Saharan Africa	0.1	33.9	10.8	8.2	0.1	32.5	10.5	7.6
All Africa wtd. GDP PPP	0.0	26.9	11.2	8.7	0.0	26.1	9.0	7.6

SSR = Share of Tariff Lines with Specific Rates (%)

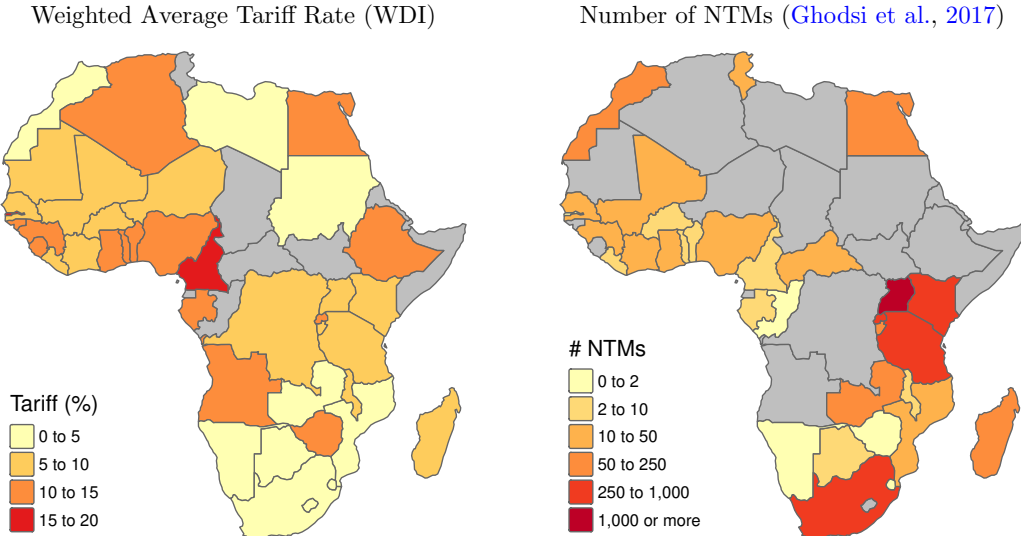
SIP = Share of Tariff Lines with International Peaks (%)

TR = Tariff Rate, Applied, Simple Mean (%)

WTR = Tariff Rate, Applied, Weighted Mean (%)

(2598) and Canada (2100). In addition, the median African country had 1 bilateral NTM with another African country (1.1 on average). Overall, this suggests that most African countries are not imposing a lot of classical NTMs; they are rather underutilizing them. Figure 7 shows the latest available estimates for tariffs and NTMs by country.

Figure 7: Trade Tariffs and Non-Tariff Measures



Notes: Figure shows weighted average tariff rate from the World Development Indicators and number of non-tariff measures from the WIIW NTM Database (Ghodsi et al., 2017). Latest estimates from 2019 are shown (if available).

3.3 Regulatory Obstacles and Border Frictions

The World Bank's Doing Business (DB) ranking recorded the time and costs (excluding tariffs) required for trading across borders¹² in all African countries, with the latest surveys done in 2019. The surveys record separately the time and cost in USD of documentary compliance (DC) and border compliance (BC) for both exporting and importing. Table 3 summarizes these results. Overall, SSA is at the bottom of the ranking, and the MENA region is not much advanced either. Weighting the estimates by countries' 2019 GDP in PPP terms also yields no improvements. The weighted estimates imply an average cost of 808 USD for exporting a container in Africa, most of which is payable at the border, and an average time investment of 170 hours, 81 of which are spent

¹²<https://archive.doingbusiness.org/en/data/explore/topics/trading-across-borders>

at the border. The costs of importing are even worse, at an average of 1177 USD per container and an average time commitment of 292 hours, 124 of which are spent at the border.

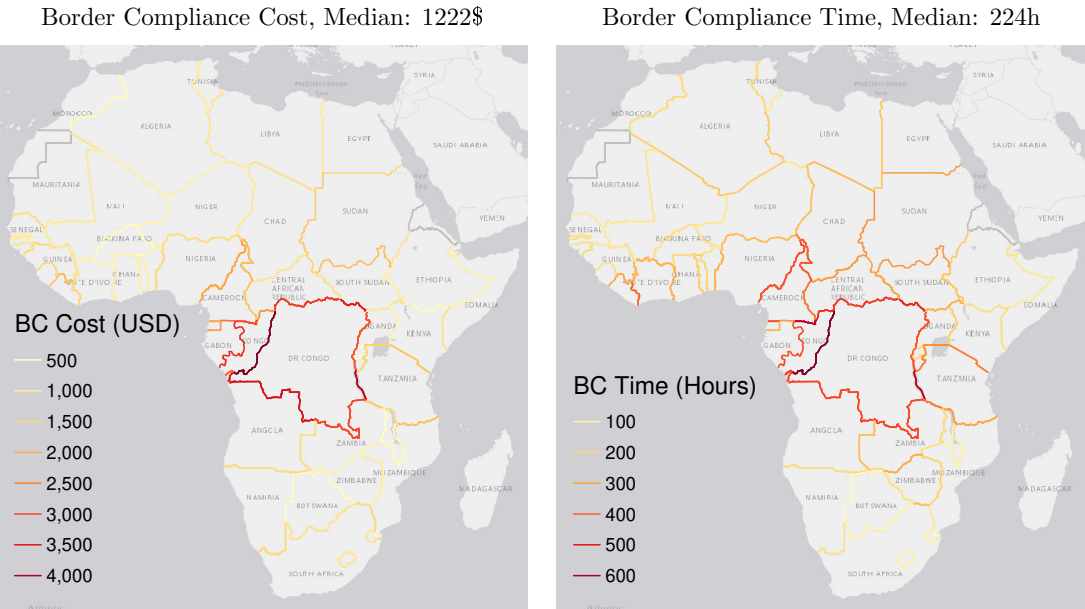
Table 3: World Bank Doing Business: Trading Across Borders in 2019

Region/Income Status	Exporting				Importing			
	USD BC	Hours DC	USD BC	Hours DC	USD BC	Hours DC	USD BC	Hours DC
OECD	149.7	34.8	12.8	2.5	106.5	26.5	9.4	3.8
Non-OECD	453.8	145.0	64.0	55.8	531.5	191.4	82.5	66.5
High income	228.4	68.0	24.8	12.6	252.1	74.3	22.1	16.0
Low income	528.8	197.1	84.1	78.9	670.7	348.0	125.9	124.3
Europe & Central Asia	117.8	47.1	11.9	12.2	91.8	42.1	10.4	11.2
South Asia	310.6	157.9	53.4	73.7	472.9	261.7	85.7	93.7
Latin America & Caribbean	513.2	99.5	55.7	36.4	625.3	106.5	55.8	44.3
Middle East & North Africa	447.0	239.7	54.1	63.1	526.0	261.8	97.3	72.4
Sub-Saharan Africa	603.1	172.5	97.1	71.9	690.6	287.2	126.2	96.1
All Africa wtd. GDP PPP	628.9	178.8	89.3	80.5	717.6	459.6	167.9	123.9

DC = Documentary Compliance, BC = Border Compliance

Figure 8 shows symmetrized exporting + importing border compliance times and costs for each border. In central African countries such as Congo, the costs are exorbitant, whereas particularly in southern Africa, they are quite efficient, coming as low as 509 USD for trades across the Rwanda-Burundi border and 40 hours for trades between Mozambique and Eswatini.

Figure 8: World Bank Doing Business: Border Compliance Frictions in 2019



Notes: Figure shows average (bi-directional) 2019 border compliance cost/time of trading a standardized product.

3.4 Border Frictions Adjusted Routes

It is difficult to take tariffs and NTMs into account when evaluating transport networks and market access because their effects depend on the value, type, and quantity of products being traded. In addition, AfCFTA has set clear aims to eliminate most inner-African tariffs in the foreseeable future. Regulatory and border frictions on the other hand are more uniformly applicable.

A critical question then is how the estimates from Table 3 can be sensibly added to road distance and travel time estimates. Surely time spent preparing documents or waiting at the border is

different from driving time. To better understand the relative cost of these times, I collect data on domestic transport costs from the 2019 DB survey for a sample of 23 (mostly landlocked) African economies where exporting/importing involved domestic transportation of 100km or more. This information is not standardized across countries and thus not published in the DB indicators. For each country surveyed, the distance in km to the border, the time in hours to the border, and the cost in USD of exporting/importing a representative product are recorded alongside the published border and documentary compliance times and costs.

To estimate the average cost of an hour spent on the road, I regress the cost of the trip on the travel time in hours while controlling for the log of the velocity and a dummy indicating whether the transport was import related.¹³ I do the same for the distance traveled. Since I am more interested in converting times into each other rather than converting cost to time, I also regress the cost of border and documentary compliance from Table 3 on the respective time required using data for all 53 available African economies. Table 4 reports the results.

Table 4: Relative Cost of Exporting/Importing Times

Cost in USD: Model:	Transport		Border	Documentary
	(1)	(2)	(3)	(4)
Constant	-711.6** (285.9)	276.7 (317.4)	217.8*** (65.28)	51.83* (29.63)
Travel Time (Hours)	15.79*** (2.074)			
Travel Distance (Km)		1.560*** (0.2987)		
Border Time (Hours)			3.988*** (0.6781)	
Documentary Time (Hours)				1.655*** (0.3954)
Log Velocity (Km/Hour)	346.3*** (85.84)	-43.95 (102.9)		
Import Dummy	106.6 (133.3)	107.7 (135.9)	-44.92 (66.38)	78.76*** (25.79)
Observations	46	46	106	106
R ²	0.448	0.415	0.471	0.388
Adjusted R ²	0.408	0.373	0.461	0.376

Heteroskedasticity-robust standard-errors in parentheses.

Signif. Codes: ***: 0.01, **: 0.05, *: 0.1

Evidently, time spent on the road, valued at 15.8 USD per hour in the average African country, is more costly than time spent at the border (4\$/h) or filing documents (1.7\$/h). The estimates imply that in the average African country, road time is $15.79/3.988 = 3.959 \approx 4$ times more costly than border time, and $15.79/1.655 = 9.540785 \approx 10$ times more costly than documentary time. To create the NTB-adjusted travel time matrix, I divide border compliance time by 4 and documentary compliance time by 10 before and add them to the OSRM estimates. Using the coefficient on distance indicating an average cost of 1.6\$/km, I also obtain an adjusted road distance matrix by dividing documentary and border compliance costs by 1.6 and adding them to the OSRM distance matrix. These estimates are roughly consistent with Djankov et al. (2010)'s result that a day of border delay is equivalent to a country distancing itself from its trade partners by ~ 70 km since $24h \times 4\$/h \div 1.6\$/km = 60$ km.

This accounting likely underestimates the true extent of frictions as I only convert time/cost to travel time/distance rather than converting both measures. Table 4 would allow converting both, but I suspect cost estimates to include labor time. Transportation economics also typically considers transport costs a function of distance rather than time whereas for personal transport

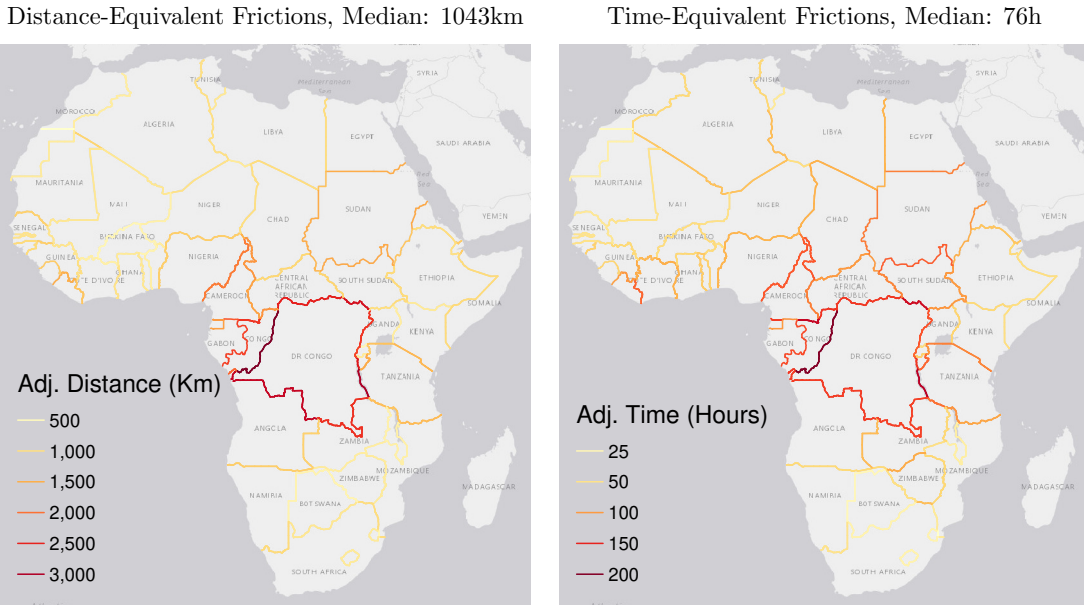
¹³I also test the interaction of travel time and the import dummy, but the term is insignificant; thus export and import time do not differ in terms of cost.

time may be more important than costs. Having two different adjusted MA measures can thus capture different aspects of frictions. Another consideration is that OSM travel speeds are too fast since they ignore congestion; thus, very large time-denominated frictions would overstate their effects. African borders may also have improved since 2019. In any case, I find that the frictions accounted in this way are sufficient to dramatically impede MA.

It remains to specify how to adjust routes between cells that are not in neighboring countries. The DB surveys do not give information about the time and cost of transiting through a country. Efficient calculation of multiple routes with OSRM also does not return the geometries of routes but only the total distance and travel time. I thus opt for a simple approach and stipulate a lump-sum transit time of 2 days on all routes transiting through 3rd countries. Using the estimates from Table 4, this yields a $48\text{h} / 4\$/\text{h} = 12\text{h}$ increase in travel time and or a $48\text{h} \times 4\$/\text{h} \div 1.6\$/\text{km} = 120\text{km}$ increase in road distance. The reader scrutinizing this generic adjustment should remember that long routes do not impact market access calculations much.

Figure 9 shows the frictions denominated in travel distance and time implied by each border crossing - again after imposing symmetry regarding the direction of travel. The median African border imposes an additional cost equivalent to 1043km of road travel or $76\text{h} = 3.2$ road days.

Figure 9: Road Distance and Time Equivalent 2019 Border Frictions



Notes: Figure shows average (bi-directional) 2019 border and documentary compliance cost/time converted to road distance/travel time following Table 4, i.e., dividing costs by 1.6 and documentary/border times by 10/4, respectively.

3.5 Border Frictions Adjusted Market Access Maps

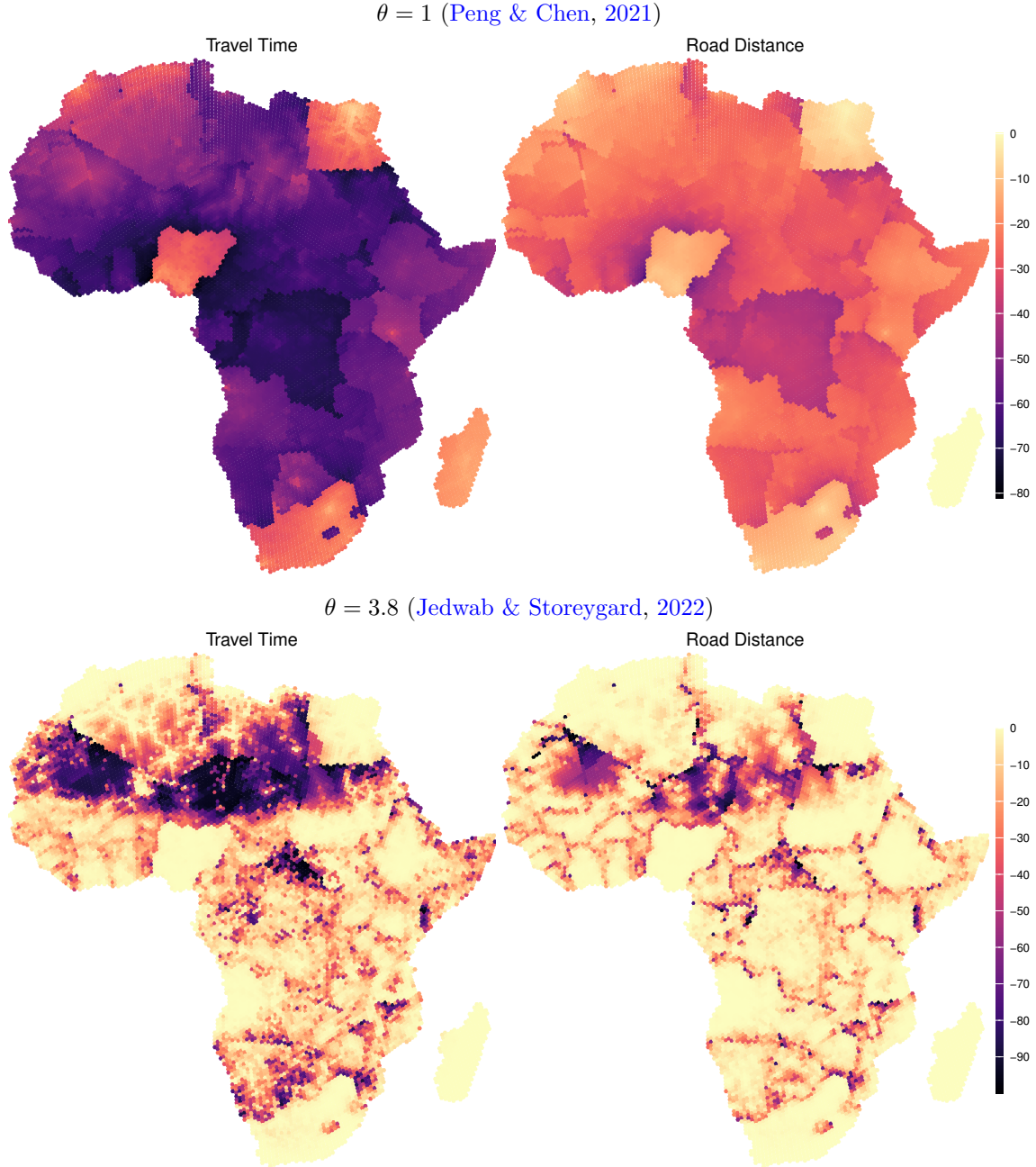
Appendix Figure A5 shows the frictions adjusted market access maps using GDP, and Appendix Figure A6 with IWI-based wealth. They indicate that, especially when θ is low, border frictions significantly obstruct access to markets in neighboring countries. The adverse effects are especially strong for cells surrounding major African markets such as Nigeria, Egypt, and South Africa.

Summing together the MA of all locations, I estimate the total cost of these frictions. Under $\theta = 1$, the estimated travel times imply a total MA of 980 billion USD/min in 2015 PPP terms, which is reduced by 52.3% to 467 billion USD/min under the 2019 trade frictions. Considering total IWI-based wealth (Figure A6) yields a similar MA reduction by 53.8%. When considering only distance, with $\theta = 1$ MA is 922 billion USD/km, and reduced by 25.5% to 687 billion USD/km under 2019 frictions. Using wealth yields a similar reduction of 27.2%. Thus, under a low trade elasticity, the African continental market could be up to twice its effective size, even with the current transport network, if regulatory and border frictions impeding cross-border trading could be eliminated. Under $\theta = 3.8$, the reduction in MA shrinks to 1.13%-1.19% in all cases, implying

that with a high trade elasticity, cross-border frictions become largely irrelevant. Evidence on inter-city migration and by Peng & Chen (2021) suggests that a lower elasticity is more plausible.

Cell-level MA losses due to border frictions range between -6.6% and -81.1% in GDP/min terms with $\theta = 1$, and between -0.1% and -99.82% with $\theta = 3.8$. Figure 10 shows their spatial distribution. Under $\theta = 1$, large parts of central Africa incur 50-80% time- and 20-50% distance-denominated losses. Cells across the border from major markets also incur very large losses. Under $\theta = 3.8$, losses are large in some cells close to borders but negligible in most populated cells.

Figure 10: Market Access Loss (%) from Border Frictions using GDP in 2015 USD PPP



Notes: Figure shows local MA %-loss from frictions (using Eq. 4 where L_j is cell-GDP from Kummu et al. (2018)).

In summary, assuming $\theta \ll 3.8$, many regions could gain significant MA from lower border frictions. In the following sections, I show that these frictions also reduce the value of (trans-African) road investments. Thus, their reduction should be a top policy priority. To simulate such investments, however, I first need to create suitable graph representations of Africa's road network.

4 Optimal Network Representations and Extensions

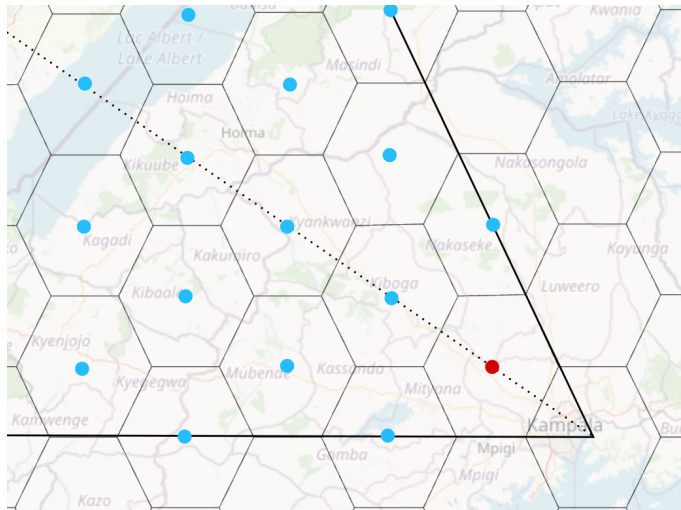
The central aim of this paper is to provide quantitative evidence on which roads should be enhanced or built. This requires accurate representations of the road network via graphs to simulate the effects of network investments. Most research creates these graphs in an ad-hoc fashion by either connecting adjacent cells in a gridded representation and parameterizing them by the connectivity along these links, or by choosing the largest roads and their intersections as nodes/edges of the graph. This section instead uses a routing engine (OSRM) to create graphs that optimally represent the road network as interpreted by the engine, implying that the optimal network graph produces road distance/travel time estimates that closely approximate those of the routing engine.

Section 4.1 demonstrates that it is possible to reduce the matrix of 144 million routes to a graph network with $\sim 12K$ nodes and $\sim 70K$ edges that reasonably approximates it. Computational constraints and tractability warrant a further reduction of the network to specific roads connecting important cities and ports. In Section 4.2, I thus also create a reduced (sparse) graph precisely representing the transport network. I then extend this graph with high-value new links connecting previously unconnected nodes (Section 4.3) and map out major transport routes (Section 4.4).

4.1 An Optimal Graph of Africa’s Entire Road Network

Previous research such as [Graff \(2024\)](#) has created a graph representation of Africa’s road network by dividing the continent into cells and computing routes connecting adjacent cells. However, cell centroids may not be of economic interest or well-connected at all. Using the full matrix of trans-African routes, I can empirically improve on this design by computing optimal edge weights that take routes to cells in the same direction as the neighboring cell into account.

Figure 11: Optimal Graph Representation of Africa’s Road Network



Notes: Figure shows 50.28km ISEA3H grid covering Uganda. In an optimal directed graph, the weight of the edge connecting Kampala to the red dot takes into account routes to all cells in this direction (red and blue dots).

Figure 11 illustrates this idea using Uganda as an example. Suppose I want to optimally weight the link from the center of Kampala to the cell with the red dot. I could simply take the road distance from the center of Kampala to the red dot, and then from the red dot to the next blue dot, etc., but then adding those distances may not well reflect routes from Kampala to blue dots. Thus, I let the direct OSRM routes to the blue dots also inform the weight attached to the link from Kampala to the red dot. Specifically, I calculate a directional route/time efficiency

$$\kappa_{ik}^m = \frac{\sum_j \delta_{ij}^m s_{ij}^{-\gamma}}{\sum_j s_{ij}^{-\gamma}} \quad \forall i, j, k \quad \text{where } \alpha_{ik,ij} < \alpha \quad \text{and } i \neq j, \quad m \in r, t \quad (5)$$

for all neighbouring cells i and k . γ is a parameter that governs spatial decay and α the (two-sided) angle up to which further points j (red dot k itself or blue dots in the direction of k) are considered.

Using spherical distances $a = i \rightarrow k$ (Kampala \rightarrow red dot), $b = i \rightarrow j$ (Kampala \rightarrow blue dot j), and $c = k \rightarrow j$ (red dot \rightarrow blue dot j) the angle $\alpha_{ik,ij}$ is calculated as

$$\alpha_{ik,ij} = \alpha_{a,b} = \arccos\left(\frac{a^2 + b^2 - c^2}{2ab}\right) \frac{180}{\pi} \quad (\text{Triangle Equation}). \quad (6)$$

The edge ik then receives a weight $\omega_{ik}^m = \kappa_{ik}^m s_{ik}$. I numerically determine α and γ using a quasi-newton algorithm by computing all shortest paths on the graph (Floyd-Warshall algorithm) and comparing it to the full 144 million road distances/travel times matrix generated by OSRM. To limit the influence of 'remote regions' on the optimal parameter choice, I exclude Madagascar and only use routes between cells where the OSRM start/end points lie within the cell.¹⁴

For travel time, this yields optimal values $\alpha^* = 29.88^\circ$ and $\gamma^* = 1$. The average shortest path takes $1.38\times$ longer than the actual route versus $2.26\times$ longer using a simple graph a la [Graff \(2024\)](#). Computing an inverse-squared distance weighted average of these ratios yields 0.93 for the optimized graph and 1.59 for the simple graph, implying that the former is slightly more efficient than the actual network at short distances to generate more realistic estimates on longer routes. When using simple inverse distance weights, the simple/optimized graphs are 2.08/1.25 times less efficient than the real network. [Wolfram \(2021\)](#) documents that road networks are more efficient on longer routes. Thus, to optimally represent a real network by a dense graph, the graph edges need to be slightly more efficient than reality.¹⁵ The optimal graph, which excludes Madagascar, has 11,582 nodes and 68,338 edges. Appendix Figure A8 plots it with duration edge weights.

4.2 An Optimal Graph of Africa's Transport Network

A sparse network graph is also needed to reduce computational complexity and increase interpretability. I construct it by sampling important cities and ports and letting OSRM compute routes between them, which I then process into an accurate graph. To sample cities, I use the updated (March 2024) world cities database from [simplemaps.com](#) sourced from the US National Geospatial Intelligence Agency.¹⁶ I derive, in multiple steps,¹⁷ the largest cities with a population of more than 100,000 within a radius of 70km in continental Africa.¹⁸ This yields 447 cities. I add populations of smaller cities within 30km of these cities to create agglomeration data. In addition, I use data on international ports compiled by the World Bank¹⁹ to select ports with a deployed capacity of more than 100,000 TEU in Q1 of 2020, which are 57 in Africa. From these, I take the largest within 100km, yielding 52 large ports at least 100km apart. I then match these ports to my 447 large cities within a 30km radius and am able to match 46. To the remaining 6 (among which Walvis Bay in Namibia), I add the population of cities/towns within a 40km radius (including Swakobsmund for Walvis Bay) to create more loosely defined 'port cities'. In total, I obtain $447 + 6 = 453$ important (port-)cities in continental Africa. Figures 12 and 14 plot them.

I then let OSRM compute precise routes between all 453 (port-)cities that are spherically less than 2000km apart. This yields 25,742 routes, shown on the LHS of Figure 12. To generate an undirected graph representation, I apply several algorithms²⁰ to intersect and segmentize the

¹⁴In particular, on this subset of 'well-defined routes,' I minimize a simple average of the ratios of the reconstructed route lengths/durations to the real ones, restricting $\gamma \in [1, 5]$ and $\alpha \in [1^\circ, 40^\circ]$.

¹⁵As a robustness exercise, I also minimize a weighted average across route-ratios with inverse squared spherical distance weights. This does not significantly alter the results, γ^* remains 1 and α^* increases slightly to 30.07° . Thus, this representation seems optimal for both medium and long routes.

¹⁶The Africapolis project (<https://africapolis.org/>) is more prevalent among researchers but does not provide precise city centroids, and the 2015 edition available at the time of writing is a bit dated.

¹⁷Concretely, I first find the largest cities within a 30km radius through an iterative algorithm that finds the largest city within 30km of each city, drops all non-selected cities, and repeats. I weight the population of cities with a higher administrative function by 5, such that national and administrative capitals are selected unless they are more than 5 times smaller than close cities. I repeat this process with an increased radius of 50km. Then, I add the populations of all cities within 30km of the selected (largest in 50km) cities to create urban agglomerations. I then remove agglomerations with a population below 100,000 and apply the algorithm one last time to find the largest agglomerations within 70km. In this last run, no additional weight is given to cities with higher administrative functions, i.e., only total population is used to select the largest urban agglomerations within 70km.

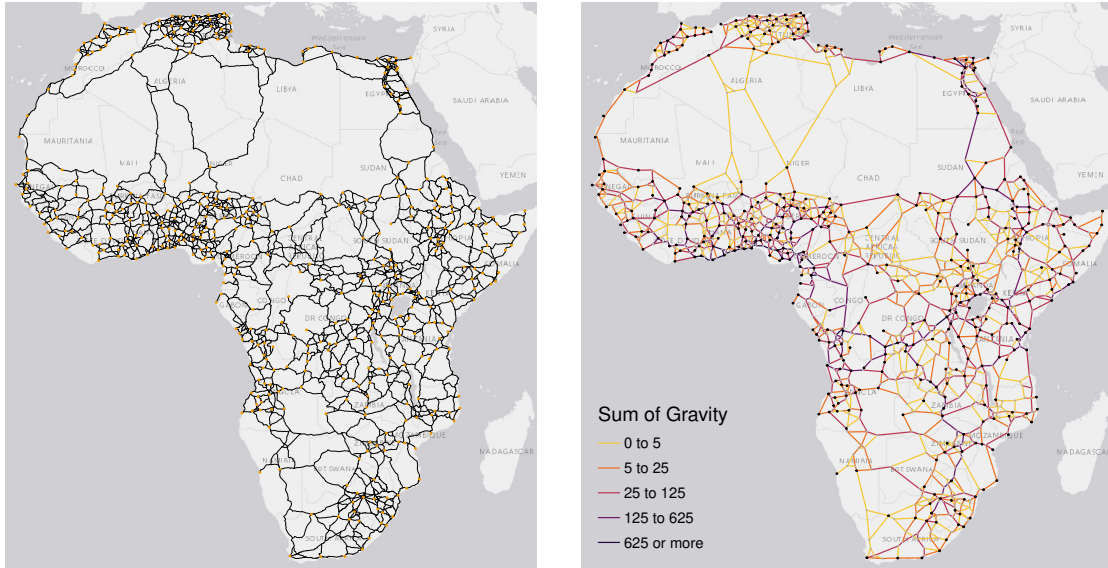
¹⁸I.e., excluding small island states, Madagascar, and also excluding cities not connected to the mainland via roads, such as Zanzibar City.

¹⁹<https://datacatalog.worldbank.org/search/dataset/0038118/Global—International-Ports>

²⁰Available in R packages *rmapshaper*, *stplanr*, *sfnetworks*, *tidygraph/igraph*, and *dbscan*.

routes, smooth them, and finally contract intersection points within 30km of each city/node.²¹ This yields a discretized network representation comprising 1,379 nodes and 2,344 edges - shown on the RHS of Figure 12. Appendix Figure A9 provides an overlay version of Figure 12, illustrating the accuracy of the network representation thus created.

Figure 12: Computing an Optimal Graph of Africa's Transport Network
25,742 Routes Connecting 453 (Port-)Cities



Notes: The LHS shows 25,742 fastest car routes connecting all 453 (port-)cities less than 2000km spherical distance apart. The RHS shows an undirected graph comprising 1,379 nodes and 2,344 edges generated from these intersecting routes.

The overall length of the transport network is 315,000km. The edges/links on the RHS of Figure 12 are colored by the appropriately scaled 'sum of gravity' across all 25,742 routes. Each route connects two cities i and j with populations P_i and P_j and road distance D_{ij} (in km) between them. Following Poot et al. (2016), migration flow can be modeled as

$$M_{ij} = G \frac{P_i^\alpha P_j^\beta}{D_{ij}^\gamma}. \quad (7)$$

In their New Zealand case study, the parameters α , β , and γ are all around 0.8-0.9. A famous early study by Zipf (1946) on US inter-city migration showed that $\alpha = \beta = \gamma = 1$ gives a good fit to the data. For simplicity, I adopt this specification and set $G = 1e-9$ to reduce the size of the estimates. The RHS of Figure 12 shows the sum of M_{ij} across all routes using the link. Darker edges are thus expected to receive higher traffic volumes. The highest volumes are expected in the Nile Delta and along the West African coastline. Due to the border closure between Algeria and Morocco since 1994, OSRM routes all car traffic between both countries through Western Sahara, yielding an unrealistic medium-sized gravity-implied flow along this link.

To parameterize the network, I add city populations within 30km of the $1379 - 453 = 926$ navigational nodes, yielding 530 or 57% of navigational nodes with populations. Figure 15 shows these as small dark nodes. In total, $453 + 530 = 983$ nodes, comprising 71.3% of the 1,379 nodes, are associated with cities. Compared to the initial network of 453 (port-)cities (large dark nodes), the population represented by this network increases by 14.7% to 444.2 million, which, according to the simplemaps world cities dataset, represents 86.3% of the African city population of 515 million.²² I also use OSRM to obtain road distance and travel time along each link, yielding edge weights representing the real road network. Figure 15 visualizes the corresponding segments.

²¹In the contraction step I first contract all nodes/intersections within 30km of the 453 cities and ports to the respective city/port centroid. I then cluster the remaining nodes with a 30km radius using density-based spatial clustering and contract these clusters to the most important node, which is the node used by the routes with the greatest 'gravity implied flows,' as further elaborated below.

²²The Africapolis 2015 estimate sums to 574 million across 9186 urban agglomerations, versus 4339 cities in the simplemaps dataset summing to 515 million. I use simplemaps because it is more up-to-date and precise.

4.3 Optimal Network Extensions

Africa's transport network is underdeveloped, and, with an average route efficiency of 0.68 vs. 0.84 for the US, far from ideal. To characterize optimal network investments on a sparse graph, including the possibility of new roads, I first need to find sensible new links and add them to the graph as potential (presently impassable) edges. I devise a network finding algorithm tailored to this task and establish its properties by letting it draw an ideal hypothetical transport network. I then apply it to the transport network graph to select high-value new links.

The algorithm begins with a complete graph where all nodes are connected and eliminates edges intercepted by other nodes which should be connected first. I illustrate it by letting it generate an ideal network between the 453 (port-)cities with a geodesic US route efficiency of ≥ 0.843 and a maximum 20° deviation from the direction of travel. Figure 13 helps explain the algorithm. It first computes the geodesic distance between some point A and another point B. Then, it computes the distance from A to all other points (cities), such as C, D, E, and F, and, using the triangle equation (Eq. 6), the angle α between AB and AC, AD, AE, and AF. It then drops points where the distance is greater than AB or $\alpha > 20^\circ$. For the remaining points (C and F), it computes the distance ACB and AFB, and compares ratios AB/ACB and AB/AFB to the US route efficiency measure of 0.843. If either C or F are found route-efficient, the algorithm concludes that there should be no direct AB link because these points should be connected via C or F. The same process is repeated taking point B as a vantage point, such that if the algorithm finds either AB or BA intercepted by other route-efficient points, this link is dropped from the undirected graph.

Figure 13: Network Finding Algorithm Illustration

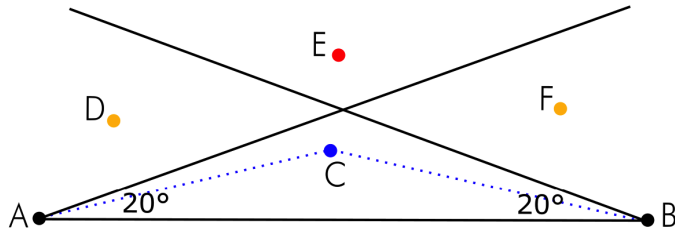


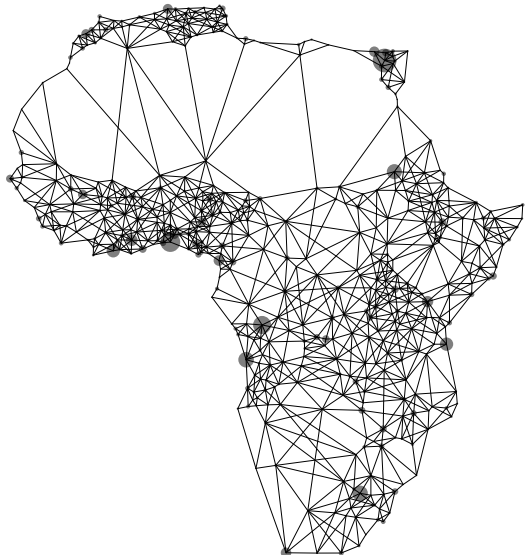
Figure 14 shows the thus generated US-grade hypothetical network connecting the 453 (port-)cities. It has 1459 edges, some of which intersect and should be broken up further.

Figure 14: Demonstration of Network Finding Algorithm

543 (Port-)City Sizes (Population)



US-Grade Hypothetical Network

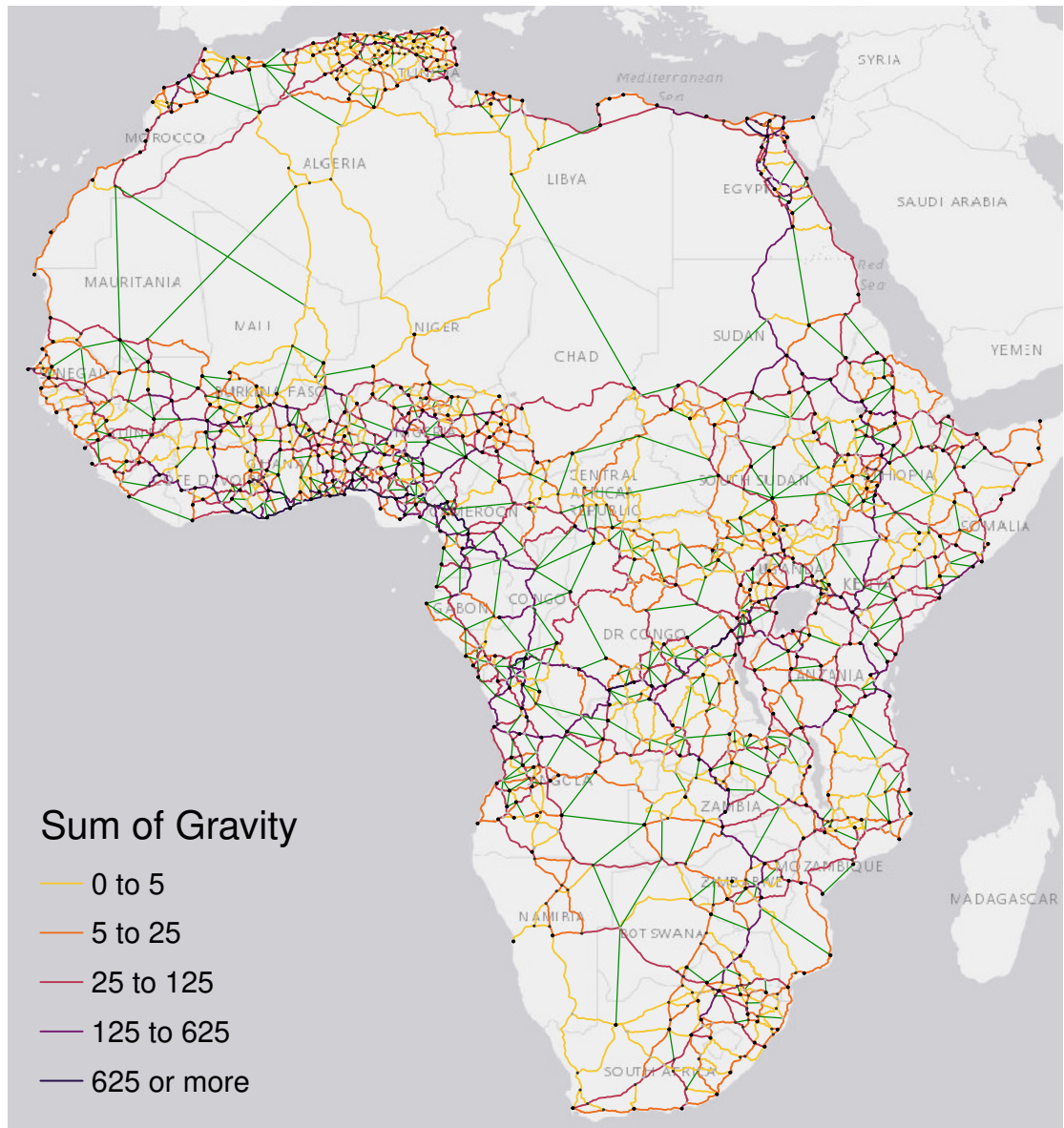


Notes: The LHS shows the 453 (port-)cities; circles reflect population. The RHS shows the result of applying the network finding algorithm described above, requiring US route efficiency of 0.834 ([Wolfram, 2021](#)) and a maximum 20° deviation.

To propose optimal network extensions, I apply the algorithm to a complete transport network graph where all 1379 nodes are fully connected. Using the US network efficiency and 20° angle criterion as illustrated above yields a staggering 2,031 new edges, shown in Appendix Figure A10. Since this is close to the number of existing edges, and many of the new links overlap, I adjust the parameters of the algorithm to generate fewer potential links. Concretely, I increase the maximum angle for intercepting nodes to $\alpha = 45^\circ$, and use the European route efficiency estimate of 0.767 by Wolfram (2021), which is lower than the US value of 0.843 partly due to Europe's more fragmented (water-bound) geography. In addition, I let OSRM compute a full road distance matrix between all 1,379 nodes and remove connections that already have a route efficiency of $2/3$ or higher. The 516 links retained by this modified algorithm, if straight, thus reduce travel distance by $\geq 50\%$.

I then verify whether these links can be constructed and remove 46 links significantly intercepted by waterbodies or protected areas. Some proposed links across the closed Morocco-Algeria border already exist. I keep them and reduce their construction costs in the network optimization process. Finally, I manually add 11 links that I consider important for improved transport flow. In total, I retain 481 new links. Figure 15 draws them as thin green lines. Exempting one crossing in northern Mali, where adding a node would add no value for routing purposes, and a similar case in central Kenya, these links don't intersect and thus imply no additional nodes to the graph.

Figure 15: Discretized and Calibrated African Transport Network incl. High-Value New Links



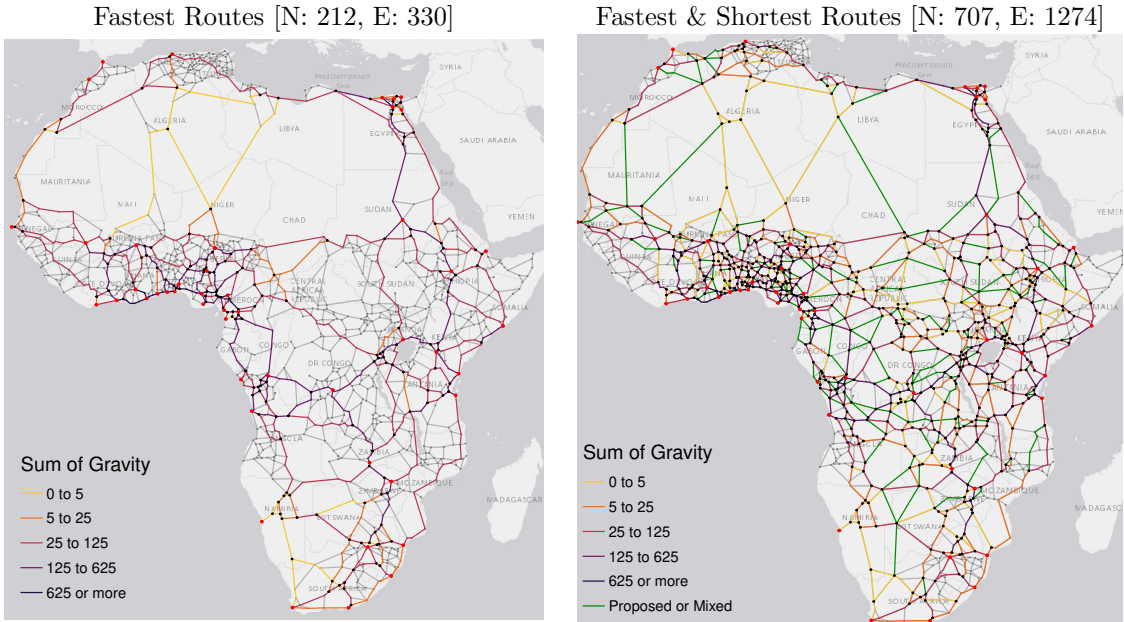
Notes: Figure shows optimal graph with 1,379 nodes and 2,344 edges (= links/road segments), including 481 feasible new links proposed by the network finding algorithm. The sum of gravity (Eq. 7) is calculated across all routes using a link.

In reality, roads constructed along these links will not be perfectly straight. I assume that new links have the same average route efficiency as existing links, which is 0.83.²³ Thus, I divide the spherical distance spanned by new links by 0.83 to estimate their road distance (edge weight), yielding 104,000km in total. In the remainder of this paper, I show simplified graphs with straight edges in all smaller plots to make them more legible. All computations, however, use edge weights corresponding to actual road distances and travel times, with existing network as in Figure 15.

4.4 Optimally Connecting Major Cities and Ports

Of particular interest to trans-African policymakers and traders are important transport routes connecting major (port-)cities across the continent. Affording special consideration to these, particularly through general equilibrium global optimization in Section 6, requires a further network reduction. To elicit these routes, I consider the subset of major agglomerations with >2 million inhabitants and ports with >1 million TEU in 2020Q1, yielding 47 major (port-)cities. I then use the parameterized network developed above to compute three sets of shortest paths between these (port-)cities: (1) fastest routes along the existing network, (2) shortest routes along the existing network, and (3) shortest routes including proposed links at route efficiency of 0.83. Figure 16 shows the outcome after (1) and the union of (1)-(3). In both cases, I contract the network, removing unnecessary intermediate nodes. Since the original graph optimally connects 453 (port-)cities, the reduced graph also optimally connects the 47 largest (port-)cities.

Figure 16: Optimally Connecting 47 Major (Port-)Cities



Notes: The LHS shows the fastest routes connecting 47 major (port-)cities with >2 million people or >1 million TEU in 2020Q1, yielding a reduced graph. The RHS shows an equivalent graph accommodating both fastest and shortest routes.

The reason for adding (2) and (3) to the network is to provide the GE planner of Section 6 with additional choices for roads to build or improve to enhance connectivity between major (port-)cities. As evident from the RHS of Figure 16, the planner has quite a few options to do that, the retained network has half the size of the full transport network.

Having thus created detailed graph representations of Africa's road network, I now examine counterfactual investments in the network and compare them in search of optimality. Section 5 characterizes MA-maximizing investments in partial equilibrium, including cost-benefit analysis, whereas Section 6 computes welfare-maximizing investments in spatial general equilibrium.

²³The route efficiency across individual links of 0.83 is larger than the overall network route efficiency of 0.68 because the latter considers full trans-African routes comprising multiple links.

5 Optimal Network Investments in Partial Equilibrium

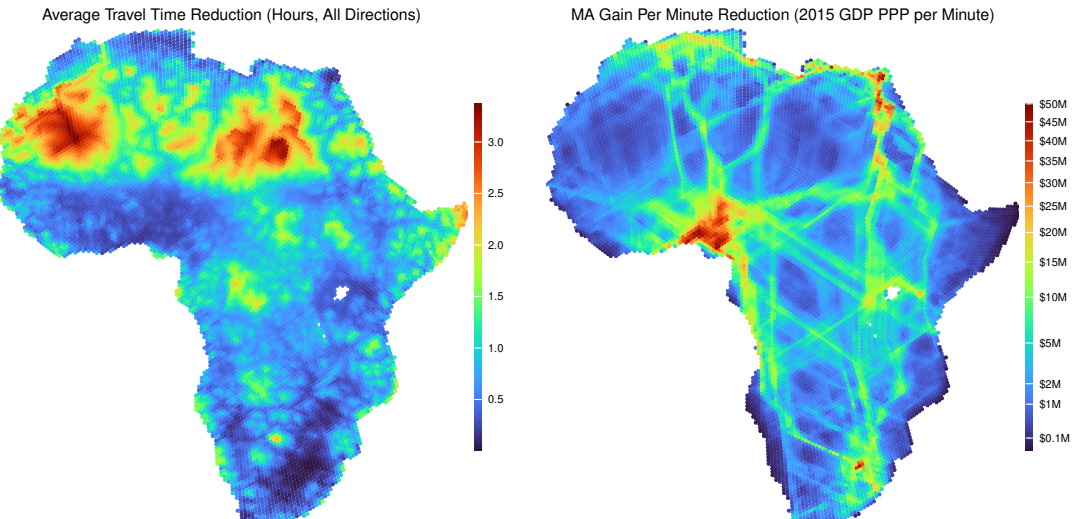
This section characterizes optimal road network investments in partial equilibrium (PE). PE estimates capture the effects of changes to the network on overall network efficiency and continental MA, keeping fixed the distribution of economic activity. Via shortest-path algorithms, PE estimates account for traders' reactions to such changes but ignore any resulting long-term shifts in activity. PE tools can also be used to compare investments in individual links or predefined investment packages. They cannot determine how a given infrastructure budget should be optimally spent on improving the network - a case considered in Section 6 characterizing optimal network investments in spatial general equilibrium (GE). This section, however, reaches important conclusions using much fewer assumptions than required for GE simulation and offers some insightful cost-benefit analyses. The PE objective of MA maximization is also fundamentally distinct from welfare maximization considered in GE. Both objectives and approaches thus produce complementary insights, and policymakers are advised to consider both rather than relying on a single approach, particularly since many difficult-to-estimate parameters are needed to produce GE results.

5.1 Local Road Network Investments

On the entire network graph (Section 4.1 and Figure A8), I simulate MA gains from small (local) road investments by enhancing the network around each node, one node at a time, and computing continental MA gains resulting from that. In the duration weighted graph, I adjust the travel time on all links such that $\min(\kappa_{ik}^t) = 50\text{km/h}$, implying $t'_{ik} = \min(t_{ik}, s_{ik}/50\text{km/h})$ for all k bordering i . 50km/h is a sensible upper bound for time efficiency as 99% of links are slower. [Wolfram \(2021\)](#) also finds very few US routes with time efficiency greater than 50km/h.

The LHS of Figure 17 shows average travel time reductions from these local investments. It ranges between 0 and 3.5 hours, which is sensible as links are 50.3km long, and a minimum travel speed of 10km/h was assumed. The LHS is thus a local time efficiency improvement potential map and summarizes the underlying graph. The RHS shows the MA gain from each local improvement divided by the investment, i.e., by the LHS. Each data point combines MA gains measured across all 11582² routes; thus, it required 11582³ shortest paths, about 1.6 trillion, to produce the plot. It indicates that MA gains per minute reduction are highest in large city centers, ranging up to 50 million USD'15. Large MA gains from local travel time reductions are evident all across Nigeria, the Nile Delta down to Khartoum, and greater Johannesburg. More interestingly, marginal MA gains are also high when connectivity between the major agglomerations like Cairo, Nigeria, the Great Lakes region, and Johannesburg is improved. The bright lines map out areas where the existing road network is already somewhat dense. Thus, the map suggests transport corridors in a purely data-driven way (although marginal PE gains cannot support large-scale investments).

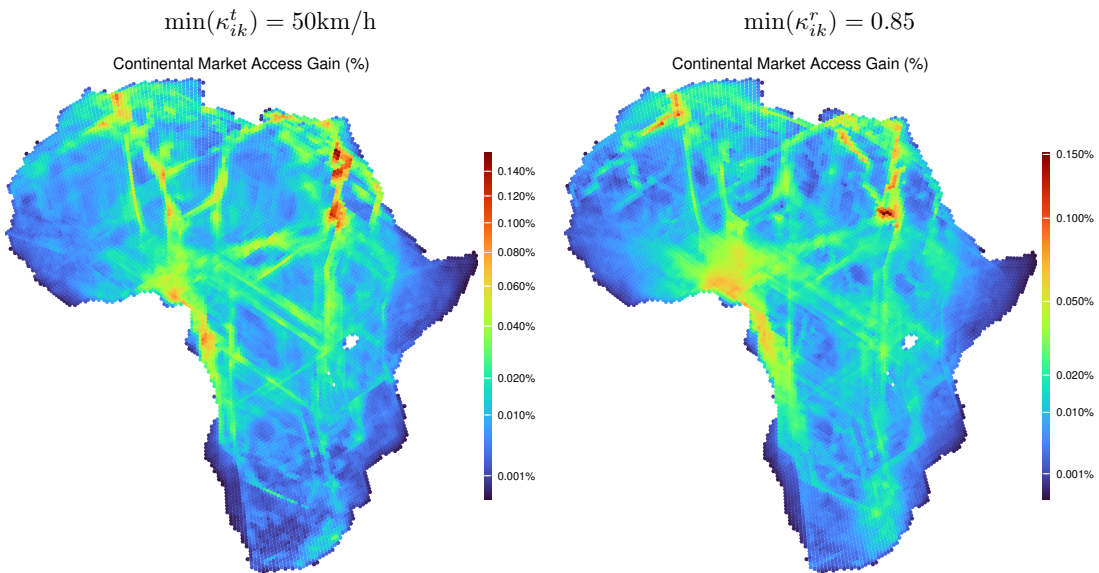
Figure 17: Local Travel Time Reduction: $\min(\kappa_{ik}^t) = 50\text{km/h}$



Notes: The LHS shows the average travel time reduction across links connecting to a node from increasing their time efficiency (Eq. 2) to $\geq 50\text{km/h}$. The RHS shows the resulting marginal MA gain measured (summed) across all trips.

A caveat is that the map does not consider MA through ports, which will only be considered in GE with several goods. Appendix Figure A11 shows the graph computed for a local road distance reduction, imposing $\min(\kappa_{ik}^r) = 0.85$. It is similar but slightly more diffuse, reflecting greater local variation in route efficiency. Further insights can be gained refraining from division by the investment and just plotting the total MA gains from heterogeneous investments in Figure 18. This map shows, for both route and time efficiency, that the largest local MA gains can be reaped by improving connectivity along the corridor between Kinshasa and Lagos, around Khartoum and upwards in the Nile Delta, and by reopening the border between Morocco and Algeria, which is closed since 1994. Simulations were also done with border frictions but did not yield interesting results at this fine local scale. Frictions do however have significant effects on marginal investments in the sparse transport network graph which I now turn to.

Figure 18: Total MA Gain from Heterogeneous Local Investments



Notes: Figure shows total MA gains measured (summed) across all trips from increasing local time efficiency to $\geq 50\text{km/h}$ (LHS) and local route efficiency to ≥ 0.85 (RHS). All links/edges connecting to a node are improved.

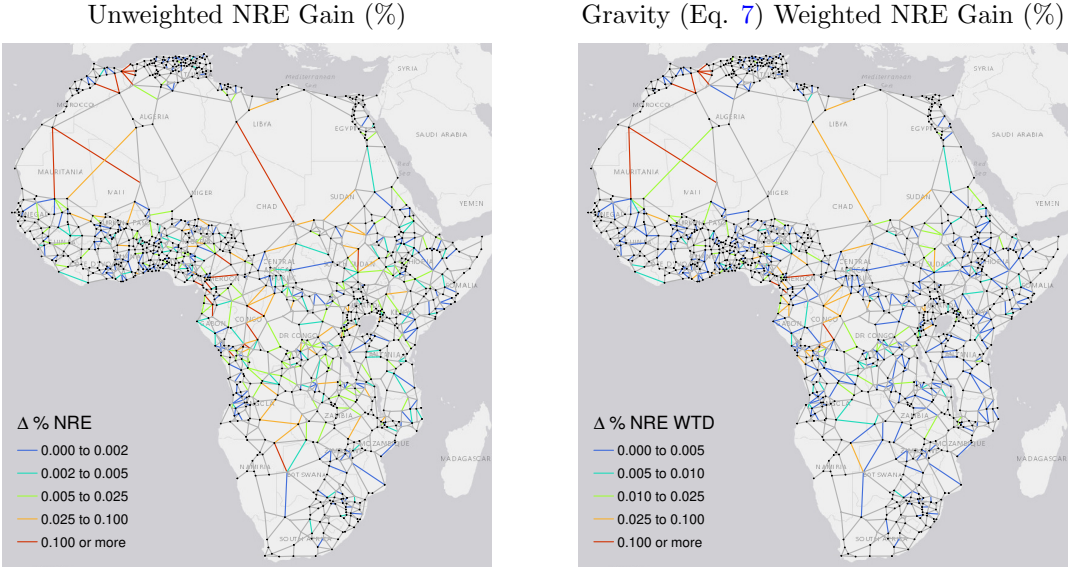
5.2 Investments in New Links

Considering the full transport network, I begin with a set of transport-oriented simulations to gauge the value of adding the 481 proposed links. Computing the route efficiency across all routes with and without the new links yields a 7.1% increase in average direct RE, from 0.68 to 0.72. When weighting routes by gravity (Eq. 7 but with the spherical distance), RE increases by 5% from 0.73 to 0.76, suggesting that travel between populated areas is more efficient (ignoring congestion).

By virtue of the smaller network size, I can also run these computations on a link-by-link basis by adding a link to the network, recomputing all shortest paths, and then computing the percentage change to the existing RE. Figure 19 shows the outcome of this process both with and without gravity weights. The results are similar regardless of weighting. The most valuable links with an impact of more than 0.1% on overall RE (up to a maximum of 0.8%) reconnect Morocco to Algeria, followed by improved trans-Saharan connections through Mauritania, Mali, and Chad. Also vital are additional links connecting southern Africa (Johannesburg) to western Africa and new links in (South-)Sudan facilitating north-south and east-west connections.

I also examine MA gains from the proposed links by computing the GDP per capita of each city as the inverse-distance weighted average of observations within 30km using data from Kummu et al. (2018) and multiplying it by city (agglomeration) population. I then calculate MA for all cities using the network and Eq. 4, and sum them to measure total MA. Setting $\theta = 1$, the total MA implied by this transport network is 1.42 billion USD/m in 2015 PPP terms, short \$1.42B/m, or around \$1M/m in the average node. With high trade elasticity ($\theta = 3.8$), total MA is below $\$1/m^{3.8}$. The MA gain from adding all proposed links is 5.5% if $\theta = 1$ and 1.9% if $\theta = 3.8$.

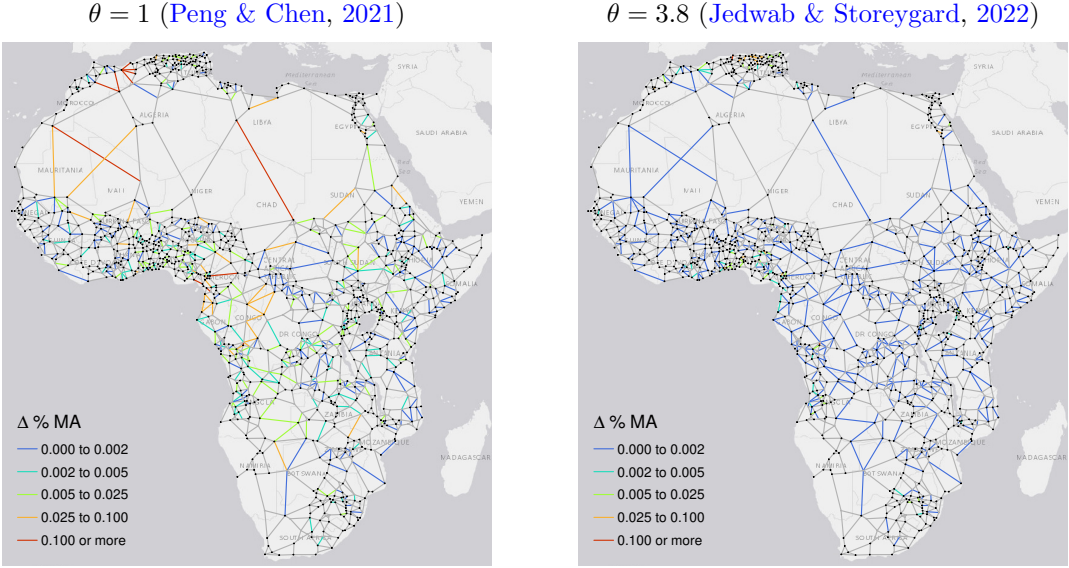
Figure 19: Percentage Gain in Network RE from Constructing Each Proposed Link



Notes: Figure shows (weighted) average route efficiency (RE) gains across all trips from building a specific link/edge.

The MA gains from adding individual links, reported in Figure 20, are similar to the route efficiency gains if $\theta = 1$. With high trade elasticity ($\theta = 3.8$), only links near agglomerations yield high returns. For the remainder of this section, I set $\theta = 1$ to limit the complexity of exposition and facilitate the interpretation of results. There are also substantive reasons for adopting this value.²⁴

Figure 20: Percentage Gain in Market Access (GDP) from Constructing Each Proposed Link



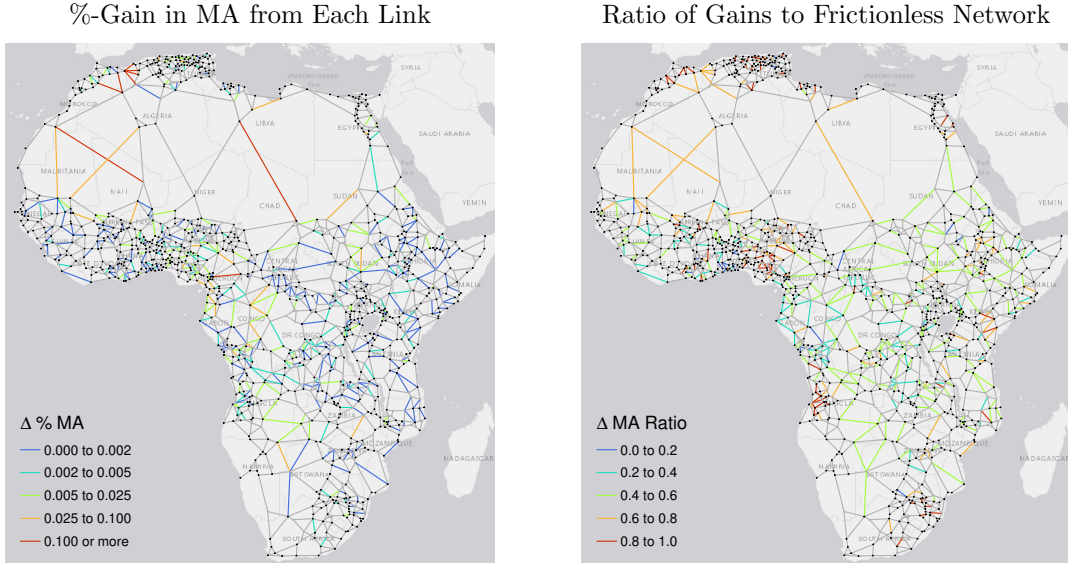
Notes: Figure shows total road-distance denominated MA gains measured (summed) across all trips from building a link.

To investigate how the presently high trade costs between borders may impact returns to link building, I add the respective export/import documentary and border compliance costs of the start and end country to each route - divided by 1.6 to turn them into kilometers following Table 4 - and also add a transit cost of $(48h \times 4\$)/1.6 = 120\text{km}$ for routes spanning any third country.

²⁴Using the Bayesian Information Criterion (BIC), Peng & Chen (2021) show that $\theta < 3$ yields decent models predicting various outcomes (incl. built-up and nightlights) by the log of MA, choosing $\theta = 1$ as their preferred value. This value is also more consistent with the evidence on inter-city migration (Poot et al., 2016; Zipf, 1946). Once considering road upgrades in Section 5.5, I find that MA gains under $\theta = 3.8$ are significantly higher than under $\theta = 1$ because upgrades also increase travel speeds at short distances in populated areas. In contrast, new links primarily improve connectivity through remote regions. Since total MA gains from road upgrades are much larger vis-a-vis new roads, setting $\theta = 1$ yields a lower bound on total MA gains from road network improvements.

Consequently, the total MA implied by the network decreases from $\$1.42B/m$ to $\$1.08B/m$, and the total gain from building all proposed links reduces to 3.9%, versus 5.5% without frictions. Thus, border frictions reduce the aggregate returns to building new roads. They also imply relatively greater gains from building domestic links. The LHS of Figure 21 shows MA gains under frictions, and the RHS the ratio of the gains with frictions to the frictionless gains (LHS of Figure 20).

Figure 21: Percentage Gains in Market Access (GDP) under Border Frictions



Notes: Figure shows absolute and relative distance-denominated MA gains from building a link under trip-level frictions.

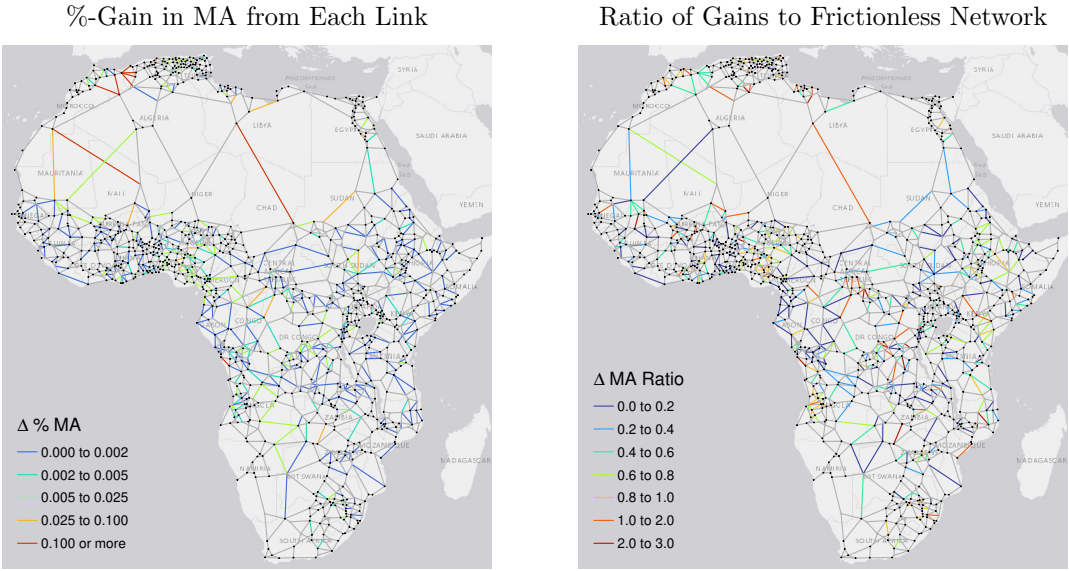
Ostensibly, frictions always reduce the gains from building links but mainly affect transnational links and links in remote areas (which are also more likely to cater to transnational traffic). New national links in populated areas (in red) yield almost the same MA gains compared to a frictionless environment. The median ratio is 0.52, implying a 48% lower return on the median link. Nevertheless, the LHS of Figure 21 suggests that certain trans-national links, especially additional trans-Saharan connections, bring the greatest MA gains even under high frictions. Thus border frictions considerably reduce the value of trans-national links and links in remote areas but do not appear capable of dramatically altering the overall distribution of returns.

However, this conclusion is tentative as it only measures border frictions at the origin and destination country border (+ lump-sum 24h transit frictions), giving traders no incentive to deviate from the frictionless route. In reality, traveling through many countries may be significantly more costly, and traders are reasonably assumed to optimize their route. To approximate this case, I ignore transit costs and add each border's average export and import cost (in km) to the respective border-crossing link. This parameterization thus conflates exporting, importing, and transit but introduces cumulative frictions prompting traders to avoid expensive borders.

Computing all shortest paths along this network has a substantial impact on trade costs. Whereas under the previous assumption routes are on average 32% more expensive than in a frictionless scenario, building these costs into the network makes them 117% more expensive, despite optimizing behavior. Total MA is reduced to $\$0.91B/m$, versus $\$1.08B/m$ under the simple transit scenario. Yet, building all proposed links in this network still increases total MA by 4%.

Figure 22 visualizes the corresponding MA gains from building each link and the ratio of MA gains to frictionless gains. Similar to Figure 21, under frictions, most gains are lower, especially from border-crossing links. The median ratio is 0.43, implying a 57% reduction in value. The RHS of Figure 22 shows that, with optimizing agents, the ratio of MA gains to the frictionless network is not bounded above by 1. Some links, colored in dark orange/red, yield greater MA gains with border frictions than without. Thus, if traders are optimizing, border frictions not only reduce average gains but also complicate the evaluation of road network investments.

Figure 22: Gains in Market Access (GDP) with Optimizing Agents



Notes: Figure shows absolute and relative distance-denominated MA gains from building a link under link-level frictions.

5.3 Road Building Costs

A central consideration for any infrastructure project is its cost-benefit ratio. In this subsection, I thus factor in heterogeneous link-building costs. The most well-known empirical work on road construction costs in developing countries is Collier et al. (2016), who analyze unit costs from 3,322 activities across 99 countries obtained from the World Bank's Road Costs Knowledge System (ROCKS) database. They find that the cost of an asphalt overlay of 40-59mm can vary by a factor of 3-4 between countries. Regressing this cost on various geographic and non-geographic factors, they find that terrain ruggedness and population density increase unit costs, whereas long roads ($>50\text{km}$) decrease it. Furthermore, conflict, corruption, the business environment, and the origin of construction firms affects unit costs. ROCKS version 2.3 used by Collier et al. (2016) runs up to 2008. In 2018, the World Bank's transport unit released an update including only projects with complete information (Bosio et al., 2018). Unfortunately, most projects in this database are road upgrades, but a few new road projects are included as well and summarized in Table 5.

Table 5: Road Building Costs: Road Costs Knowledge System (ROCKS) - 2018 Update

Work Type	N	Length (km)	Cost (M\$'15)	Cost/km
<i>Continental Africa</i>				
New 1L Road	1	99.0	21.15	0.214
New 2L Highway	4	122.0	59.53	0.611
<i>All Low and Lower-Middle Income Countries</i>				
New 1L Road	6	59.5	7.65	0.135
New 2L Highway	6	84.5	44.09	0.611
New 4L Expressway	1	84.8	328.08	3.869
<i>All Countries</i>				
New 2L Highway	7	50.0	43.03	0.682
New 4L Expressway	24	74.9	213.01	5.152

Notes: Statistics are aggregated across projects using the median. Costs are in millions of 2015 USD. The raw costs in current USD were deflated at their project end date using the US GDP deflator with base year 2015.

According to the final column of Table 5, which provides median costs per km in millions of constant 2015 USD, the median new African road in the 2-lane highway category (implying one lane in each direction) costs \$611K/km. This estimate, though derived from only four projects, is consistent with other estimates: a 2014 report by the African Development Bank (African

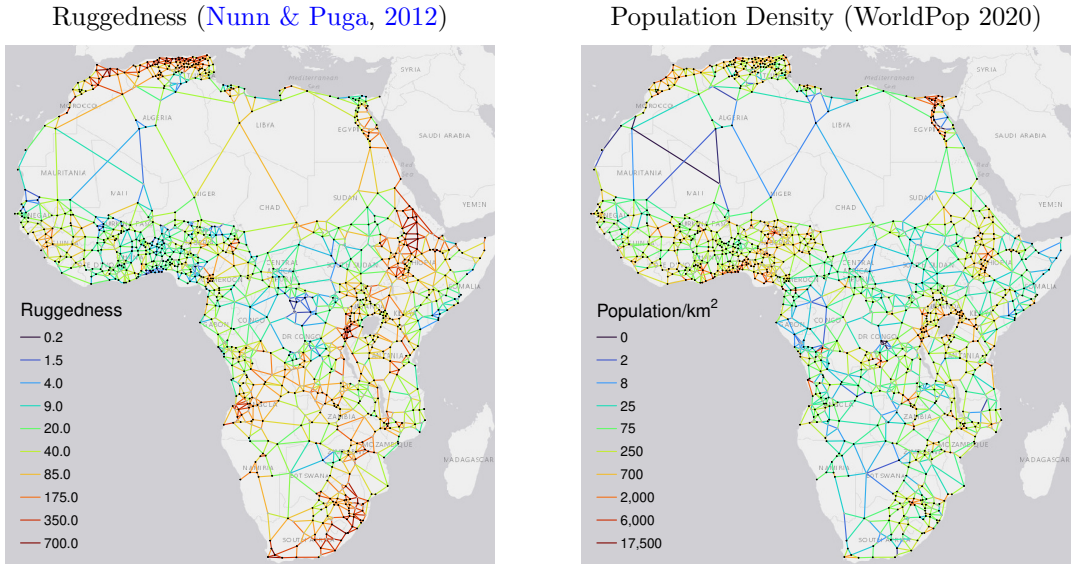
(Development Bank, 2014) analyzes 172 Projects contracted between 2000 and 2008 and reports a median cost of 227,800 2006 USD per lane-km. This figure includes road upgrades. Multiplying by 2 for a 2-lane highway and inflating by 16% to 2015 USD yields 528,800 USD per lane-km.

Following Collier et al. (2016), I allow for heterogeneity in road construction costs. Since it is difficult to measure (ever-changing) political conditions across the continent, I follow Fajgelbaum & Schaal (2020) and Graff (2024) and only consider average returns to ruggedness and distance, as well as population. My preferred specification is

$$\ln\left(\frac{\text{cost}}{\text{km}}\right) = \ln(120,000) - 0.11 \times (\text{dist} > 50\text{km}) + 0.12 \times \ln(\text{rugg}) + 0.085 \times \ln\left(\frac{\text{pop}}{\text{km}^2} + 1\right). \quad (8)$$

The first part is taken from Eq. (21) of Fajgelbaum & Schaal (2020). The 120,000 USD/km constant makes the mean cost/km across all existing links approximately equal to \$611K/km. The population coefficient is averaged across Tables 4 and 5 of Collier et al. (2016), following Fajgelbaum & Schaal (2020), which obtain the other coefficient in this way. The tables suggest that Collier et al. (2016) regressed the log of cost on the population density (in 100 people/km²), but applying the coefficient to the levels density yields peak construction costs above \$10M/km near large cities, which I regard as unrealistic. Thus, I use the natural log of the population density and add 1 to avoid negative values in remote regions. This effectively reduces the relevance of this term and remains close to Fajgelbaum & Schaal (2020). I extract ruggedness from the original 30 arc-second layer by Nunn & Puga (2012) within a 3km buffer around existing and proposed links, and do the same for population from the WorldPop 2020 population layer at 1km resolution.²⁵ Figure 23 shows ruggedness and population density thus estimated for each link.

Figure 23: Ruggedness and Population Density within 3km Buffer around Links



Notes: Figure shows average ruggedness and total population within a 3km (two-sided) buffer around (straight) links.

Appendix Figure A12 shows the corresponding cost estimates from applying Eq. 8.²⁶ I divide the cost of building Algeria-Morocco links by 3 as these are, to a large extent, already constructed. The distribution of costs is roughly consistent with African Development Bank (2014), whose 1st and 3rd quartile estimates, appropriately converted, are 386,000 and 987,500 USD'15/km. Reconstructing the total existing network comprising 315K km of roads is estimated to cost \$186B USD'15, and the proposed extension of 104K km costs \$56B. Figure A12 suggests that roads in unpopulated and relatively flat areas such as Congo and the Sahara are cheapest. This may be erroneous since both exhibit rather extreme weather conditions and human security risks. Collier et al. (2016) unfortunately don't consider temperature, humidity, and landcover variables. More research is thus needed to refine estimates of road construction costs in developing countries.

²⁵It is possible to track the terrain around existing roads more closely, but being more realistic with existing links complicates comparison with potential new links. Thus, I opt for a simpler approach of considering terrain within a broad 3km buffer in the direction of travel for both existing and potential new links.

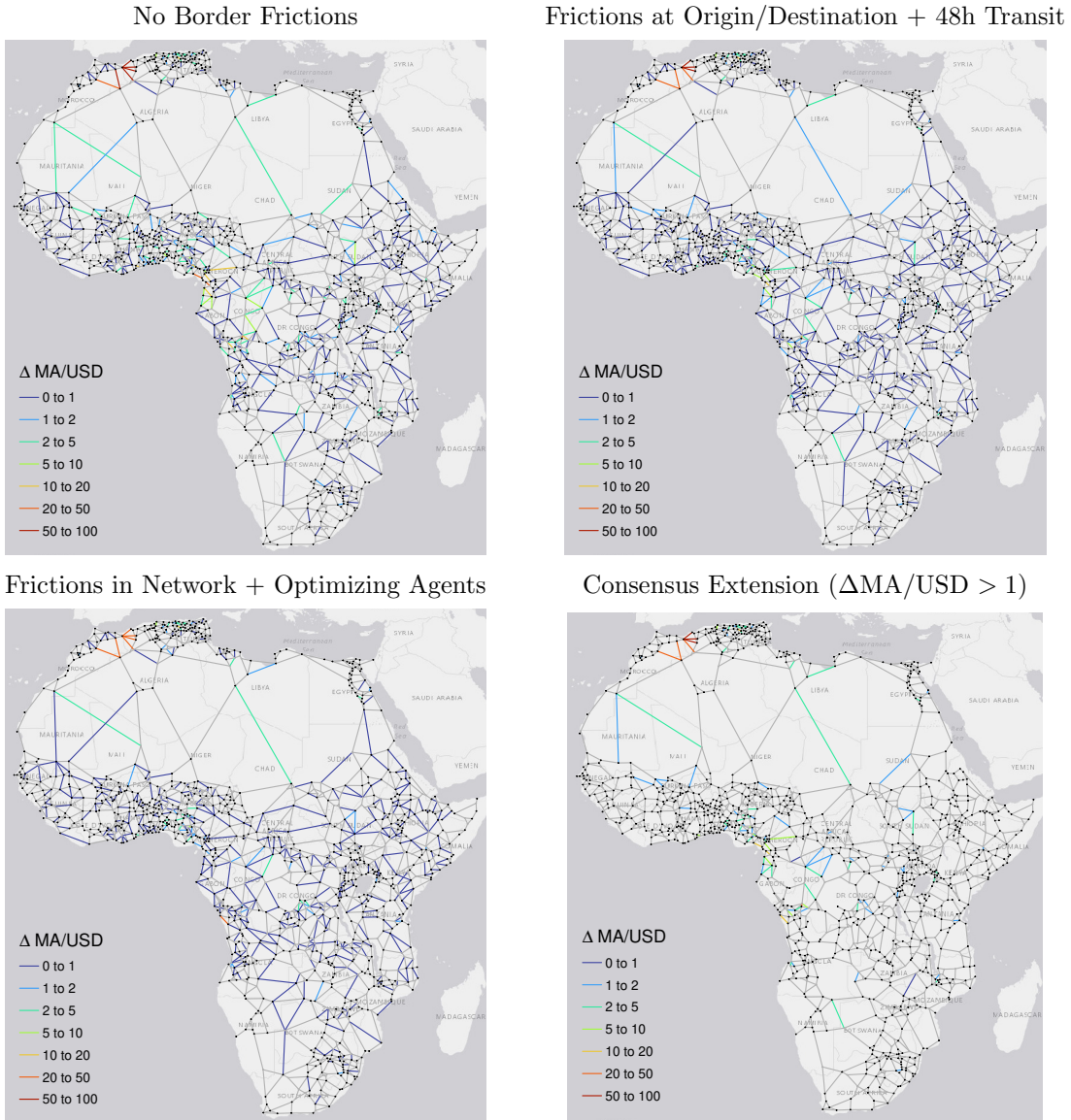
²⁶Figure 31 provides the same information, including upgrading costs. I thus relegate Figure A12 to the Appendix.

5.4 Cost-Benefit Analysis: Building New Links

Comparing the proposed extensions at cost of \$56B to the total MA gain of 5.5% of \$1.42B/m, amounting to \$77.6M/m or \$77.6B/km, yields a MA return of \$1.4/km per USD invested, in short, \$1.4/km/\$. If border frictions are added, the MA gain from the network extensions is only 3.9% or \$41B/km, implying a return of \$0.76/km/\$. If frictions are built into the network and agents optimize, the MA gain is 4% or \$36.4B/km, implying a return of \$0.65/km/\$. Either way, current frictions reduce the gains from the proposed investment package by around 50%.

Since the total MA gains are below \$1/km/\$ under frictions, a limited investment package focusing on critical links is more sensible. Figure 24 shows the gain in \$/km/\$ of different links under the three assumptions about border frictions, and a consensus extension including only links above \$1/km/\$ in the frictionless case and at least one of the two scenarios with frictions.

Figure 24: Cost-Benefit Analysis (USD/km MA Gain per USD Invested)



Notes: Figure shows MA returns in USD/km per USD invested in link building under different types of border frictions.

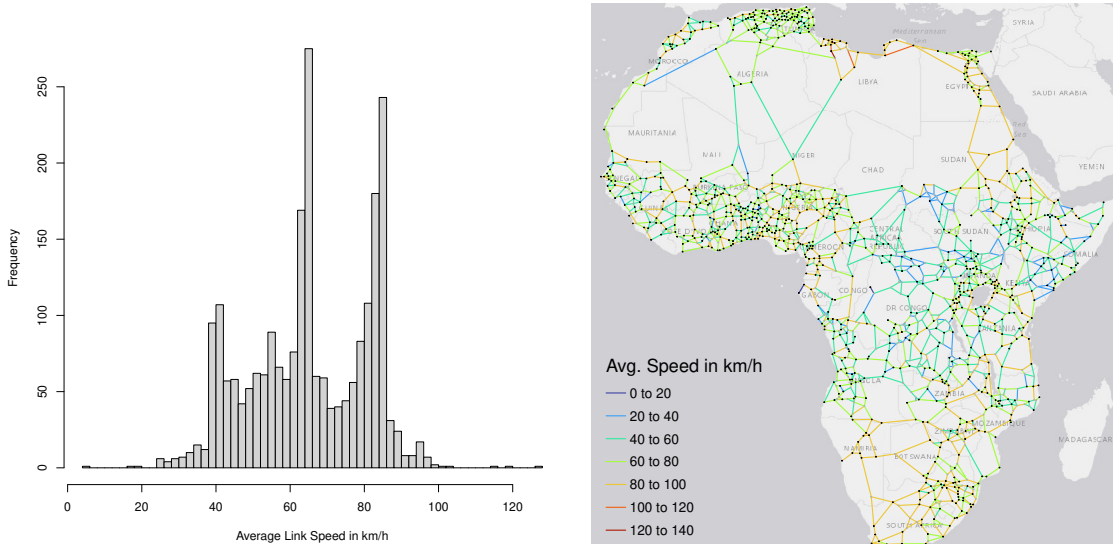
Figure 24 indicates that, even without frictions, 66.5% of the proposed links yield a MA return of <\$1/km/\$, and only 19.5% of links yield MA returns >\$2/km/\$. Some links, especially in West Africa (Cameroon) and Congo (Kinshasa), yield up to \$20/km/\$ returns. Reopening the Morocco-Algeria border would yield even higher returns on any border-crossing link. The consensus extension combining at least break-even links in MA terms includes 105 links (21.8% of the proposed

481). This package's estimated cost is \$12.1B. In the frictionless scenario, it yields a 4% MA gain amounting to \$57.5B/km, implying a return of \$4.75/km/.²⁷ Excluding the 6 links bridging the Morocco-Algeria border still yields a 2.9% MA gain of \$41.8B/km or \$3.45/km/. Under the most restrictive cumulative frictions scenario, the MA gain (excl. Morocco-Algeria links) drops to \$22B/km (2.4%) or \$1.82/km/. Thus, this package, which includes 4 additional trans-Saharan links, is only sensible if MA gains generate high economic gains (more in Section 5.9).

5.5 Upgrading of Existing Links

Since constructing new roads is expensive and the quality of African roads is low in many regions, upgrading the existing network is another vital policy option. While routing engines cannot perfectly consider road quality, OSM has an elaborate tagging system to indicate the surface and smoothness of roads, which is taken into account in OSRM routing and travel time estimates. Figure 25 shows the average travel speed in km/h along each link, indicating sizeable heterogeneity. The distribution of travel speeds is trimodal, with slow links around 40km/h, medium links around 65 km/h, and fast links around 85km/h. The three fastest links at travel speeds around 120km/h are in Libya, which satellite imagery reveals are newly asphalted straight roads through flat desert. The slowest link at a travel speed of 5km/h is in Gabon and connects the coastal cities of Libreville and Port-Gentil via a ferry (in absence of a viable road). Apart from these extremes, most links in populated areas have travel speeds ≥ 60 km/h. Slower links with travel speeds < 60 km/h, or even < 40 km/h, are prevalent in central Africa (Congo, Central African Republic, Chad, (South-)Sudan) and around the Horn of Africa (Northern Kenya, Somalia, South-Sudan, peripheral Ethiopia). The three trans-Saharan links connecting Algeria and Libya to Mali and Niger also have average travel speeds around 50km/h. Thus, Figure 25 (and Appendix Figure A1) suggests that mainly roads connecting the different populated macro-regions in Africa need upgrading.

Figure 25: Average Link Speeds in Africa's Transport Network



Notes: Figure shows average link speeds calculated at the link-level using the OSRM R API (accessed June 2024).

The MA measure implied by the current network speed is \$1.75T/min. Letting all links have a speed of ≥ 100 km/h yields a MA of \$2.48T/m, a 42.1% increase.²⁸ This is dramatically higher than the 5.5% gain from adding all proposed links (disregarding speed). To determine whether this discrepancy is an artefact of the way of denominating MA, I also compute MA gains from the proposed links, assuming average speeds of either 100km/h or 65km/h, the median link speed in the existing network. Adding all new links at 65km/h yields a 5.7% MA gain - comparable to the 5.5% measured earlier - whereas assuming a speed of 100km/h yields a 14.1% increase. This highlights the importance of road quality considerations. Since new roads are typically high quality, the 100km/h assumption and associated 14.1% MA gain without border frictions may be

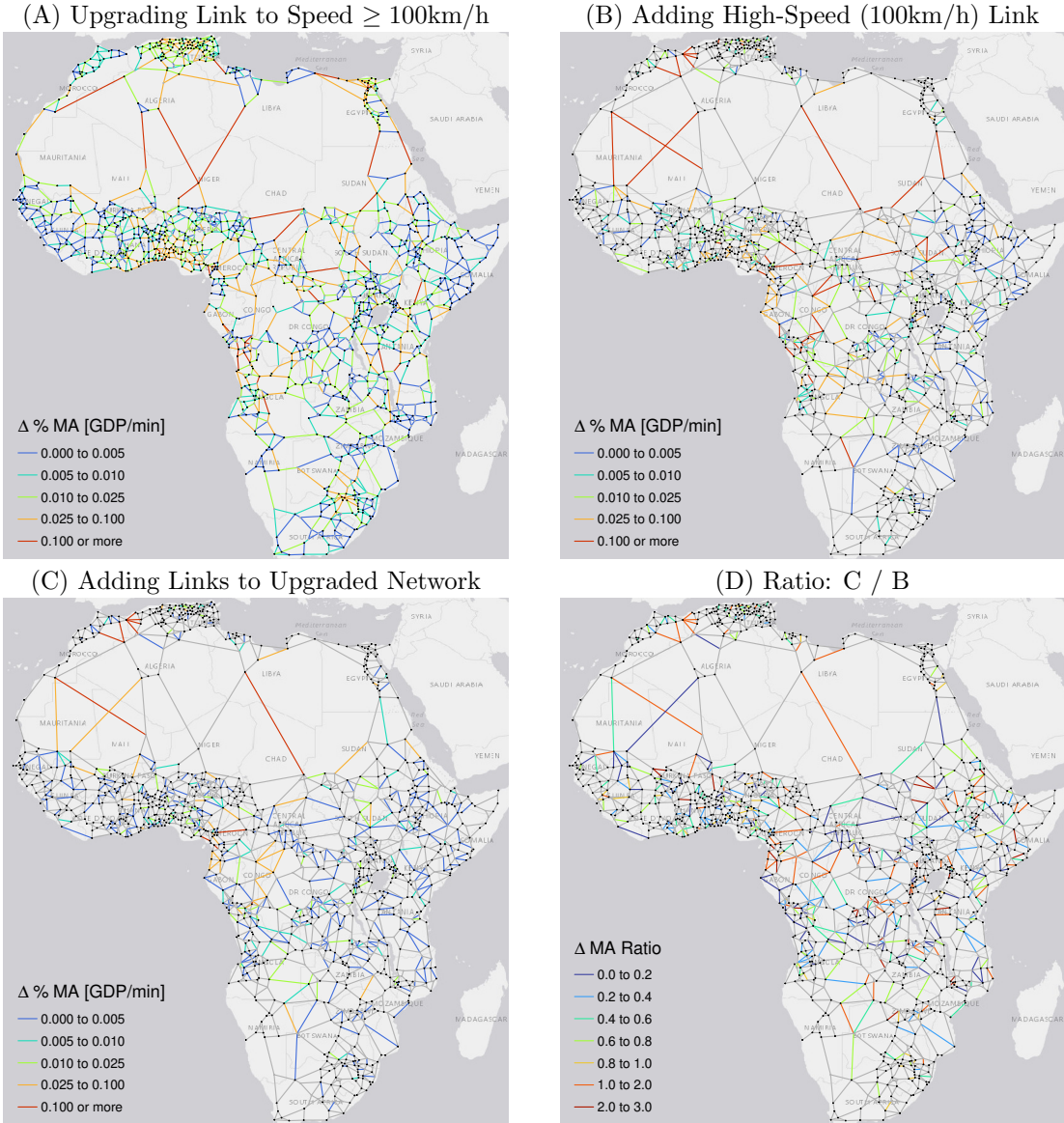
²⁷These returns are based on recalculating shortest paths and MA after adding all 105 links.

²⁸The Histogram in Figure 25 suggests 100km/h as a natural efficiency target for transport roads. This target is also sensible as different maximum speed regulations may exist beyond it.

more realistic. In total, eliminating all frictions, upgrading all existing links to $\geq 100\text{km/h}$, and adding the proposed links at 100km/h , would increase MA to $\$2.62\text{T/min}$, a 50% improvement. This affirms that the largest gains (42%) can be reaped from improving existing roads. Gains from new roads are higher without improvements to existing roads due to optimizing behavior.

All of these scenarios can be simulated on a link-by-link basis. Figure 26 reports three scenarios that are policy relevant: upgrading existing links to $\geq 100\text{km/h}$, building new links at 100km/h with the existing network unchanged, and building new links at 100km/h on an upgraded network. The final panel shows a ratio indicating the relative MA gains under the latter two scenarios.

Figure 26: MA Gains (GDP/min) from Upgrading Links and Adding High-Speed Links



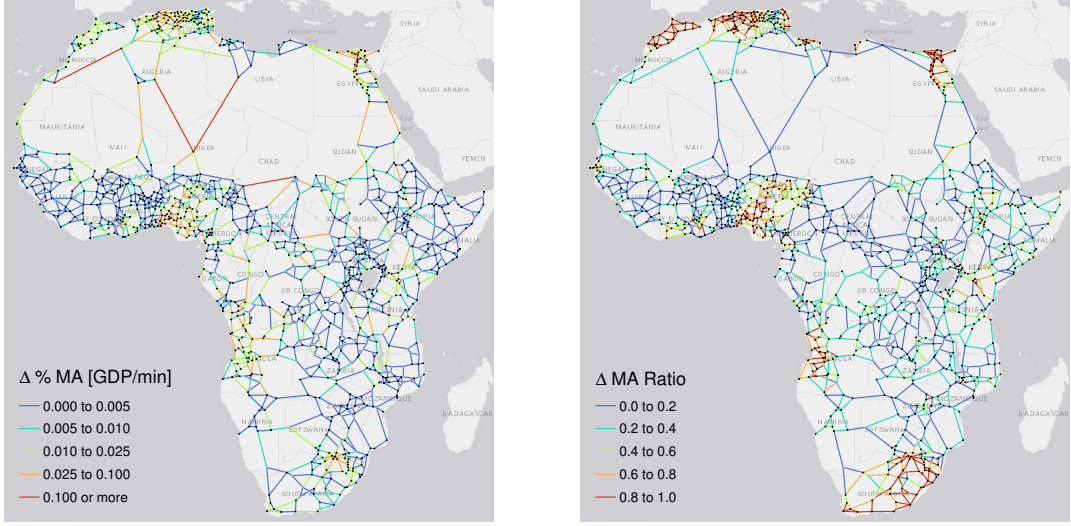
Notes: Figure shows total MA gains from upgrading a link and building a new link before/after upgrading all links.

Panel A signifies that improving major north-south/east-west roads and roads in metropolitan areas yields significant MA gains. Panels B and C are congruent to previous results that new high-speed north-south/east-west roads are most impactful, with lower average gains under the upgraded network. Panel D signifies that, whereas most links yield smaller returns under an upgraded network (ratio < 1), some links, including re-opening the Morocco-Algeria border and the two proposed north-west south-east oriented trans-Saharan connections, yield higher returns if the existing network is fully upgraded. Notably, these are also particularly high-value links from a pure route efficiency standpoint and included in the consensus extension of Figure 24.

Another major area of necessary improvement is border frictions. Applying current frictions, i.e., dividing border time by 4 and documentary time by 10 (Table 4) and adding a 48h transit through 3rd countries, yields a MA of \$982B/min, which is only 56.1% of the \$1.75T/min without frictions. When improving all links to a speed of $\geq 100\text{km/h}$, total MA increases to \$1.24T/min, which is 50% of the \$2.48T/min without frictions and only 27% more than the \$982B/min under the current network, compared to a 42% increase without frictions. Figure 27 reports link-level gains and a comparison to frictionless gains (Panel A of Figure 26). The results are unequivocal: border frictions particularly diminish MA gains from upgrading remote and transnational links.

Figure 27: Percentage Gains in Market Access (GDP/min) under Border Frictions

%-Gain in MA from Improving Link Ratio of Gains to Frictionless Network

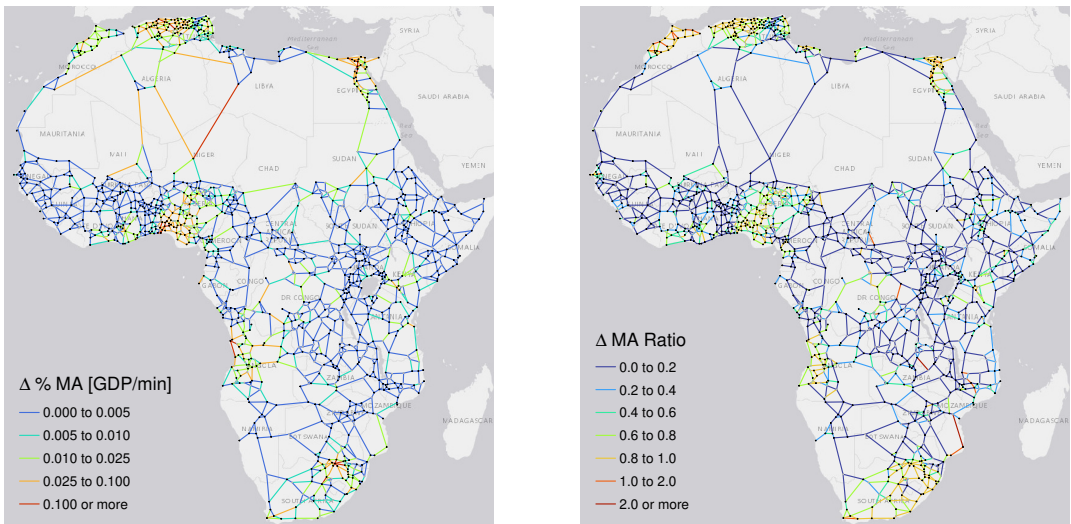


Notes: Figure shows absolute and relative MA gains from upgrading a link under trip-level frictions.

The exercise is again repeated by incorporating average export/import frictions into border-crossing links. This reduces MA to \$820B/min, or 47% of the frictionless value. With all links upgraded to 100km/h, the MA is \$1.04T/min, only 42% of the MA gain without frictions, but still 27.3% more MA than without road improvements. These numbers reflect an average 6x travel time increase under frictions, which rises to 8.6x with an upgraded 100km/h network. Figure 28 shows gains under the cumulative frictions case. The effects are similar and stronger than in Figure 27. Because of the optimizing behavior away from expensive links, the RHS of Figure 28 again includes a few links whose upgrading under frictions yields greater MA gains than without frictions.

Figure 28: Gains in MA (GDP/min) under Border Frictions with Optimizing Agents

%-Gain in MA from Improving Link Ratio of Gains to Frictionless Network



Notes: Figure shows absolute and relative MA gains from upgrading a link under link-level frictions.

5.6 Road Upgrading Costs

For cost-benefit analysis, I also estimate the cost of upgrading roads. The ROCKS database distinguishes several types of road improvements. Table 6 summarizes the four most common ones: 'Upgrading', 'Reconstruction', 'Asphalt Mix Resurfacing', and 'Strengthening'. To obtain a summary statistics for the cost of upgrading, I compute a weighted average of the median costs/km across types, using the number of works (N) times the median length of the work in km as weights. This yields an average upgrade cost estimate of \$326M/km. Thus, upgrades are, on average, only about half as costly as new highways priced at \$611M/km (see Table 5). However, road upgrades in Africa are $\sim 60\%$ more costly than the low- and lower-middle income country average of \$205M.

Table 6: Road Upgrading Costs: Road Costs Knowledge System (ROCKS) - 2018 Update

Work Type	N	Length (km)	Weight	Cost (M\$'15)	Cost/km
<i>Continental Africa</i>					
Upgrading	28	103.5	2898	49.73	0.513
Reconstruction	27	33.0	891	20.20	0.116
Asphalt Mix Resurfacing	14	133.8	1874	16.93	0.143
Strengthening	11	110.0	1210	42.97	0.316
Weighted Average		104.0		35.77	0.326
<i>All Low and Lower-Middle Income Countries</i>					
Upgrading	68	61.8	4199	20.63	0.320
Reconstruction	53	73.0	3869	20.20	0.162
Asphalt Mix Resurfacing	35	143.9	5036	15.50	0.090
Strengthening	26	92.0	2392	20.89	0.316
Weighted Average		95.9		18.90	0.205

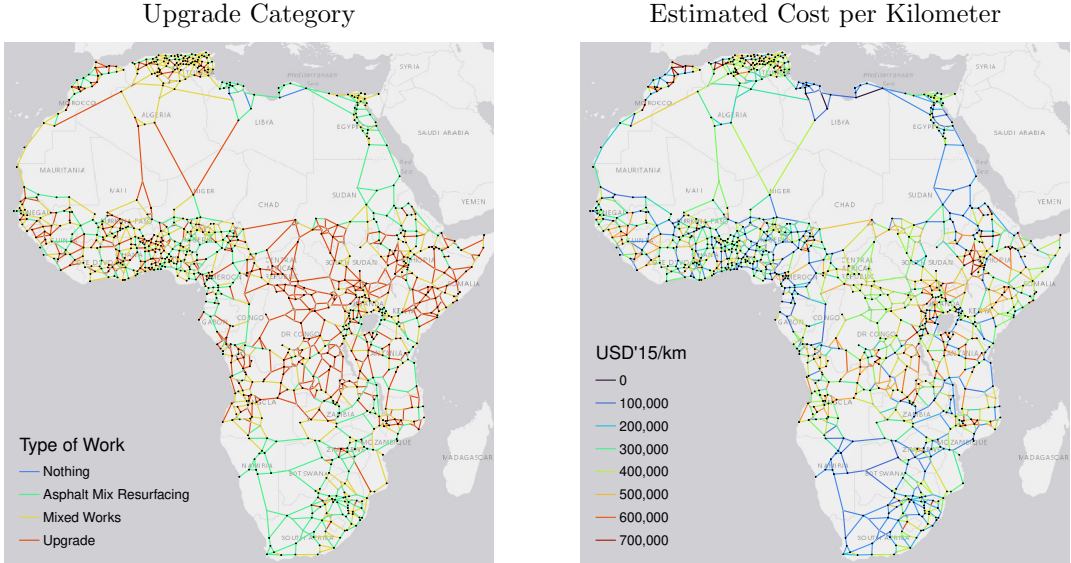
Notes: Statistics are aggregated across projects using the median. The 'Weight' column is the number of projects (N) times the median length (Length). This is used to compute a weighted average across different work types. Costs are in millions of 2015 USD. The raw costs in current USD were deflated at their project end date using the US GDP deflator with base year 2015.

These estimates are consistent with [African Development Bank \(2014\)](#), who report an average cost of 180,300 USD'06/lane-km for a category called 'Rehabilitation,' yielding 418,500 USD'15/km for 2-lane highways. Their 1st and 3rd quartile estimates translate to 254,900 and 673,100 USD'15/km, respectively. As mentioned earlier, [African Development Bank \(2014\)](#) lump together 'Upgrading' with new construction at a median price of 528,800 USD'15/km. Their estimate is thus between the 'Upgrading' estimate of \$513K in Table 6 and new construction at \$611K from Table 5.

Upgrading a link to allow speeds of 100km/h should require different types of road work depending on the existing condition of the road. It is unrealistic to assume that this is a continuous function of the distance of travel speed from 100km/h. For example, two roads with travel speeds of 85 and 90km/h likely both require a full asphalt resurfacing to bring them to 100km/h. Since the distribution of speeds in Figure 25 is trimodal, I propose the following three categories: (1) roads with a travel speed below 60km/h require a full 'Upgrade' at an average cost of \$513K/km; (2) roads with travel speeds of 60-79km/h may require mixed works at an average cost of \$326K/km; (3) roads with travel speeds of 80km/h and higher require an 'Asphalt Mix Resurfacing' at \$143K/km on average. To introduce heterogeneity in these cost estimates, I use Eq. 8 and modify the intercept such that the median (across all routes, regardless of their upgrade type) is close to the respective category medians: For category (1), the intercept is ln(101,600), for category (2) it is ln(64,600), and for category (3), it is ln(28,400). In addition, I clip estimates at the 2.5th and 97.5th percentile to guard against outliers, such that, e.g., 'Asphalt Mix Resurfacing' costs remain between \$94K/km and \$206K/km. Figure 29 reports the classification and estimated unit costs.

The entire central-African network and trans-Saharan connections via Mali and Niger, as well as most of the network around the horn of Africa, is classified as requiring a full upgrade, at costs around \$400K/km due to mostly flat terrain and small population density. The total cost of upgrading the entire 315K km transport network is thus estimated at \$106B (in 2015 USD), comprising \$57.8B full road upgrades, \$35.6B mixed works, and \$12.3B mixed asphalt resurfacing.

Figure 29: Estimated Network Upgrading Cost per Kilometer



Notes: Figure shows stipulated work required to upgrade a link to speed $\geq 100\text{km/h}$ (LHS) and estimated cost/km (RHS).

5.7 Cost-Benefit Analysis: Road Upgrading

Comparing this cost to the total MA gain of 42% or \$701B/min implies a return of \$6.6/min/\$. With border frictions, the MA gain is reduced to 27% or between 214 and 253 billion USD/min in the two scenarios, implying a 2/2.4 \$/min/\$ return in the cumulative/simple frictions scenarios, respectively. Thus, road upgrades yield significantly higher average returns than fresh construction.

It remains to gauge the returns to upgrading individual links. Figure 30 shows estimates following the same schema as Figure 24, signifying that upgrading links in populated areas and critical trans-continental connections yields significant returns. The consensus package again includes links where the MA return in \$/min/\$ is greater than 1 in the frictionless case and at least one of the scenarios with frictions. It suggests prioritizing upgrading roads near urban centers and important trans-continental links. The package comprises 1255 links, 53.5% of all links, and costs \$45B. It yields a frictionless 33.1% MA gain of \$552B/min or 12.3\$/min/\$.

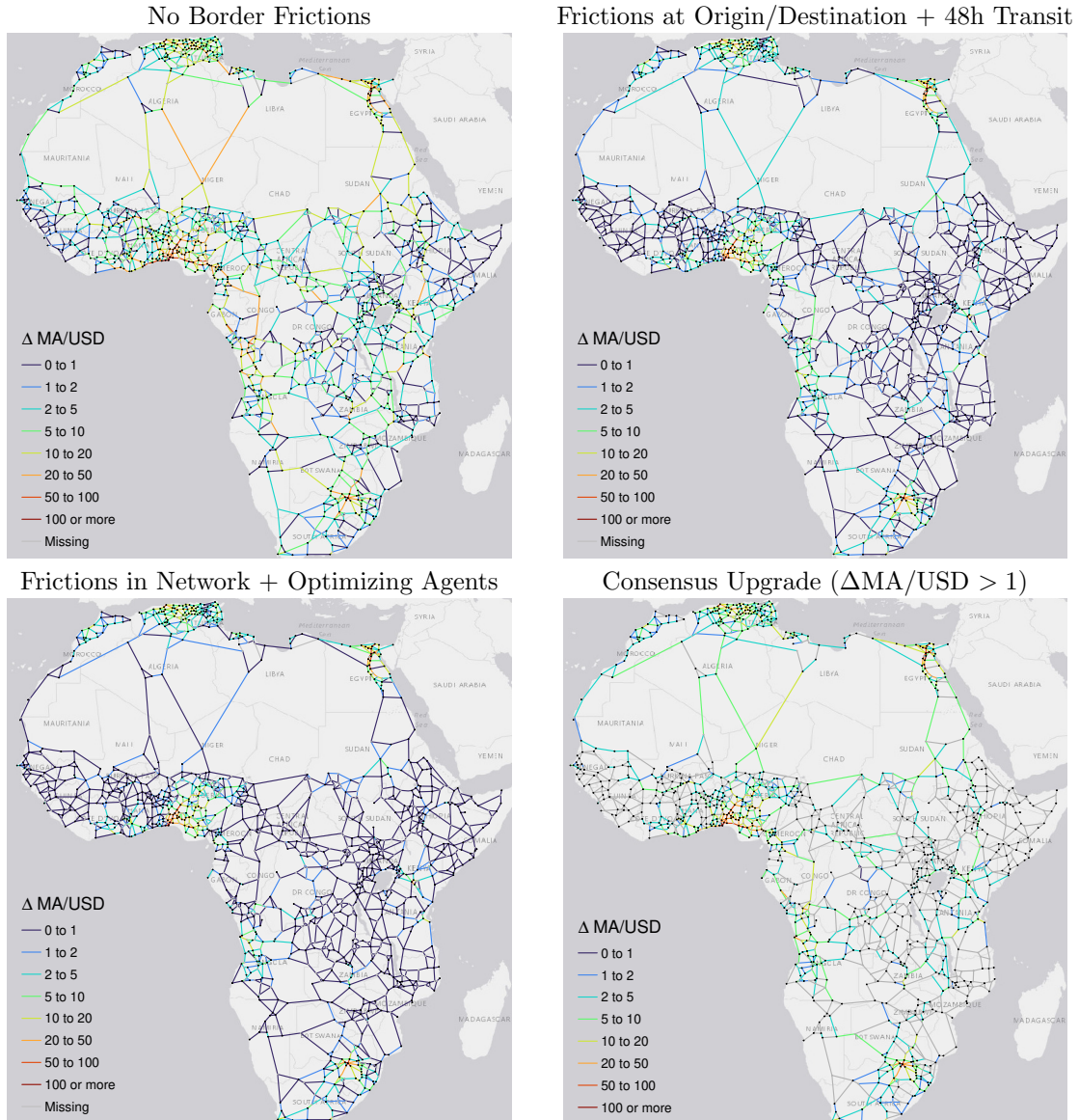
5.8 Cost-Benefit Analysis: Joint Scenarios

Combining road construction and upgrading costs (see Figure 31), I also perform cost-benefit analysis for joint scenarios where building new links and upgrading existing ones are part of the choice set. Due to the different intercepts in Eq. 8, the cost of building a new link is always greater than upgrading an existing one *ceteris paribus*.

All proposed road works combined cost 161 billion USD'15 (around 200 billion in current USD). They yield a frictionless MA gain of 50%, amounting to \$831B/min or \$5.2/min/\$. The more restrictive cumulative frictions case yields a 31% MA gain, amounting to \$241B/min or \$1.5/min/\$. Figure 32 provides the full link-level analysis, including three consensus packages with MA gains above 1, 2 and 4 \$/min/\$, at costs of 60.9, 36.6, and 17 billion USD'15, respectively:

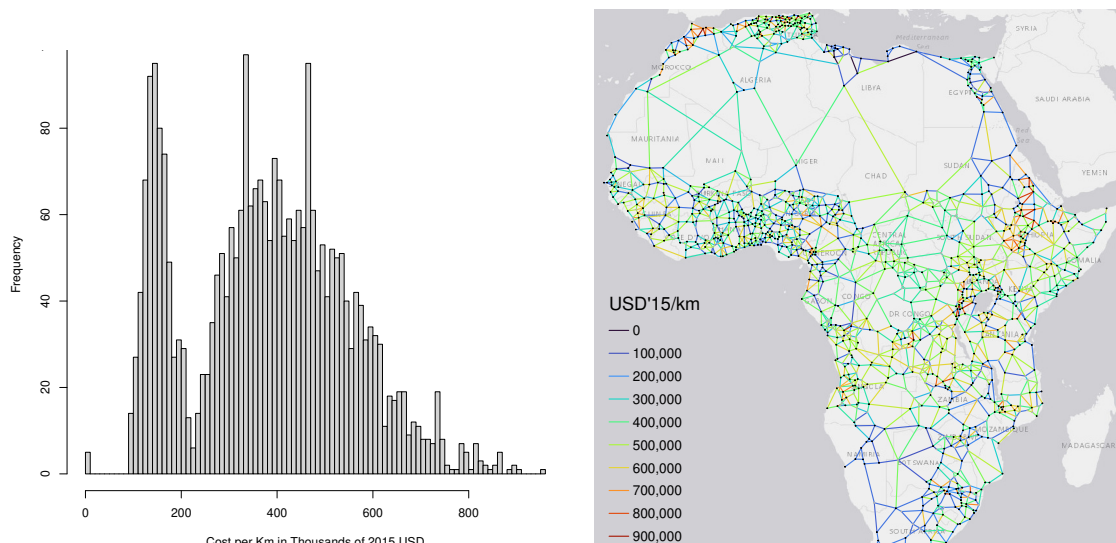
- The > \$1 package comprises upgrading 54% of links and building 30% of proposed links. It yields a 38% MA gain of \$636B/min or \$10.4/min/\$ without frictions and 26.8% | \$251B/min | \$4.1/min/\$ or 28% | \$221B/min | \$3.6/min/\$ under simple or cumulative frictions.
- The > \$2 package comprises upgrading 37% of links and building 18% of proposed links. It yields a 30.6% MA gain of \$511B/min or \$14/min/\$ without frictions and 24% | \$225B/min | \$6.1/min/\$ or 25.7% | \$201.5B/min | \$5.5/min\$ under simple or cumulative frictions.
- The > \$4 package comprises upgrading 22.4% of links and building 8.9% of proposed links. It yields a 20% MA gain of \$340B/min or \$20/min/\$ without frictions and 19.5% | \$182B/min | \$10.7/min/\$ or 21.3% | \$167B/min | \$9.8/min/\$ under simple or cumulative frictions.

Figure 30: Cost-Benefit Analysis (USD/min MA Gain per USD Invested)



Notes: Figure shows MA returns in USD/min per USD invested in link upgrading under different types of border frictions.

Figure 31: Estimated Network Building/Upgrading Cost per Kilometer



Notes: Figure shows combined cost/km of building new (fast) links and upgrading existing links to speed $\geq 100\text{km/h}$.

The first two packages are prone to generate a much greater developmental impact than the high-yield package, which primarily addresses low connectivity in the already large markets.

5.9 Macroeconomic Cost-Benefit Analysis

A critical question neglected so far is whether these investments are macroeconomically feasible. How do MA gains translate into medium-term economic gains, and are these gains large enough to justify such expenses, potentially even on a debt-financing basis?

The medium-term economic returns to increased MA are very difficult to estimate, especially on such a large scale. The only large-scale analysis I am aware of is [Donaldson & Hornbeck \(2016\)](#). The authors regress changes on the log of land values across 2,327 US counties between 1870 and 1890 on changes in the log of MA, and find an elasticity of 0.5, which is quite robust to different choices of θ . This suggests that in the medium run MA translates into economic activity at a ratio of 2:1. However, present-day Africa is very different from the historical US.

Thus, instead of estimating economic returns to MA gains in Africa, I present an attempt to determine what the returns would need to be in order to justify the investment. This will take the form of a reverse macroeconomic present discounted value (PDV) calculation. African GDP in 2022 was 2.81 trillion 2015 USD. The median growth rate in 2000-2022 was 4.1%. If we are pessimistic about African growth, let it be 3% going forward. I discount the future by 10%. This is a reasonable rate given that stock market returns are generally below this - the MSCI World has a long-term return rate of 8-9%. Emerging market bonds yield even lower returns, around 6%, according to the EMBI index by JP Morgan. So at the macroeconomic scale, it is very difficult to invest with more than 10% returns. I also assume that the horizon of policymakers is 30 years and disregard benefits accruing after 30 years. With these assumptions, I calculate the change in the macroeconomic growth rate of Africa that would be necessary to break even in PDV terms for each of the three scenarios proposed above as well as the full/consensus construction and upgrade scenarios considered in Sections 5.4 and 5.7. Table 7 reports these calculations.

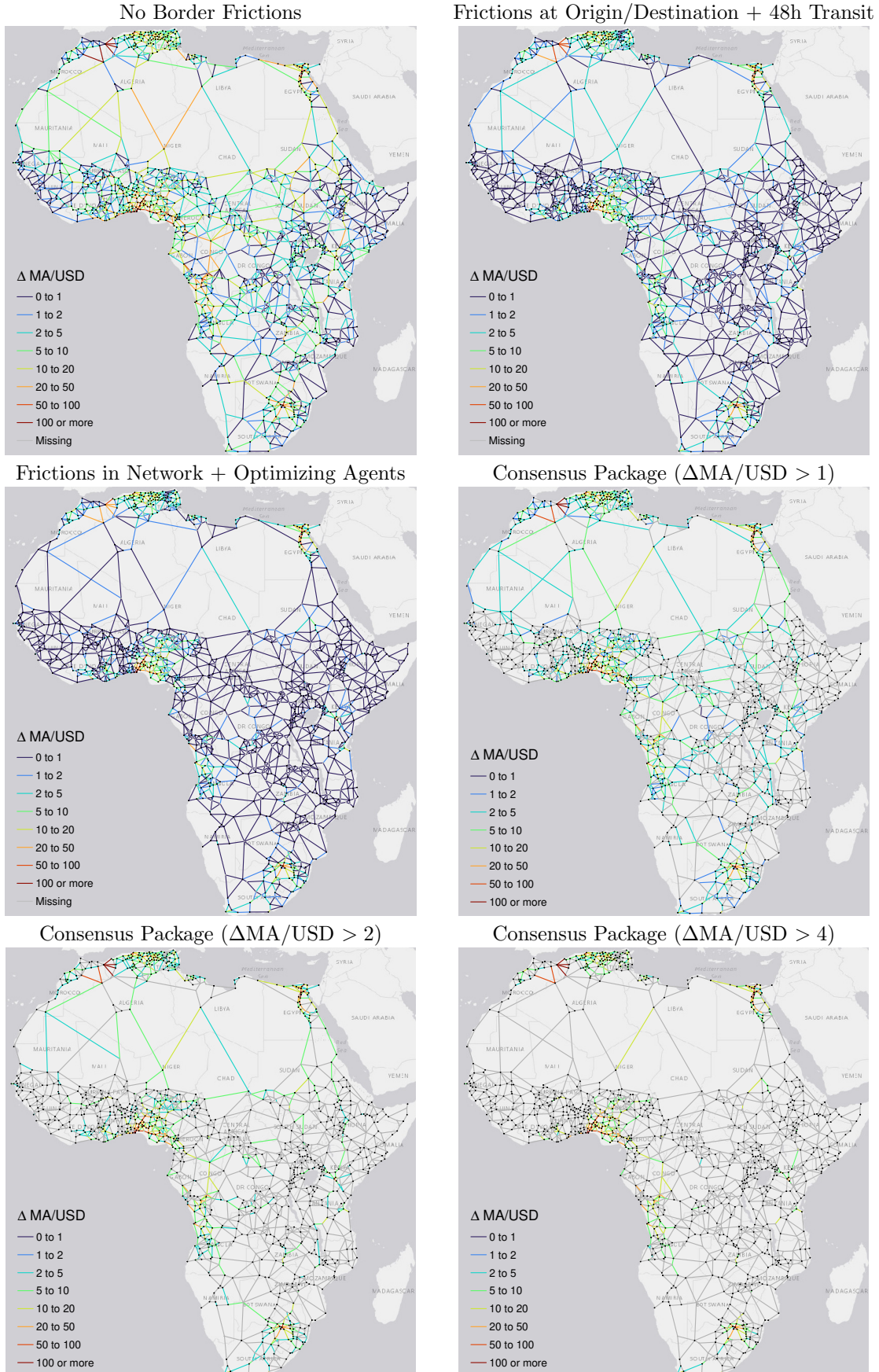
Table 7: Break Even Changes in the Macroeconomic Growth Rate for Different Investments

Work Package	Cost	%ΔMA	BEG (4.1%)	BEG (3%)
Full Extension (\uparrow RE)	\$56.1B	3.9 – 5.5	0.31% → 4.113	0.50% → 3.015
Consensus Extension (\uparrow RE)	\$12.1B	2.4 – 4.0	0.07% → 4.103	0.11% → 3.003
Full Upgrade (\uparrow TE)	\$105.7B	27.0 – 42.1	0.58% → 4.124	0.94% → 3.028
Consensus Upgrade (\uparrow TE)	\$45.0B	21.2 – 33.1	0.25% → 4.110	0.40% → 3.012
All Links > \$1/min/\$	\$60.9B	26.8 – 38.1	0.33% → 4.114	0.54% → 3.016
All Links > \$2/min/\$	\$36.6B	24.0 – 30.6	0.20% → 4.108	0.32% → 3.010
All Links > \$4/min/\$	\$17.0B	19.5 – 20.4	0.09% → 4.104	0.15% → 3.005

Notes: Table shows the cost in 2015 USD PPP of different investment packages, their MA %-gain under the worst frictions and frictionless scenarios, and the change in Africa's macroeconomic growth rate needed to break even after 30 years under realistic (4.1%) and pessimistic (3%) baseline growth.

I illustrate their interpretation using the largest consensus package containing all links with $>\$1/\text{min}/\$$ marginal returns. It costs \$60.9B and yields a MA gain between 26.8% (worst frictions scenario) and 38.1% (no frictions). Under the 4.1% baseline growth scenario, the growth rate needs to change by 0.33% to 4.114% to yield a return of \$60.9B in PDV terms after 30 years. Comparing the 26.8% lower bound to 0.33% yields a ratio of 81:1. Thus, if changes in MA translate to changes in the growth rate at 81:1 or higher, the package is macroeconomically feasible. This appears very plausible given the results of [Donaldson & Hornbeck \(2016\)](#). However, many things can go wrong. First, growth could be slower at 3%, requiring a 0.54% increase in the growth rate or a return ratio above 50:1. Then, the package could end up being more expensive for various reasons related to terrain, weather, corruption or delays. Assuming it turns out twice as expensive, this would require a ratio above 25:1. Finally, if the investment is financed through debt, it could adversely affect both the total costs and the macroeconomic growth rate by limiting fiscal space and worsening credit ratings. Such forces could lower the required return ratio to as low as 10:1. Nevertheless, this still appears reasonably achievable; thus, overall, these back-of-the-envelope calculations suggest that large-scale *optimal* investments in Africa's road network are macroeconomically feasible.

Figure 32: Cost-Benefit Analysis: Joint Scenarios (USD/min MA Gain per USD Invested)



Notes: Figure shows MA returns in USD/min per USD invested in link building and/or upgrading under different types of border frictions. It also shows 3 different 'consensus packages' containing high-returns links with and without frictions.

6 Optimal Network Investments in General Equilibrium

Having simulated many scenarios in partial equilibrium by modifying one link at a time or jointly adding/improving a selection of (high marginal value) links and computing MA returns, this section goes a bold step further and considers welfare-maximizing network investments in general equilibrium (GE). In particular, using a quantitative framework established by [Fajgelbaum & Schaal \(2020\)](#), I optimize over the space of networks after setting an infrastructure budget. The framework accommodates trade in multiple goods and requires exogenous productivities for the production of each good in each location. Cities must have different productive endowments to create incentives for trade. For my application to the African network, this is a strong limitation, firstly because such city-level productivity data is unavailable, and secondly because global optimization with many goods traded on a large network is computationally infeasible.

To remedy the lack of detailed productivity data, I follow [Armington \(1969\)](#), [Fajgelbaum & Schaal \(2020\)](#), and [Graff \(2024\)](#) and assume that products are differentiated by city of origin and each city produces just one good. To overcome the dimensionality problem, I perform simulations on two different network graphs: (1) on the full transport network from Section 4.3 with 1379 nodes and $2344 + 481 = 2825$ edges, I let small, medium, large, and port-cities produce different goods. This creates incentives for regional trade between cities of different sizes and with coastal ports, but limited incentives for trans-African trade. (2) On the reduced network connecting 47 major cities and ports from Section 4.4 with, in the simplest case, only 212 nodes and 330 edges, I let the largest 17 cities produce differentiated products. Other (port-)cities are categorized.

In my model specification and parameterization, I largely follow [Graff \(2024\)](#). I set the existing level of infrastructure along each link from city j to city k , I_{jk} , to the average link speed in km/h

$$I_{jk} = \text{speed}_{jk} \quad \forall j, k. \quad (9)$$

I_{jk} is bounded from below by the present speed ($I_{jk}^{\min} = I_{jk}$), which is zero for proposed links. It is also bounded from above by the greater of 100km/h and the present speed, denoted by $I_{jk}^{\max} = \max(I_{jk}^{\max}, 100)$. I then calculate the (per km/h) infrastructure building cost δ_{jk}^I as

$$\delta_{jk}^I = \text{upgrade cost}_{jk} / (I_{jk}^{\max} - I_{jk}), \quad (10)$$

where upgrade cost $_{jk}$ corresponds to the cost per km of building each link or upgrading it to 100km/h from Figure 31, multiplied by the link length in km. Since in the model of [Fajgelbaum & Schaal \(2020\)](#) the lower bound on I_{jk} is simply a constraint on how a given infrastructure budget may be spent, I set the baseline budget equal to $\delta_{jk}^I \times I_{jk}$. I then consider a social planner with a budget of approx. 1/3 of the cost of all proposed work (upgrading and construction) in addition to the baseline budget. The planner can freely choose which links to build/upgrade at cost δ_{jk}^I .

In reality, most road upgrade/construction decisions are discrete, but the quantitative framework does not allow a discretization of optimal infrastructure investments. The results may instead be interpreted as 'partial' upgrades/completion. For example, suppose a road at 80km/h has a speed of 90km/h after the optimization. In that case, we may conclude that the planner decided to upgrade $(90-80)/(100-80) = 50\%$ of the road.²⁹ The model also features iceberg trade costs of the form

$$\tau_{jk}^n(Q_{jk}^n, I_{jk}) = \delta_{jk}^\tau \frac{(Q_{jk}^n)^\beta}{I_{jk}^\gamma}, \quad (11)$$

such that traders need to send $1 + \tau_{jk}^n$ units of a good for one unit to arrive. Following [Graff \(2024\)](#), who averages estimates from [Atkin & Donaldson \(2015\)](#) for Nigeria and Ethiopia, I set

$$\delta_{jk}^\tau = 0.1159 \times \ln(\text{distance in miles}_{jk}). \quad (12)$$

²⁹While this interpretation is plausible, the cost per km of building/upgrading segments decreases for roads longer than 50km (Eq. 8, following [Collier et al. \(2016\)](#)), and it is thus not realistic that the planner considers prices δ_{jk}^I inelastic to the quantity (length) constructed. In addition, if the planner partially builds a new links, we must assume that the remainder corresponds to a dirt road that can be constructed free of cost. Thus, the framework may slightly overstate the amount of infrastructure that can be constructed on a given budget.

The trade cost positively depends on the flow of good n across link $j \rightarrow k$, Q_{jk}^n , subject to an elasticity β , an effect Fajgelbaum & Schaal (2020) describe as 'congestion forces'. It also depends negatively on the level of infrastructure I_{jk} , subject to an elasticity γ . Following Graff (2024), I set $\gamma = 0.946$ and $\beta = 1.177$.³⁰ As discussed at length by Fajgelbaum & Schaal (2020), the lagrangian objective of the model is only convex if $\beta > \gamma$, in which case a unique global solution to the network design problem can be computed. If $\beta < \gamma$, the problem becomes non-convex and yields a local optimum, which Fajgelbaum & Schaal (2020) further refine using simulated annealing methods. They denote this case as 'increasing returns to infrastructure' (IRS) and show that the optimal network is more tree-like, with larger investments in fewer links. Graff (2024)'s parameterization implies $\beta > \gamma$. This may, however, not hold for large transnational networks; thus, following Fajgelbaum & Schaal (2020), I also examine the IRS case assuming $\gamma' = \beta^2/\gamma = 1.465$.³¹

Fajgelbaum & Schaal (2020)'s model has a normalized inequality-averse Cobb-Douglas utility function giving the utility of a single worker in location j in terms of consumption and housing

$$u_j(c_j, h_j) = \left[\left(\frac{c_j}{\alpha} \right)^\alpha \left(\frac{h_j}{1-\alpha} \right)^{1-\alpha} \right]^{1-\rho} / (1-\rho), \quad (13)$$

where ρ controls the level of inequality aversion. Following Graff (2024), I assume $\alpha = 0.7$, which is based on estimates by Porteous (2022), and $\rho = 0$ (no inequality aversion), but I also explore $\rho = 2$ (moderate inequality aversion). Following Graff (2024), I set $h_j = 1 - \alpha$, i.e., the local housing availability is proportional to the current population. Total consumption in location j is $C_j = L_j c_j$, which in turn is a CES aggregate over N traded goods with elasticity of substitution σ

$$C_j = \left[\sum_{n=1}^N (C_j^n)^{\frac{\sigma-1}{\sigma}} \right]^{\frac{\sigma}{\sigma-1}}. \quad (14)$$

In line with the international trade literature, Fajgelbaum & Schaal (2020) and Graff (2024) use $\sigma = 5$, following recommendations by Atkin & Donaldson (2022). Both assume that the largest $N - k$ cities produce their own good and mostly conduct single-country simulations.³² Since I have few cities per country, it is also plausible to interpret σ as an Armington (1969) elasticity, and here a meta-study by Bajzik et al. (2020) suggests a median value of 3.8. These values apply to the trans-African network simulation case where I let 17 megacities produce differentiated products. In the case of only 4 goods produced by small, medium, large, and port cities, such elasticities generate near autarky equilibria. I thus assume σ values as low as 1.5 to generate realistic trade flows in this case. Goods are produced according to a linear technology

$$Y_j^n = Z_j^n L_j^n. \quad (15)$$

Due to lack of better measures,³³ I set city productivity Z_j^n equal to the predicted International Wealth Index of Lee & Braithwaite (2022) (Figure A2). Since the original estimate is only available for SSA, I use the imputed version of Krantz (2023) (Figure A3) and compute the productivity of each city as the inverse-distance-weighted average of cells within 30km of the city centroid. I assume

³⁰The value for γ is informed by estimates of the costs of road delays to African truckers by Teravaninthorn & Raballand (2009). The value of β is informed by estimates on the cost of traffic congestion by Wang et al. (2011). Fajgelbaum & Schaal (2020) use $\beta = 0.13$ and $\gamma = 0.1$, but their characterization of infrastructure (I_{jk}) in terms of road-lane km yields significantly larger values than the formulation in terms of km/h adopted from Graff (2024).

³¹Fajgelbaum & Schaal (2020) page 1439 simulate an IRS case by inverting the ratio of β and γ keeping β fixed.

³²Graff (2024) sets $N = 6, k = 2$ (with one international good produced outside the country and one agricultural good produced by smaller cities) and conducts simulations for every African country. Fajgelbaum & Schaal (2020) set $N = 10, k = 1$ and conduct simulations for France, Spain, and Western Europe.

³³Graff (2024) uses nightlights divided by city population to form the productivity measure. While this is a viable approach, the task of measuring differences in city productivity across countries encourages the use of richer data sources. Lee & Braithwaite (2022) combine daylight satellite imagery and OSM data in an iterative ML framework that has proven able to predict wealth within and across SSA countries reliably. As an attempt to verify, taking a city-population weighted average of the IWI by countries yields a correlation of 0.62 with the 2020 World Bank national GDP/capita estimate and a correlation of 0.73 with the log of GDP/capita. Using NASA's Black Marble nightlights, on the other hand, only yields a correlation of 0.15 between city-population weighted nightlights/capita and national GDP/capita. However, using the log of nightlights/capita yields a 0.58 correlation with GDP/capita and a 0.65 correlation with the log of GDP/capita. While this appears more promising, a visual comparison, provided in Appendix Figure A13 for the interested reader, shows that the IWI is higher in larger cities in richer countries - in line with much scientific evidence. The nightlights measure appears quite noisy and imprecise.

that average household wealth, aggregated at the city level, approximates worker productivity. Footnote 33 shows that national average urban wealth strongly correlates with GDP per capita.

I also calibrate the productivity of international ports so that overall production matches national accounts data. Averaging estimates from the UN National Accounts Main Aggregates database between 2020 and 2022 yields that imports were equal to 26.5% of African GDP. Since my network does not include foreign locations,³⁴ the imported goods will have to be produced by port cities. Assuming that port outflows in 2020Q1 are proportional to the inflows, multiplying outflows from the 52 largest ports by a factor of 37 yields (precisely) an imports measure summing to 26.5% of the total production volume using the IWI as productivity measure. These imports need to be divided by port city population to yield productivities. Since the framework of Fajgelbaum & Schaal (2020) endogenously allocates labor to different tasks, letting port cities produce both a domestic and international variety would obscure this calibration. Thus, I compound both tasks so that port cities use all labour to produce a mixed international variety at productivity

$$Z_j^{\text{intl.}} = \text{IWI}_j + \frac{37 \times \text{Outflow in TEU } 2020 \text{ Q1}_j}{\text{City Population}_j}. \quad (16)$$

The resulting increase in purchasing power implies that a part of the equilibrium consumption of port cities is exported. For simplicity, I assume the export share is equal to the share of international productivity in total city productivity and adjust consumption and welfare accordingly. Another implication of this calibration is that I am constrained to fixed labor scenarios. The mobile labor case, examined by Graff (2024) for national African road networks and by Fajgelbaum & Schaal (2020) for France, Spain, and Western Europe, lets workers reallocate to more productive and better-connected locations - implying potentially large changes in the production of imports.

6.1 Optimal Regional Network Investments

Due to computational constraints, I parameterize the full transport network graph from Section 4.3 with 1379 nodes and 2825 edges using only $N = 4$ traded goods, three of which are produced by cities (agglomerations) of sizes 0-200K, 200K-1M, and >1M, respectively, and the fourth, international good, is produced by port cities. This incentivizes regional trade between larger and smaller cities, hinterland cities and coastal ports. I think of these goods as consumption bundles. Small cities may specialize in agriculture, medium-sized cities in simple manufactured goods, and large cities in diverse manufacturing. Ports provide a bundle of international goods.

Due to their compound nature, the elasticity of substitution between them should be significantly lower. My benchmark specification is $\sigma = 1.5$, which is the lowest value where the model delivers robust solutions. In equilibrium, all cities still consume > 85% of their own output, and large/port cities > 96%. This seems much when aggregate data suggests that at least 25% of consumption is imports, but such are the limitations of using the framework on a large network.

Table 8 summarizes city populations and productivities. The majority of people, 283 million, live in large interior cities (agglomerations) with >1 million people, and nearly 120 million live near large ports. Port cities are the most productive, even without international (import-related) productivity. When adding intl. productivity, their total production volume almost doubles from 7 to 12.7 billion IWI points, higher than the 9.3 billion IWI points produced by major interior cities. The median intl. productivity is 27 IWI points, but the mean is much higher at 2748, indicating high import volumes in some port cities with small populations. Top of the list is Egypt's Sokhma Port (towards the Red Sea), with a population of 1000 and intl. productivity of 134,656, followed by Egypt's Port Said, with a population of 894,850 (within a 30km radius) and intl. productivity of 1,264. Other ports with intl. productivity above 500 include Tanger Med and Walvis Bay. Since

³⁴It would be difficult to add foreign markets to an already large network. In theory, this could be done by adding additional nodes for ports and separating the city from the port in this way, but for any goods to flow to these locations, they need to have populations. Since flows are an equilibrium outcome, they would have to be calibrated to match the data by reverse engineering the model, which is quite complicated solving for populations of multiple ports. The framework may also have difficulties computing optimal flows along zero-cost links.

utility functions are mildly concave ($\alpha = 0.7$) and the planner maximizes utility, the comparatively small populations of these port cities downweights their importance for network optimization.

Table 8: Productivity and Population by City Type

City Type Count	1-200K 625	200K-1M 248	>1M 59	Port 51
<i>Population</i>				
Sum	48.9M	112.2M	283M	117.2M
Mean	77.5K	422K	3.29M	2.3M
Median	66.1K	361K	1.64M	1.04M
<i>Productivity</i>				
Total	1.50B	3.76B	9.28B	12.67B
Total Domestic	1.50B	3.76B	9.28B	6.97B
Domestic Mean	30.37	35.48	43.64	52.87
Domestic Median	26.58	31.49	43.10	53.64
International Mean	0	0	0	2784.44
International Median	0	0	0	27.15

Notes: Table shows population and productivity (IWI) summarized for cities of different sizes and port-cities. International productivity (for imports) is the second term in Eq. 16.

Figure 33 provides an overview of the calibrated network structure. Like Fajgelbaum & Schaal (2020), I conduct all simulations assuming cross-good-congestion, as it is realistic to assume that the same roads are utilized to transport different goods. The maximum investment volume in this network comprising all proposed roads and upgrades is 161 billion USD'15. To create an interesting allocation problem, I assume the social planner has \$50B, around 1/3 of the needs.

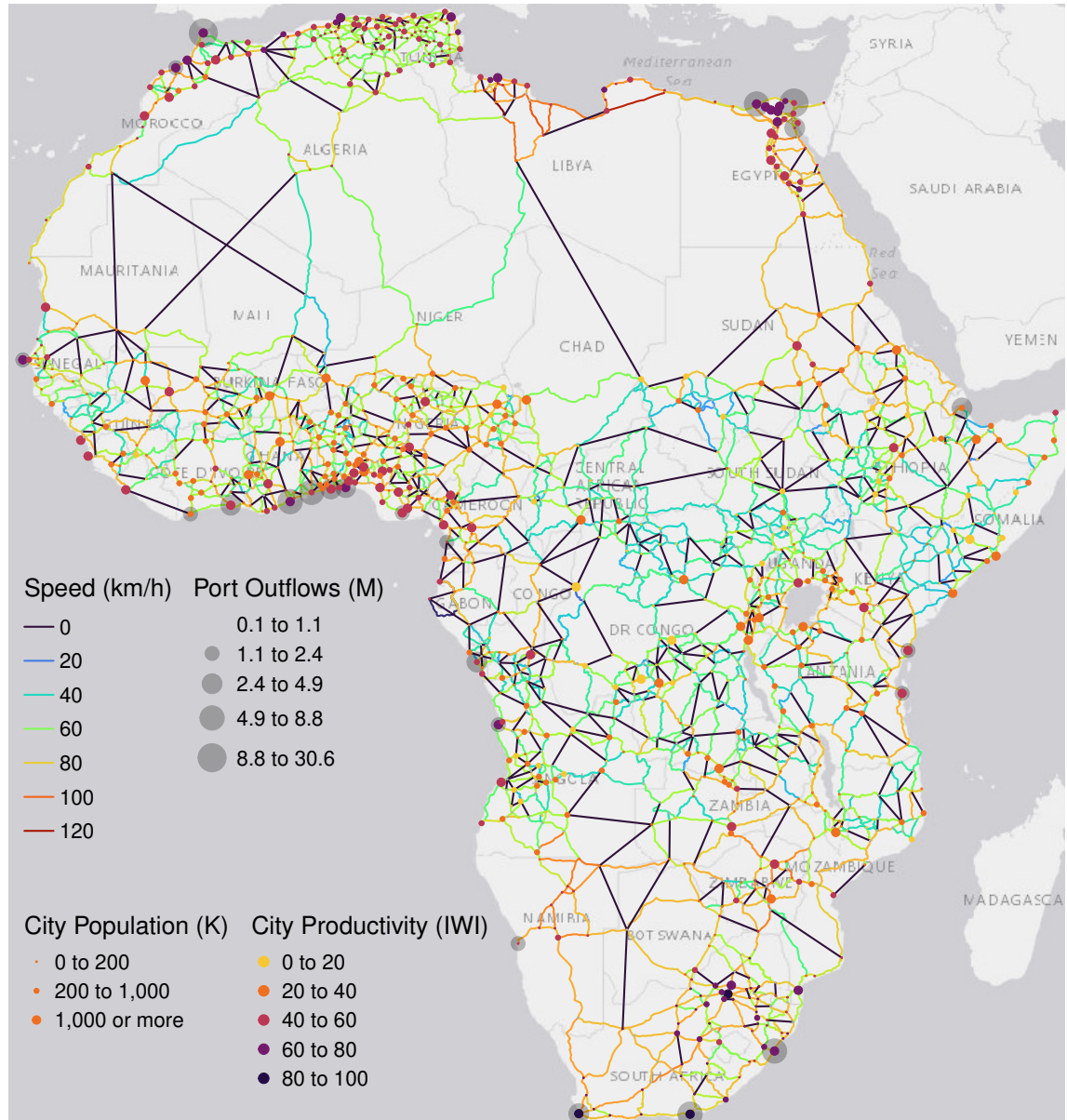
6.1.1 Decreasing Returns to Scale in Infrastructure

Under decreasing returns (DRS) ($\gamma < \beta$), the \$50B social planner focuses on connecting high-productivity large cities and port cities to surrounding smaller cities, particularly where road connectivity is inferior. Fajgelbaum & Schaal (2020) find that, in equilibrium, more infrastructure is allocated to regions with lower levels of infrastructure, higher population, and greater worker productivity. Figure 34 visualizes the optimal allocation. The left panel shows network speed post optimization, the middle panel the speed difference to the current network, and the right panel the percentage to which the stipulated work on each link was completed. Thus, the right panel measures the extensive margin of road work, the middle panel the intensive margin.

Overall, this planner commissions road activities equivalent to 130,562km of fully built/upgraded road segments, of which 94,008km are upgrades at a cost of \$29B, and the remaining 36,554km are fresh construction at a cost of \$21B. These activities induce a non-risk-averse model-implied utilitarian welfare gain of 5.8% and a market access gain of 23.2%. The welfare gain is proportional to a consumption gain of 8%. Both are spatially heterogeneous, with utility per worker gains ranging from a 15% loss (1st percentile) to a 158% gain (99th percentile), at a median gain of 12%. The gains are negatively correlated with the IWI ($r = -0.31$) and also with population ($r = -0.14$), indicating that they are mildly redistributive. The MA gains are lower than the consensus packages of Section 5.8, where the second package at a cost of \$36.6B yields a 30.6% MA gain. This difference is due to the welfare maximizing motive and limited incentives for continental trade. Notably, PE packages invest more in major markets and trans-African links connecting them.

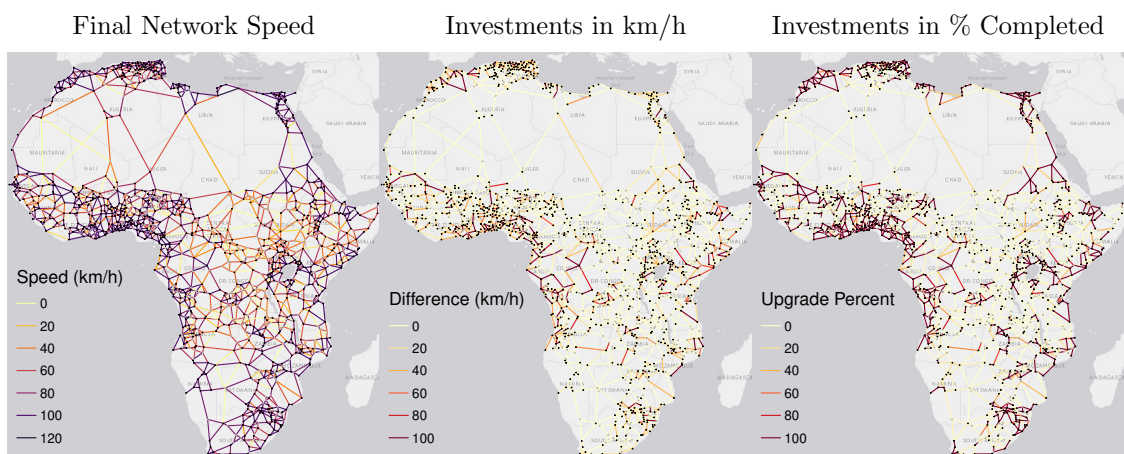
To better understand the planner's optimal allocation, I also examine the flow of goods. Figure 35 visualizes the average flow (across both directions) along each link. The scales are logarithmic, owing to significant differences in the magnitudes of flows. The geographic reach of flows differs by city size. Most small and medium-sized cities' trade is 'local', whereas large cities and ports send their goods to far-away destinations. Only these goods are shipped on trans-Saharan roads, explaining why the planner hardly invests in them.

Figure 33: Calibrated Network for Regional Trade (4 Goods) General Equilibrium Simulations



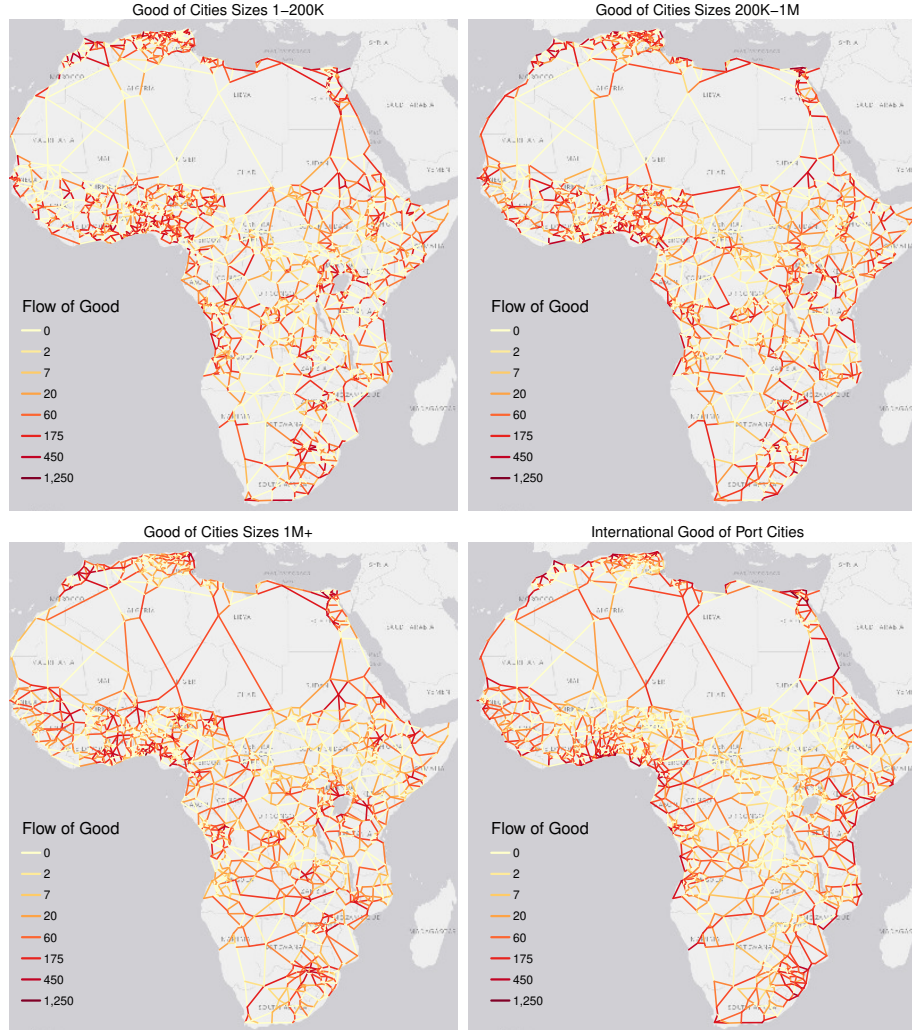
Notes: Figure shows network calibrated with speed, city population and productivity (IWI) and port outflows → Eq. 16.

Figure 34: Optimal \$50B Regional Network Investments under Decreasing Returns



Notes: Figure shows the optimal spatial allocation of a \$50B social planner. Investments in km/h are bounded above by 100km/h. The %-completed is the invested amount (speed) divided by the difference of the initial speed from 100km/h.

Figure 35: Flow of Goods Following \$50B Investments under Decreasing Returns



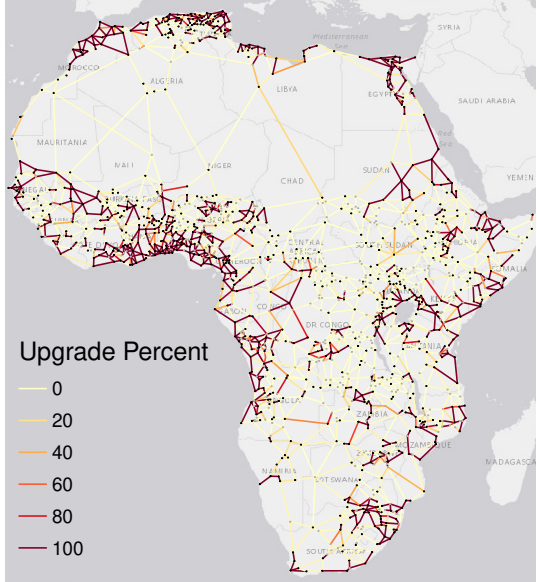
Notes: Figure shows the equilibrium flow of goods produced by difference (port-)cities on a logarithmic scale.

Despite the relatively low elasticity of substitution ($\sigma = 1.5$), all cities primarily consume their output. The median small (0-200K) city's own consumption share is 85.5%; for medium-sized cities (200K-1M), it is 93.5%; large cities (>1M) 96.7%, and for port cities, even 98.9% own consumption. Further lowering σ gives smaller own consumption shares but introduces numerical stability issues in the more complex increasing returns case. Yet, optimal infrastructure is relatively insensitive to σ . Appendix Figure A14 shows optimal network investments in percent of work completed, and below it the flow of major-city goods and local welfare gains, for σ values of 1.5, 2, and 4.

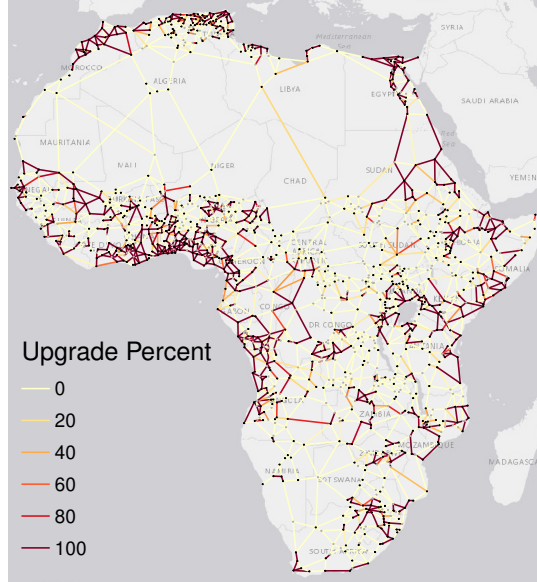
Higher elasticities induce more localized infrastructure investments in the vicinity of large cities, more concentrated trade around these centers, and reduced welfare gains, both overall and particularly in remote locations. As alluded to earlier, assuming $\sigma = 4$ yields a near-autarky equilibrium where small/large cities consume 97%/99.8% of their output. The overall welfare gain of 0.19% is minimal and also non-redistributional, at a correlation of $r = 0.25$ with the IWI versus $r = -0.31$ under the benchmark elasticity. At $\sigma = 2$, $r = 0.07$, indicating a relatively even distribution of welfare gains. Yet the optimal infrastructure allocation is largely unaffected, except for specific locations such as Juba in South Sudan. Under $\sigma = 4$, the planner fully connects Juba to surrounding cities through four new roads and one upgrade (see Figure 33). Under lower elasticities, these works are only partially completed. Another notable example is the proposed trans-African connection through Chad, connecting Libya with central and eastern Africa. Under $\sigma = 1.5$, the planner chooses to construct ~30% of this road, but under $\sigma = 4$, no work is done. Thus, trans-African connections are less important under high σ . The optimal allocation is also relatively insensitive to the presence of imported goods produced by ports. Appendix Figure A15 shows that without imports, investments shift slightly towards interior roads.

Figure 36: Optimal \$50B Network Investments under Decreasing Returns: Different Scenarios

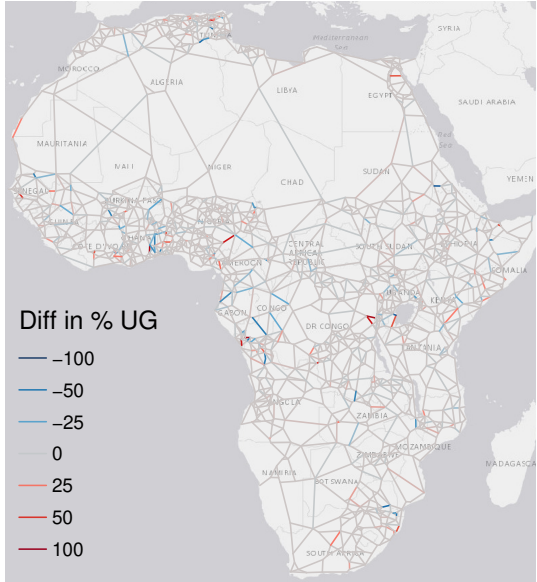
Non-Inequality Averse Planner, No Frictions
Builds 130,562km - 72% Upgrades at \$29B



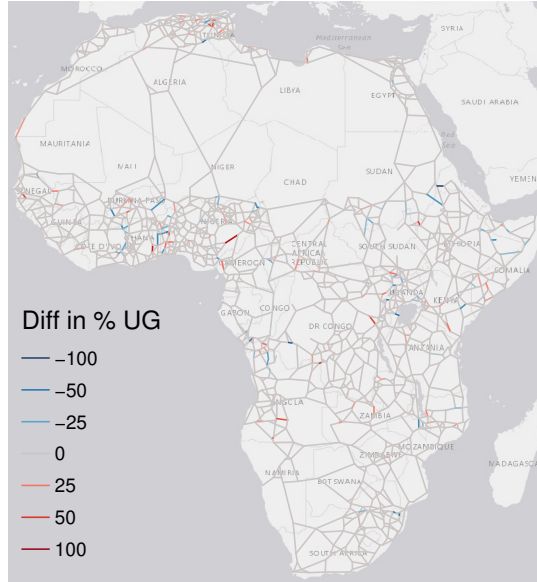
Inequality Averse Planner, No Frictions
Builds 126,989km - 69.4% Upgrades at \$27.8B



Non-Inequality Averse Planner, With Frictions
Builds 130,930km - 72.5% Upgrades at \$29.3B



Inequality Averse Planner, With Frictions
Builds 127,101km - 69.7% Upgrades at \$28B



Notes: Figure compares optimal allocations with/without an inequality averse planner and border frictions. Friction results show the difference in upgrade percentage points (% completed) to the frictionless case.

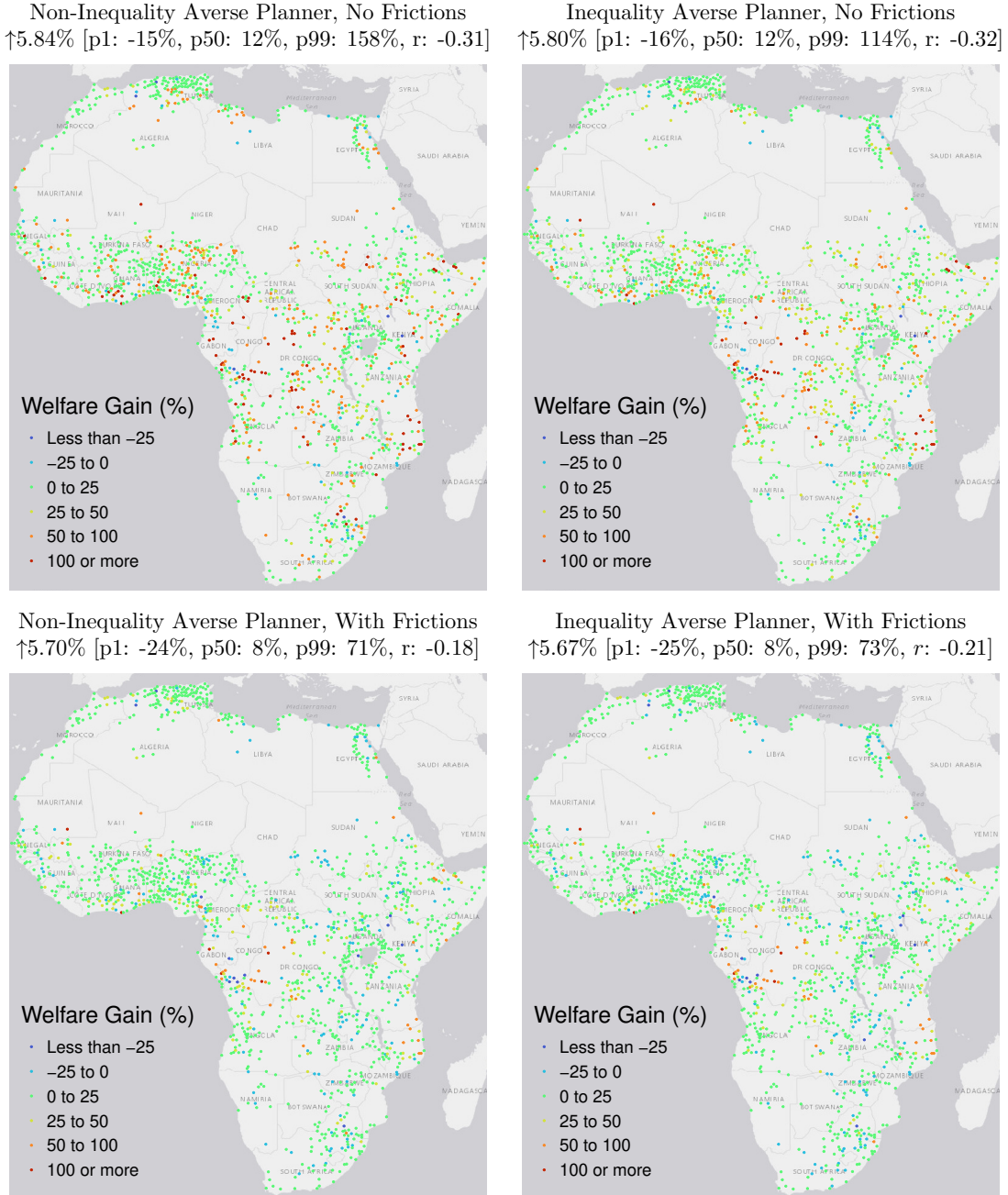
Another important factor influencing optimal investment allocations is the planner's regard for alleviating inequalities (ρ). The benchmark assumes $\rho = 0$ (no inequality aversion). Unfortunately, setting $\rho = 2$ or even 1.5 is computationally infeasible on the large network.³⁵ However, since housing (h_j) is fixed, the consumption share α is an alternative way of controlling the planner's regard for inequality - albeit less effective than the ρ parameter. Figure 36 shows optimal network investments under $\alpha = 0.1$, which simulations on small random networks reveal has almost the effect of $\rho = 2$. Under inequality aversion, investments in peripheral links increase slightly. For example, the planner better connects Juba and upgrades the link connecting Khartoum to Egypt.

What happens under border frictions? I investigate this by adding the distance-equivalent border frictions (Figure 9) to δ_{jk}^τ (Eq. 12). Surprisingly, optimal regional network investments change very little; the planner slightly reduces investments on certain links, many of which are

³⁵Similar to lowering σ too much, inequality aversion makes the planner's objective too complex.

close to borders, and expands others instead. The bottom half of Figure 36 shows the difference to the frictionless case. However, their effects on trade flows and welfare are considerable. Appendix Figure A16 shows the optimal flows ratio. To say the least, the adjustment is complex; the ratio is not bounded above by 1. Rather, flows through expensive border-crossing links are redirected to less expensive border-crossing links. Overall consumption and welfare gains are reduced slightly, and particularly in remote cities which would trade more without frictions.

Figure 37: Local Utilitarian Welfare Gains under Decreasing Returns



Notes: Figure shows welfare gains from allocations with/without an inequality averse planner and border frictions.

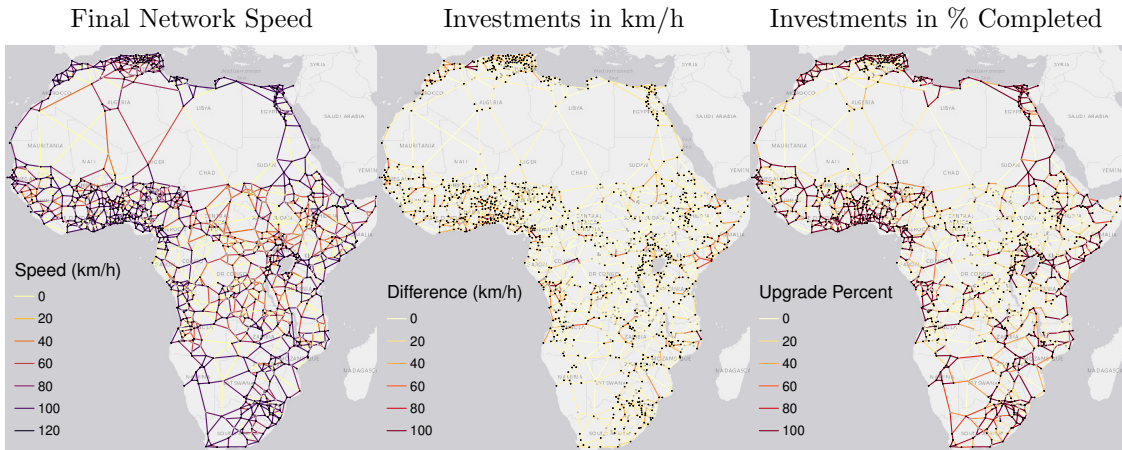
Figure 37 shows the bespoke heterogeneity in welfare gains. For the inequality-averse planner ($\alpha = 0.1$), I recalculated welfare gains by re-solving the model under $\alpha = 0.7$ using the optimal investments of the $\alpha = 0.1$ planner. In both scenarios, workers in Congo, Zambia, Mozambique, Nigeria, Cote d'Ivoire, Ghana, Sudan and Somalia gain the most. In the inequality-averse case, the gains are slightly more equitable at $r = -0.32$ (vs. -0.31) correlation with the IWI. The bottom panel shows that median welfare gains are reduced from 12% to 8% under frictions. Remote regions benefit less from the investments, and gains are less redistributive at $r = -0.18$ / -0.21.

6.1.2 Increasing Returns to Scale in Infrastructure

More than any parameter considered so far, the returns to infrastructure govern its optimal allocation. The benchmark specification is decreasing returns ($\gamma < \beta$). [Fajgelbaum & Schaal \(2020\)](#) make this assumption drawing on a study of the determinants of driving speed in large U.S. cities by [Couture et al. \(2018\)](#). [Graff \(2024\)](#)'s calibration also implies decreasing returns, but his parameters are derived very indirectly from the literature (not from econometric estimates) and thus form a sparse evidential basis. It may well be that trans-African connections, much less prone to congestion than inner-city roads, exhibit increasing returns ($\gamma > \beta$).

Follow [Fajgelbaum & Schaal \(2020\)](#), I invert the ratio of β and γ keeping β fixed, setting $\gamma' = \beta^2/\gamma = 1.465$. I then approximate the global optimum of the now non-convex optimization problem with simulated annealing and [Fajgelbaum & Schaal \(2020\)](#)'s random rebranching algorithm, whose desirable properties they establish. Figure 38 shows optimal network investments under IRS.

Figure 38: Optimal Network Investments under Increasing Returns



Notes: Figure shows the optimal allocation of a \$50B social planner under increasing returns to infrastructure ($\gamma > \beta$).

The 50 billion IRS planner commissions 166,549km of road work, considerably more than the DRS planner at 130,562km. Of these, 163,701km or 98.3% are upgrades at a cost of \$48.2B, and only 2,848km is new construction at \$1.8B. Compared to the DRS case (Figure 34), the investments are more dispersed, and the planner builds/upgrades fewer roads near large cities. The difference is particularly manifest in southern Africa, where the IRS planner chooses to resurface roads in the entire region. In contrast, the DRS planner only invests locally around Cape Town and Johannesburg. The total welfare gain of 7.51% is higher than the 5.84% gain under DRS, consistent with [Fajgelbaum & Schaal \(2020\)](#) and [Gorton & Ianovichina \(2021\)](#). The IRS investment is also better for MA, yielding 26.9% gain in total MA, versus 23.2% under DRS. It is also more equitable, with welfare gains ranging from -6% (p1) to 103% (p99) at median gain of 12% as in the DRS case, and slightly more redistributional at $r = -0.32$ IWI correlation. However, not everyone benefits under this scenario. For example, the IRS planner does not build new roads to better connect Juba, which are deemed relatively too expensive compared to upgrades in other regions.

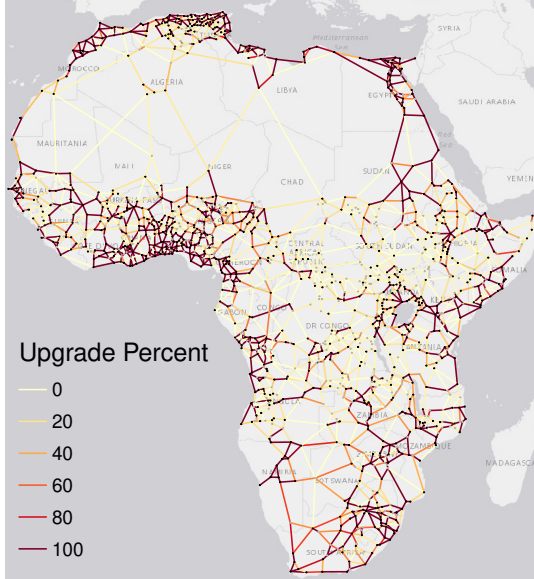
Under IRS, consumption flows in all goods, reported in Appendix Figure A17, are much larger than under DRS. This is also reflected in cities' own consumption shares. Under the benchmark $\sigma = 1.5$, small/medium/large/port-cities consume 52%/80%/88%/96% of their produce, considerably less than under DRS. Appendix Figure A18 shows that optimal investments are again relatively insensitive to σ . Raising σ lets them become more concentrated around cities; for example, under $\sigma = 1.5$, the planner builds/upgrades a long road into central DRC, unlike under $\sigma = 4$. Trade flows again become more local, and welfare gains decrease but remain larger than under DRS and, importantly, redistributional, at an IWI correlation of $r = -0.2$ even under $\sigma = 4$. The optimal allocation mildly reacts to ignoring imported goods, as Appendix Figure A19 shows.

Can a more inequality-averse planner still improve the spatial allocation? Figure 39 shows the

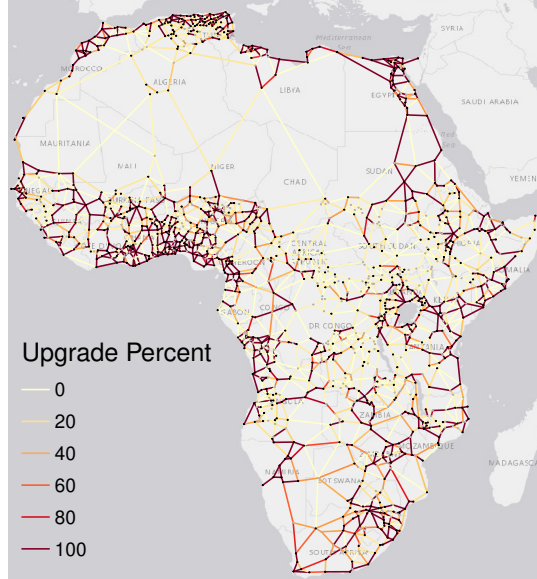
optimal investments.³⁶ The averse planner invests slightly more in countries like Angola, Congo, Sudan, and Somalia and less in northern, southern, and western Africa. Notably, (s)he upgrades an additional road in Congo but reconnects Morocco to Algeria using one instead of three links and does not upgrade a link connecting Algeria to Libya. Border frictions added at the bottom of Figure 39 (difference view) have a relatively small impact on the allocation but significantly change optimal flows (see Appendix Figure A20), and reduce welfare gains.

Figure 39: Optimal \$50B Network Investments under Increasing Returns: Different Scenarios

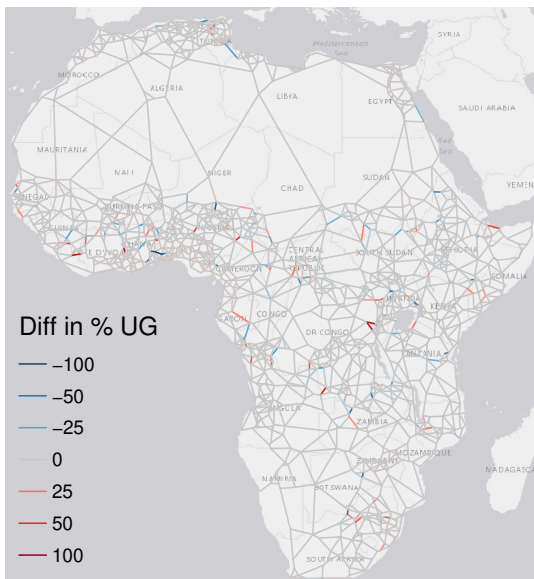
Non-Inequality Averse Planner, No Frictions
Builds 166,549km - 98.3% Upgrades at \$48.2B



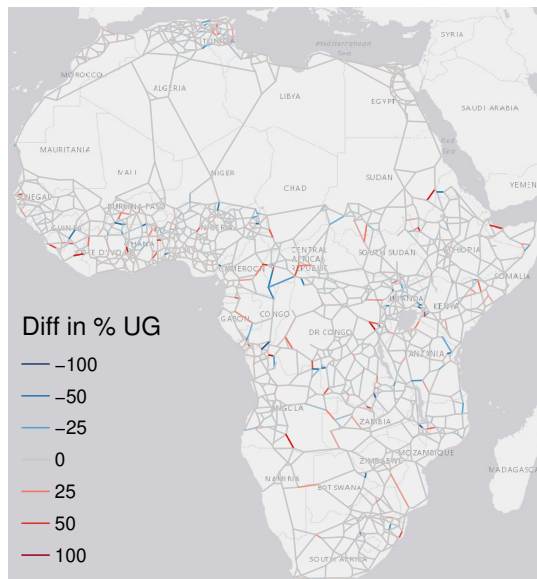
Inequality Averse Planner, No Frictions
Builds 165,798km - 98.5% Upgrades at \$48.6B



Non-Inequality Averse Planner, With Frictions
Builds 166,337km - 98.4% Upgrades at \$48.3B



Inequality Averse Planner, With Frictions
Builds 165,605km - 98.4% Upgrades at \$48.5B



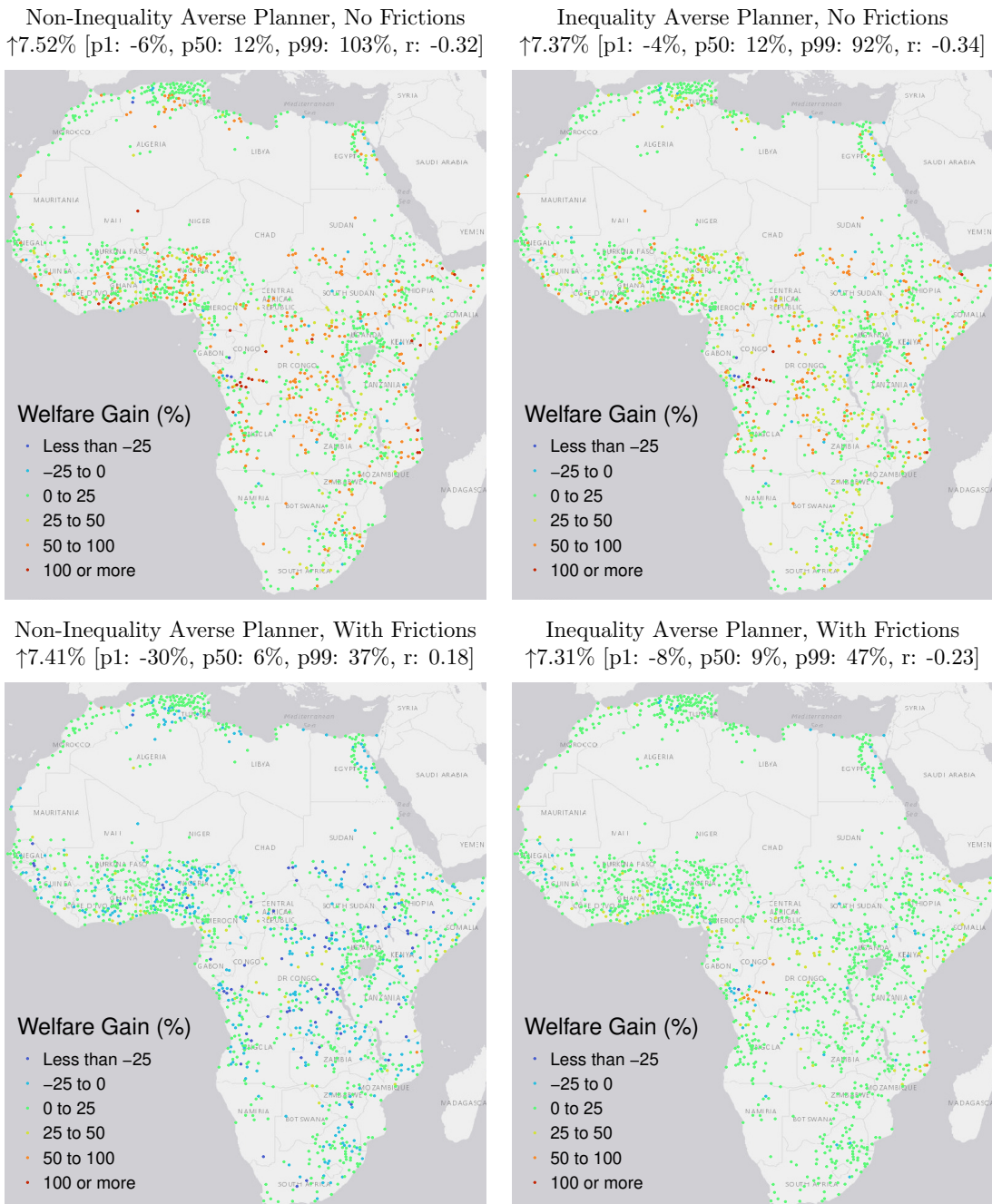
Notes: Figure compares optimal allocations under IRS with/without an inequality averse planner and border frictions.

Figure 40 shows welfare gains for IRS scenarios. Gains under the inequality-averse planner are again slightly lower on average but more equal and redistributive at $r = -0.34$, up from $r = -0.32$. Due to the concave utility of consumption, the welfare gains are highest in more remote cities, which are now better connected. These results are consistent with [Gorton & Ianchovichina](#)

³⁶Due to bespoke numerical challenges, I again test this setting $\alpha = 0.1$ to compute the optimal infrastructure allocation and re-solve the spatial model with $\alpha = 0.7$ afterwards.

(2021). The frictions case under IRS is particularly interesting. The non-averse planner achieves an aggregate welfare gain of 7.41%, but the median city only gains 6%, with welfare losses up to -30% in remote cities due to trade diversion. The gains become non-redistributional at IWI correlation of $r = 0.18$. In stark contrast, the averse planner achieves a slightly lower aggregate welfare gain of 7.31%, but the median city gains 9%, the overall distribution of city-level gains is much more positive, and the gains are redistributional at $r = -0.23$.³⁷ Overall, the IRS allocation with inequality-averse planner yields socially optimal outcomes and significantly enhances regional connectivity through >160K km of road upgrades and 2.5K km of strategic new roads. Currently, there is no empirical evidence supporting the IRS case, but suitable data on trade costs, traffic flows, and road upgrades along African highways could produce such evidence.

Figure 40: Local Utilitarian Welfare Gains Under Increasing Returns



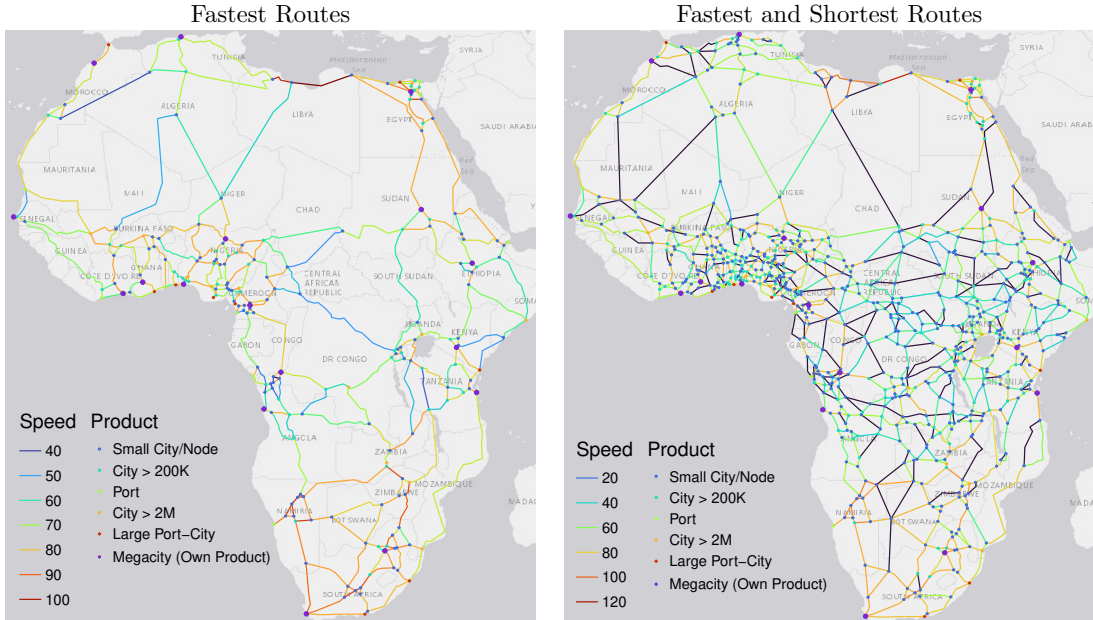
Notes: Figure shows welfare gains from IRS allocations with/without an inequality averse planner and border frictions.

³⁷This result, verified by re-solving the model under both allocations and frictions with the same parameters, is purely the outcome of 'minor' strategic differences in road investments as shown in the bottom half of Figure 39.

6.2 Optimal Trans-African Network Investments

Having examined optimal regional network investments by letting cities of different sizes and ports trade with each other, I now examine optimal investments in trans-African roads connecting the largest 47 (port-)cities on the reduced networks developed in Section 4.4. To create strong incentives for trans-African trade, I let 17 large and strategically located megacities produce their own goods. Other cities are classified into large port cities (population >1M and outflows >1M TEU in 2020Q1), large cities (population >2M), ports (outflows >0), medium sizes cities (population >200K) and small cities otherwise. Figure 41 shows the classified networks.

Figure 41: Trans-African Network Connecting Large Cities: Parameterization



Notes: Figure shows networks connecting 47 large (port-)cities with link speeds and a classification of traded products.

These networks are consistent with the larger network considered so far and parameterized using the same routing data. Edges are contracted by summing distances and travel times and recalculating travel speeds on the new, longer edges. Appendix Figure A21 provides an equivalent representation of the fastest-routes network with real roads along the original edges, illustrating that some of these 'long edges' are a patchwork of different roads at heterogeneous travel speeds.

6.2.1 Fastest Route Investments under Decreasing Returns

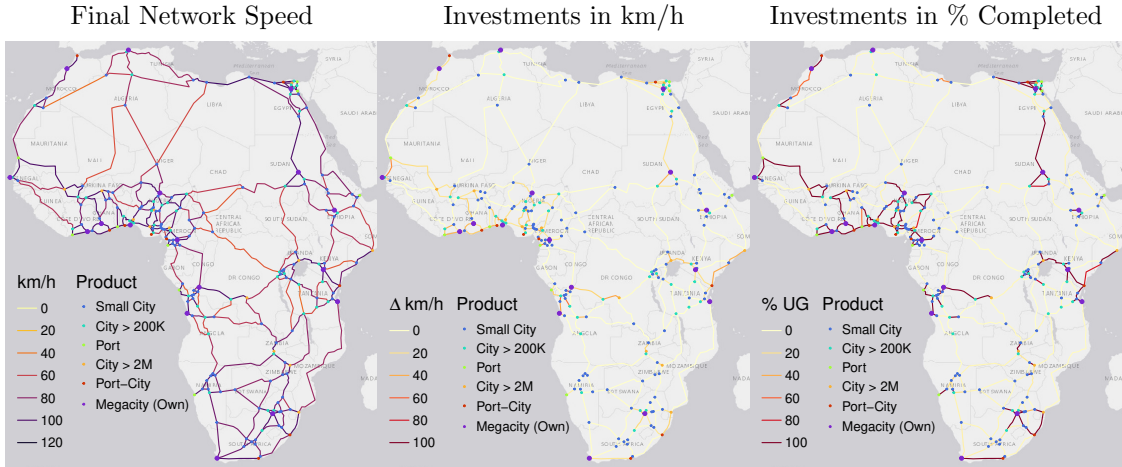
I begin by considering just upgrades along the existing fastest routes. These sum to a total cost of \$33B. I assume the planner has \$10B to invest in trans-African roads - about 1/3 of the total needs. The parameterization otherwise follows the previous subsection, with added international productivity in port cities to account for imports. I use $\sigma = 3.8$ as benchmark elasticity following Bajzik et al. (2020) and Armington (1969), but also run simulations with $\sigma = 5$ and $\sigma = 2$.

Figure 42 shows that under DRS ($\gamma < \beta$), the \$10B planner mainly invests in connections between large cities, megacities, and ports. This includes better connecting Khartoum to upper Egypt, Kampala to Mombasa, Kinshasa to Mbaji-Mayi, and improving connectivity in West Africa, particularly along the extended coastline between Abidjan and Yaounde. In total the planner completely upgrades 40,164km of roads. The welfare gains of only 0.04% are very small and nonredistributional at $r = 0.13$ correlation with the IWI. Similar to the $\sigma = 4$ cases considered above, the equilibrium is close to autarky: small cities consume >95% and megacities >99.7% of their own produce. Appendix Figure A22 visualizes the flow of goods.

Unlike the four good case on the full network, optimal investments are quite sensitive to the value of σ . Appendix Figure A23 provides a comparison. While σ values of 3.8 and 5 yield relatively similar results (under $\sigma = 5$ the planner interestingly better connects Kinshasa to

Bukavu/Rwanda), the $\sigma = 2$ planner spends much more on roads crossing central Africa. Notably, a significant fraction of the budget is devoted to upgrading an expensive road across the DRC connecting Bukavu/Rwanda to Bangui in the Central African Republic. (S)he also better connects Khartoum to West Africa and upgrades a segment in Algeria common to two trans-Saharan roads, instead of better connecting Khartoum to Egypt, Dakar to Bamako, and Mombasa to Mogadishu.

Figure 42: Optimal Trans-African Network Investments



Notes: Figure shows the optimal allocation of a \$10B social planner investing in the trans-African fastest routes network.

In the model, σ governs consumers' love for trans-African variety, but we may also reinterpret σ from the production side as a propensity to form trans-African regional value chains (RVCs). Thus, the results signify that, under decreasing returns to infrastructure, significant efforts to upgrade central African roads - the worst on the continent - are only sensible if consumers' love for variety or the propensity to form RVCs is relatively strong. Ignoring imports again shifts optimal investments slightly to interior roads, as the upper middle panel of Appendix Figure A23 shows.

With inequality aversion ($\rho = 2$), the optimal allocation, reported in Figure 43 and further in Appendix Figure A24 for different σ values, changes slightly. The planner invests more in poorer countries such as Angola, Congo, and Somalia/Ethiopia, and less in other regions. Welfare gains are again small at maximally 0.5% under $\sigma = 2$ (and 0.03% under the benchmark $\sigma = 3.8$) and thus not reported in further detail. But their distribution remains modestly non-redistributive at $r = 0.13$. Consumption remains relatively autark, with megacities consuming >99.7% of their own produce under the benchmark $\sigma = 3.8$, and >98.7% under $\sigma = 2$.

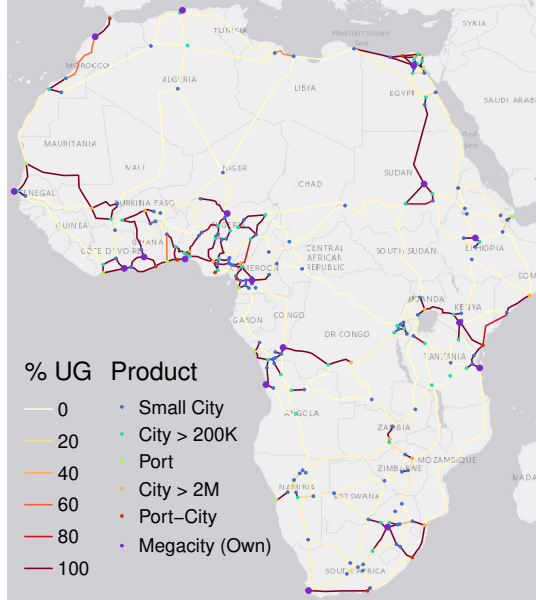
The optimal investment allocation is also largely unaffected by the inclusion of border frictions into δ_{jk}^τ (Eq. 12), as the bottom panel of Figure 43 and the lower middle panels of Appendix Figures A23 and A24 show. Since in PE (Section 5), frictions had a significant impact on optimal allocations, this suggests that the iceberg formulation (Eq. 11) with logarithmic distance (Eq. 12) may not be the most appropriate way to include them. Better accounting for border frictions in quantitative spatial models with endogenous infrastructure thus invites further research.

6.2.2 Fastest Route Investments under Increasing Returns

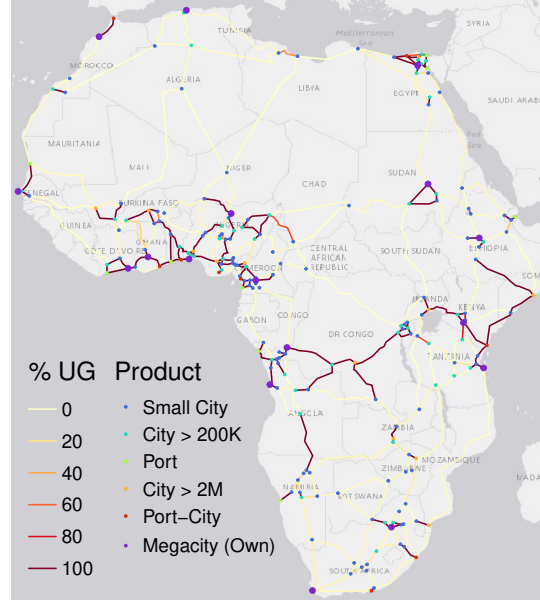
Surprisingly, with increasing returns to infrastructure ($\gamma > \beta$), the optimal allocation, reported in Figure 44 and, in more detail, Appendix Figure A26, hardly changes. Only locally there are minor differences to Figure 42 in terms of which segments are upgraded. This suggests that the returns to infrastructure are less important when restricting the planners' choice to important transport routes. The propensity to trade long distances, governed by σ , is the key parameter governing optimal allocations. However, interestingly, trade flows still increase considerably under IRS, as Appendix Figure A25 shows. The total welfare gains from the investment at 0.16% are still small but considerably larger than the 0.04% under decreasing returns. But they remain non-redistributional ($r = 0.14$), and megacities consume more than 98.2% of their own produce. Appendix Figure A27 provides sensitivity analysis with very similar results to the DRS case.

Figure 43: Optimal \$10B Trans-African Network Investments: Different Scenarios

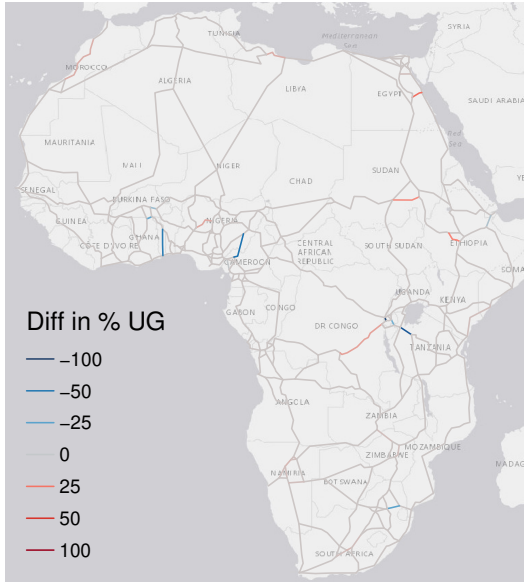
Non-Inequality Averse Planner, No Frictions
Upgrades 40,164km



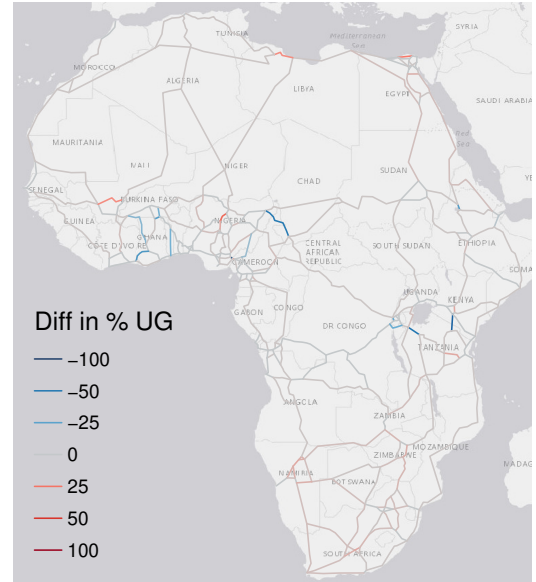
Inequality Averse Planner, No Frictions
Upgrades 37,407km



Non-Inequality Averse Planner, With Frictions
Upgrades 40,273km



Inequality Averse Planner, With Frictions
Upgrades 37,857km



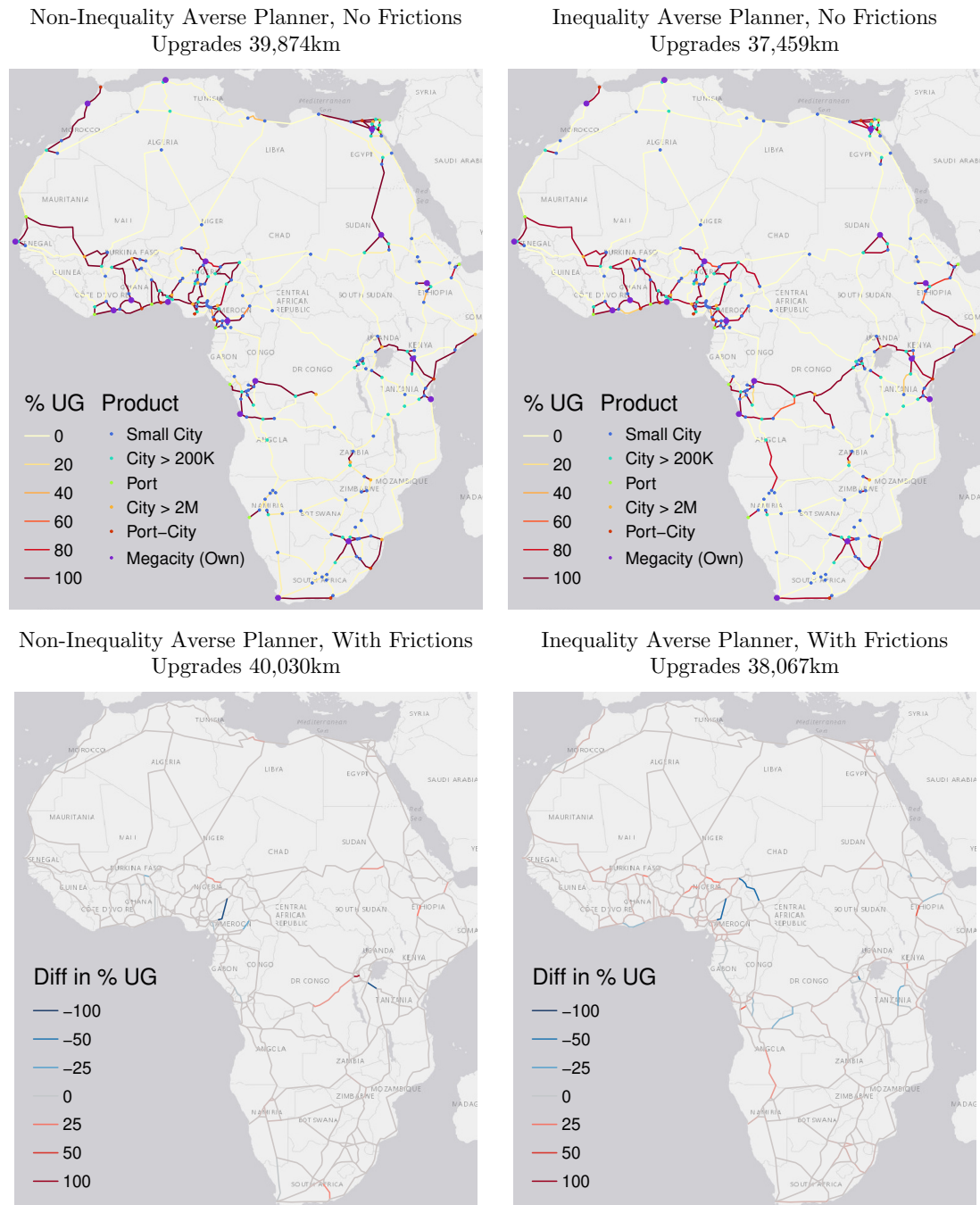
Notes: Figure compares optimal allocations (in % upgraded) with/without inequality averse planner and border frictions.

As under DRS, making the planner inequality averse ($\rho = 2$) redistributes investments to poorer regions, particularly in DR Congo, Angola, and Sudan/Ethiopia. The allocation is again relatively insensitive to including border frictions, the most notable difference being cross-border roads into Nigeria from Cameroon and Chad, which are not upgraded under frictions. The average cost of crossing the Nigerian border is estimated equivalent to 1944km of road distance.

Thus, the distribution of optimal investments in trans-African roads depends on the elasticity of substitution (σ) and the planner's inequality aversion (ρ). The central African infrastructure gap evident from Figures 2 and 4 is particularly interesting. This vast area is largely unpopulated; hence, the optimal regional planner of Section 6.1 does not place much infrastructure there. The non-averse trans-African planner in this section does the same under standard assumptions of $\sigma = 3.8$ or $\sigma = 5$. With inequality aversion ($\rho = 2$) (s)he fully upgrades the road from Kinshasa

to Bukavu and builds roads in Angola and Somalia. However, significant efforts to close the gap in northern central Africa require elasticities as low as $\sigma = 2$ (see Appendix Figures A23, A24, A27, and A28). In other words, it requires optimism about the development of trans-African trade and RVCs to prioritize upgrading these roads. Presently, trade between ECOWAS and the EAC + IGAD combined makes up 0.2% of total inner-African trade and 0.7% of inner-African trade between different regional economic communities. Closing the central African infrastructure gap is likely to increase these shares significantly, but, as discussed, only a policy priority if σ is lower than typically assumed. Another priority is the reduction of border frictions, which, as Figures 8-9 show, are extremely high along Congolese borders. Appendix Figures A23 and A24 show that under frictions and $\sigma = 2$, the planner reduces investments on the Bukavu-Bangui link by around 25% - and likely by more if frictions were incorporated into the framework in a better way. Thus, this intriguing link is not a reasonable present policy option for a \$10B social planner.

Figure 44: Optimal \$10B Trans-African Network Investments under IRS: Different Scenarios



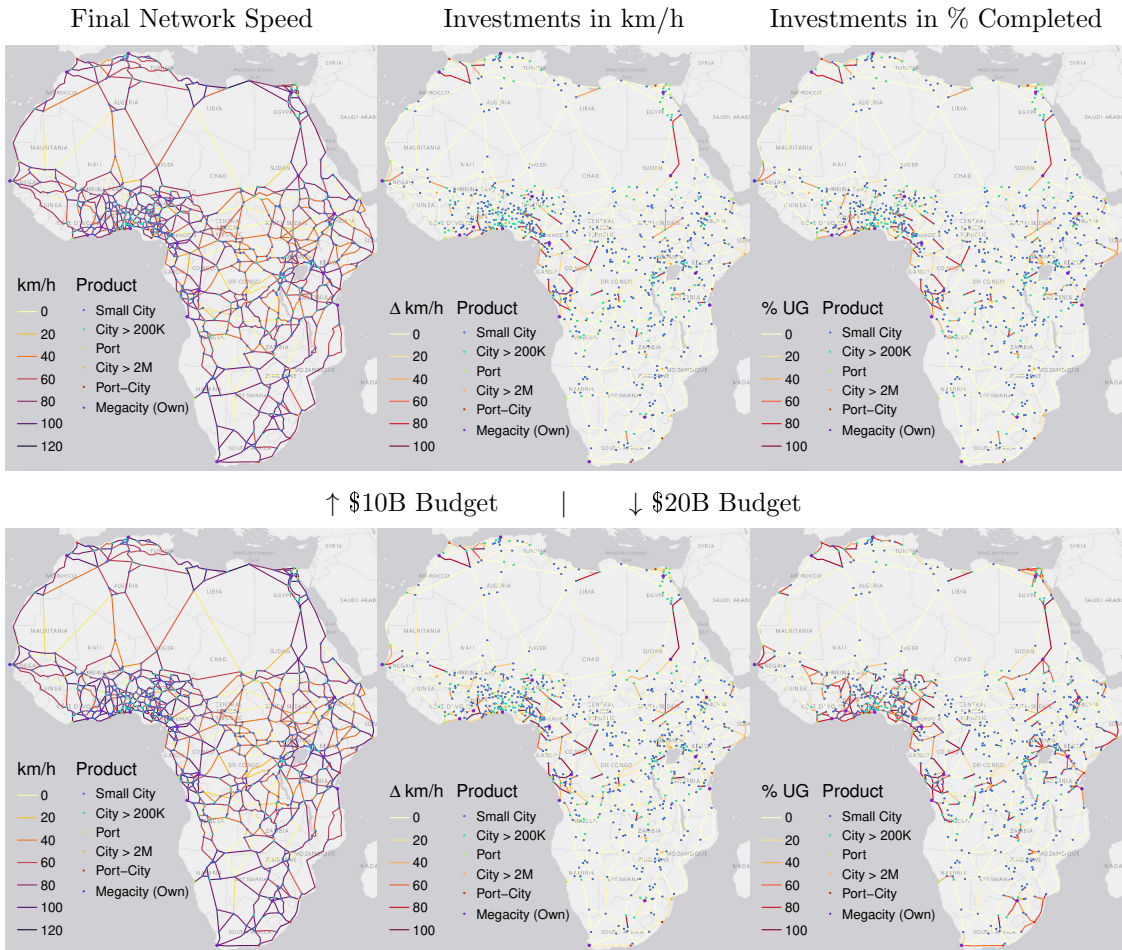
Notes: Figure compares optimal allocations (in % upgraded) under IRS with/without inequality aversion and frictions.

6.2.3 Fastest and Shortest Route Investments

It remains to consider the trans-African network comprising both fastest and shortest routes. With 707 nodes and 1274 edges, it gives the planner considerably more choices to improve trans-African connectivity. The total potential investment volume into this network is \$93B. Therefore, a planning budget of only \$10B imposes a tight resource allocation problem. To loosen the resource constraint a bit, I additionally consider a \$20B planner. With 22 goods, the model takes modern non-linear optimizers to their limits. I can only solve it by assuming strong duality, which, following Fajgelbaum & Schaal (2020), requires $\gamma < \beta$ and $\beta \leq 1$. Hence, I set $\beta = 1$.

Figure 45 shows both planner's allocations. Ostensibly, they are more similar to the optimal regional investments from Section 6.1 than those in fastest routes. Both planners better connect Khartoum to Egypt, build/upgrade roads surrounding Juba, Kampala, Kinshasa, Luanda, Mbandaka, Dakar, and many West African cities, and better connect Morocco to Algeria. Thus, even with a richer trade characterization incentivizing trans-African trade, investments in major trans-African roads are not a priority if planners can divert away from them, at least under $\sigma = 3.8$.

Figure 45: Optimal Trans-African Network Investments: Shortest Routes



Notes: Figure shows optimal allocations of \$10B & \$20B planners investing in the trans-African shortest routes network.

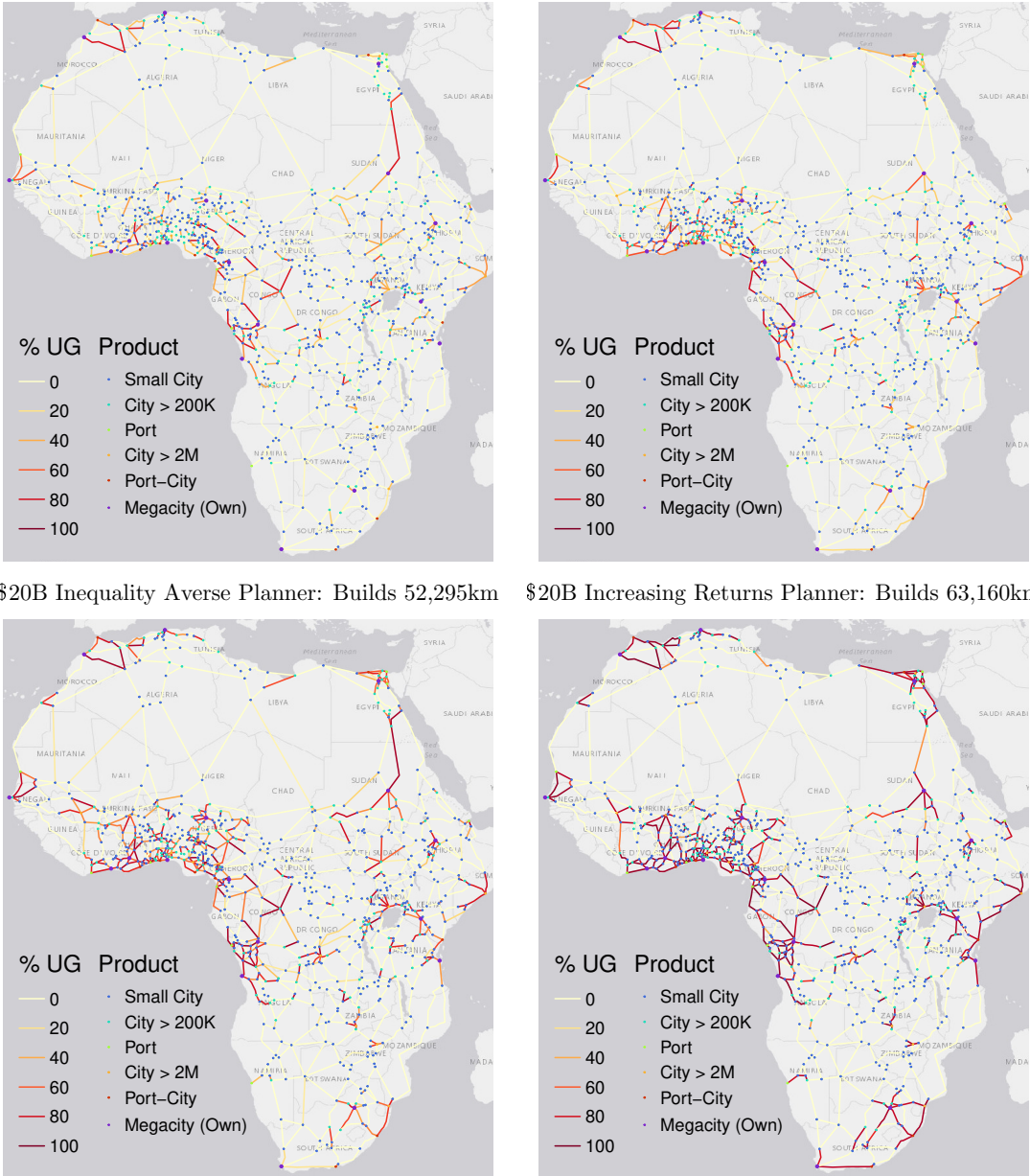
Appendix Figure A30 provides results for different σ values, including the impact of border frictions. Under $\sigma = 2$ the planners again become more cosmopolitan and, notably, invest mildly in new trans-Saharan links (not in upgrading existing ones), links better connecting Cape Town to Botswana and further north, and significantly improve the connectivity of Luanda, Kinshasa and other Congolese cities to West Africa. Building new trans-Saharan links rather than upgrading existing ones is a particularly interesting choice. Likely these links are significantly more expensive than modelled taking into account just terrain and population, thus this allocation is not cost-efficient. But it clearly shows the planners desire to enable more route-efficient travel between North- and Sub-Saharan Africa. Compared to the network with only fastest routes, the flow of

goods is much more focused on nearby cities. The welfare gains under $\sigma = 3.8$ are small at 0.12%/0.21% for the \$10B/\$20B planner and mildly redistributive ($r = -0.08 / -0.1$). When lowering σ to 2, the welfare gains increase to 1.34%/2.11%. Appendix Figure A31 provides details.

To cut short the discussion of different scenarios, Figure 46 reports results for inequality averse planners ($\rho = 2$) and IRS planners ($\gamma > \beta$). Averse planners again invests more in central Africa, Angola and Somalia. IRS planners expend more efforts connecting Morocco to Algeria and the populated regions around Kinshasa and Luanda to West Africa, while reducing connectivity from Khartoum to Egypt and around major cities such as Juba. Aggregate welfare gains again drop slightly to 0.1%/1.7% under averse planners, and increase to 0.52%/0.91% under the IRS planners. Appendix Figures A32 and A33 analyze their sensitivity to different σ values.

Figure 46: Optimal Trans-African Network Investments: Shortest Routes: Different Scenarios

\$10B Inequality Averse Planner: Builds 21,491km \$10B Increasing Returns Planner: Builds 26,848km



Notes: Figure illustrates optimal \$10B and \$20B allocations under IRS ($\gamma > \beta$) or inequality averse planners.

Overall, the results even under $\sigma = 2$ are quite regionally focused. I thus also run simulations for $\sigma = 1.5$, generating much larger trade flows and incentives for pan-African investments. Appendix Figures A34 and A35 reports these results for different planners. The investments are indeed much more pan-African. Research on Armington elasticities between African cities could disambiguate.

7 Summary and Conclusion

Using detailed routing data, large and accurate network graphs, and a rich economic geography including population, wealth/gdp, trade through ports, border frictions, road construction and upgrading costs, this paper rigorously examines Africa's full continental road network and characterizes optimal investments into it in partial and general equilibrium (PE and GE).

Presently, Africa has 1.6 million km of non-residential roads, around 30% of which are paved. This fraction differs significantly by country and road type. Particularly in central Africa, the Sahara, and the Horn of Africa region, most roads are unpaved and rough, severely limiting trans-African connectivity. The network's overall route efficiency (RE) of 0.68 is acceptable but considerably lower than that of the US network at 0.84. The time efficiency and average travel speed along many roads is significantly worse than in other world regions. Particularly the aforementioned regions can only be traversed at speeds around 40km/h. In addition, cross-border frictions substantially impede continental market access (MA). Estimates suggest that crossing the median border in Africa is as costly as 1043km of road distance, and the time commitment is equivalent to 3.2 days of travel time. These frictions induce an aggregate MA loss between 26% and 78%. Locations across the border from major markets such as Nigeria suffer MA losses of up to 80%.

Given a detailed network and economic geography, optimal road investments still depend on the geographic scale and magnitude of the investment and the planner's objective (MA or welfare maximization with/without inequality aversion). Structural parameters such as the trade elasticity/elasticity of substitution and returns to scale in infrastructure also noticeably impact optimal spatial allocations, as do heterogeneous road construction costs and border frictions. The paper navigates this complexity via a graduated approach, starting with high-resolution small-scale PE investments and gradually progressing towards lower-resolution GE simulations where social planners spend large amounts. This requires different network representations and methods.

Considering first local network investments surrounding 50.3km equally spaced grid cells, I find that increasing connectivity in densely populated high-activity areas such as West Africa around Nigeria, greater Johannesburg, East Africa between Bukavu and Nairobi, Sudan around Khartoum, Upper Egypt, Kinshasa and Luanda, and in corridors connecting these economic areas where transport roads are already present, yields the greatest marginal MA gains. Figures 17 and A11 map out such corridors of high marginal gains, synthesizing rich data on the road network and the distribution of economic activity via an optimally weighted graph.

To increase the scale of investments to entire roads or collections of segments, I build a detailed representation of the transport network connecting 447 important cities and 52 ports along the fastest routes. My network graph has 1379 nodes and 2344 edges (links), summing to 315K km. I apply a network finding algorithm and find 481 potential new links summing to 104K km. Building them all would raise RE by 7.1%, from 0.68 to 0.72, and MA (denominated in road distance) by 5.5%. The most valuable links increasing RE/MA by more than 0.1% are new trans-Saharan roads through Mauritania, Mali, and Chad and reopening the closed Morocco-Algeria border. Some new roads in central and southern Africa would also significantly increase RE/MA. When border frictions are activated, the MA gain drops from 5.5% to 3.9%, with particularly high losses on remote and border-crossing links. The median link yields a 50% lower MA gain under frictions.

According to the World Bank ROCKS database, the median 2-lane highway in Africa costs \$611K 2015 USD per km. Using a heterogeneous road costs prediction model considering road length, terrain ruggedness, and population density, I estimate the cost of the existing transport network at \$186B USD'15, and the proposed extension of \$104K km at \$56B, yielding an average MA return of \$1.4/km per \$ invested in new links, which drops to ~\$0.7/km/\$ if frictions are added.

Examining road quality measured by travel speed, I find that upgrading all links to $\geq 100\text{km/h}$ yields a time-denominated MA gain of 42.1%. New links yield a 14.1% MA gain if built at 100km/h on top of the existing (slow) network. Upgrading the entire network to fast links and also building the proposed ones could yield a 50% MA gain. There is significant heterogeneity in the value of upgrading links, with trans-Saharan links yielding the greatest MA gains. Applying border frictions

lets the total MA gain from upgrading all links drop to 27%. Again, particularly peripheral and transnational links lose value. I estimate the cost of upgrading the entire network at \$106B, comprising \$67.8B full upgrades, \$36.5B mixed works, and \$12.3B asphalt resurfacing. Upgrading all roads yields average gains of \$6/min per \$ spent, which drops to \$2.4/min/\$ under frictions.

To raise average returns, I consider investment packages targeting high marginal gain links (both upgrades and new roads). I propose three packages with links at marginal gains >1 , 2 , or 4 \$/min/\$. They cost \$60.9B/\$36.6B/\$17B, yield frictionless MA gains of 38.1%/30.6%/20%, and 26.8%/24%/19.5% under frictions. These packages are globally macroeconomically feasible under frictions if they can raise Africa's aggregate growth rate (4.1%) by 0.33%/0.2%/0.09%. For the $>\$1$ (\$60.9B) package, this would require that growth in MA translates into economic growth at a rate of $\geq 81:1$. This is plausible in light of empirical results suggesting economic returns to MA gains as high as 2:1, but there are several factors that could raise the cost of these packages considerably and lower the macroeconomic returns, especially if they are financed through debt.

Calibrating a general equilibrium framework by [Fajgelbaum & Schaal \(2020\)](#) permitting global optimization over the space of networks, I also derive optimal investments in spatial equilibrium, letting a welfare-maximizing social planner spend a fixed infrastructure budget. My calibration accounts for trade in multiple goods and through international ports. I consider cases with/without inequality aversion, imports, cross-border frictions, and increasing returns to infrastructure. I also simulate with different values for the elasticity of substitution (σ). Due to the computational complexity of the problem, I split the simulations into two parts. In Part 1, a regional planner improves connectivity between small/medium/large cities and ports. In Part 2, a trans-African planner optimally invests in continental transport roads connecting 47 major (port-)cities.

The regional planner with a budget of \$50B optimally connects large cities and ports with each other and surrounding smaller cities, focusing on populated/productive areas. An inequality-averse planner invests slightly more in the poorer central African and the Horn of Africa regions. With increasing returns to infrastructure, the investments become less concentrated around large cities, and the planner upgrades more roads (building few new ones). This increases welfare gains to 7.4%, up from 5.8% under decreasing returns. With inequality aversion, the gains become more equitable at minor aggregate losses, and the planner upgrades more roads in central Africa. Due to concave utility of consumption, remote cities gain more despite receiving less infrastructure.

The trans-African planner, endowed with \$10B, also mostly improves regional connectivity under standard assumptions of σ between 3.8 and 5. Much is invested along the West African coastline, but also in better connecting Dakar to Bamako, Khartoum to Egypt, Kampala to Mombasa, and Kinshasa to Mbuji Mayi. An inequality-averse planner fully connects Kinshasa to Bukavu/Rwanda and further to Mombasa, Mogadishu, and Addis Ababa. Thus, the planner upgrades a corridor crossing populated central Africa. At low $\sigma = 2$, both planners also close the large infrastructure gap in sparsely populated northern central Africa by upgrading roads from Rwanda/Bukavu and Khartoum to West Africa. Thus, optimal trans-African investments depend critically on the propensity to trade. Only at low σ do major infrastructure gaps in central Africa become a policy priority. High border frictions reduce equilibrium investments along affected links.

In conclusion, the paper characterizes optimality for road network investments at different spatial scales and economic objectives from a pan-African perspective. It thus provides broad guidance for policymakers interested in improving Africa's road infrastructure. An overarching finding is that trans-African roads are neither MA nor welfare maximizing compared to benefits from improved local connectivity in populated areas or between nearby cities and coastal ports. This is especially true under border frictions, which reduce the value of trans-African links. Yet, these links are essential for trans-African trade under AfCFTA to pick up. A general policy recommendation is thus to prioritize regional connectivity improvements, reduce border frictions, and invest in trans-African roads along specific high-yield links/corridors. The graphical results provided in the paper and appendix should be helpful in prioritizing continental and regional investments, with detailed data and results available upon request. The multi-level approach combining routing engines, PE, and GE analysis can also be adapted to further examine specific regions/investments. Towards this end, a new [Julia library](#) for general equilibrium analysis is utile.

References

- Abbasi, M., Lebrand, M. S. M., Mongoue, A. B., Pongou, R., & Zhang, F. (2022, March). *Roads, Electricity, and Jobs: Evidence of Infrastructure Complementarity in Sub-Saharan Africa* (Policy Research Working Paper Series No. 9976). The World Bank. Retrieved from <https://ideas.repec.org/p/wbk/wbrwps/9976.html>
- ADB. (2010). *African development report 2010: Ports, logistics and trade in africa*. African Development Bank. Retrieved from <https://www.afdb.org/en/documents/document/african-development-report-2010-27559>
- African Development Bank. (2014). *Study on road infrastructure costs: Analysis of unit costs and cost overruns of road infrastructure projects in africa* (Tech. Rep.). Abidjan, Côte d'Ivoire: African Development Bank Group. Retrieved 2023-05-23, from https://www.afdb.org/fileadmin/uploads/afdb/Documents/Publications/Study_on_Road_Infrastructure_Costs-_Analysis_of_Unit_Costs_and_Cost_OVERRUNS_of_Road_Infrastructure_Projects_in_Africa.pdf
- Alder, S. (2016). Chinese roads in india: The effect of transport infrastructure on economic development. *SSRN Working Paper*. Retrieved from <https://ssrn.com/abstract=2856050> doi: 10.2139/ssrn.2856050
- Armington, P. S. (1969). A theory of demand for products distinguished by place of production (une théorie de la demande de produits différenciés d'après leur origine)(una teoría de la demanda de productos distinguiéndolos según el lugar de producción). *Staff Papers-International Monetary Fund*, 159–178.
- Asher, S., & Novosad, P. (2020, March). Rural roads and local economic development. *American Economic Review*, 110(3), 797-823. Retrieved from <https://www.aeaweb.org/articles?id=10.1257/aer.20180268> doi: 10.1257/aer.20180268
- Atkin, D., & Donaldson, D. (2015). *Who's getting globalized?: The size and implications of intra-national trade costs* (No. w21439). National Bureau of Economic Research Cambridge, MA.
- Atkin, D., & Donaldson, D. (2022). The role of trade in economic development. In *Handbook of International Economics* (Vol. 5, pp. 1–59). Elsevier.
- Bajzik, J., Havranek, T., Irsova, Z., & Schwarz, J. (2020). Estimating the armington elasticity: The importance of study design and publication bias. *Journal of International Economics*, 127, 103383.
- Barnes, R. (2020). dggridr: Discrete global grids [Computer software manual]. Retrieved from <https://CRAN.R-project.org/package=dggridR> (R package version 2.0.4)
- Baum-Snow, N., Henderson, J. V., Turner, M. A., Zhang, Q., & Brandt, L. (2020). Does investment in national highways help or hurt hinterland city growth? *Journal of Urban Economics*, 115, 103124.
- Bonfatti, R., Gu, Y., & Poelhekk, S. (2019). *Priority roads: The political economy of Africa's interior-to-coast roads* (Discussion Papers No. 2019-04). University of Nottingham, GEP. Retrieved from <https://ideas.repec.org/p/not/notgep/2019-04.html>
- Bosio, E., Arlet, J., Comas, A. A. N., & Leger, N. A. (2018). Road costs knowledge system (rocks)–update. *The World Bank, Washington, DC*.
- Burgess, R., Jedwab, R., Miguel, E., Morjaria, A., & Padró i Miquel, G. (2015). The value of democracy: evidence from road building in kenya. *American Economic Review*, 105(6), 1817–1851.
- Collier, P., Kirchberger, M., & Söderbom, M. (2016). The cost of road infrastructure in low-and middle-income countries. *The World Bank Economic Review*, 30(3), 522–548.
- Couture, V., Duranton, G., & Turner, M. A. (2018, 10). Speed. *The Review of Economics and Statistics*, 100(4), 725-739. Retrieved from https://doi.org/10.1162/rest_a_00744 doi: 10.1162/rest_a_00744

- Djankov, S., Freund, C., & Pham, C. S. (2010). Trading on time. *The Review of Economics and Statistics*, 92(1), 166–173.
- Donaldson, D., & Hornbeck, R. (2016). Railroads and american economic growth: A "market access" approach. *The Quarterly Journal of Economics*, 131(2), 799–858.
- Faber, B. (2014). Trade integration, market size, and industrialization: evidence from china's national trunk highway system. *Review of Economic Studies*, 81(3), 1046–1070.
- Fajgelbaum, P. D., & Schaal, E. (2020). Optimal transport networks in spatial equilibrium. *Econometrica*, 88(4), 1411–1452.
- Fiorini, M., Sanfilippo, M., & Sundaram, A. (2021). Trade liberalization, roads and firm productivity. *Journal of Development Economics*, 153, 102712.
- Foster, V., & Briceño-Garmendia, C. (2010). *Africa's infrastructure: a time for transformation*. World Bank.
- Gennaioli, N., La Porta, R., Lopez-de Silanes, F., & Shleifer, A. (2013). Human capital and regional development. *The Quarterly Journal of Economics*, 128(1), 105–164.
- Ghodsi, M., Grübler, J., Reiter, O., & Stehrer, R. (2017). *The evolution of non-tariff measures and their diverse effects on trade* (wiw Research Report No. 419). Vienna. Retrieved from <https://hdl.handle.net/10419/204191>
- Gorton, N. E., & Ianovichina, E. (2021, November). *Trade Networks in Latin America : Spatial Inefficiencies and Optimal Expansions* (Policy Research Working Paper Series No. 9843). The World Bank. Retrieved from <https://ideas.repec.org/p/wbk/wbrwps/9843.html>
- Graff, T. (2024). Spatial inefficiencies in africa's trade network. *Journal of Development Economics*, 103319.
- Jedwab, R., Kerby, E., & Moradi, A. (2017). History, path dependence and development: Evidence from colonial railways, settlers and cities in kenya. *The Economic Journal*, 127(603), 1467–1494.
- Jedwab, R., & Moradi, A. (2016). The permanent effects of transportation revolutions in poor countries: evidence from africa. *Review of Economics and Statistics*, 98(2), 268–284.
- Jedwab, R., & Storeygard, A. (2022). The average and heterogeneous effects of transportation investments: Evidence from sub-saharan africa 1960–2010. *Journal of the European Economic Association*, 20(1), 1–38.
- Krantz, S. (2023). Mapping africa's infrastructure potential with geospatial big data and causal ml. *SSRN Working Paper*. Retrieved from <https://ssrn.com/abstract=4537867> doi: 10.2139/ssrn.4537867
- Kummu, M., Taka, M., & Guillaume, J. H. (2018). Gridded global datasets for gross domestic product and human development index over 1990–2015. *Scientific Data*, 5(1), 1–15.
- Lamarque, H., & Nugent, P. (2022). *Transport corridors in africa*. Boydell & Brewer.
- Lee, K., & Braithwaite, J. (2022). High-resolution poverty maps in sub-saharan africa. *World Development*, 159, 106028.
- Mayer, M. (2023). missranger: Fast imputation of missing values [Computer software manual]. Retrieved from <https://CRAN.R-project.org/package=missRanger> (R package version 2.2.1)
- Moneke, N. (2020). Can big push infrastructure unlock development? evidence from ethiopia. *STEG Theme*, 3, 14–15.
- Nunn, N., & Puga, D. (2012). Ruggedness: The blessing of bad geography in africa. *Review of Economics and Statistics*, 94(1), 20–36.
- Peng, C., & Chen, W. (2021). *Roads to development? Examining the Zambian context using AI-Sat* [Working Paper]. Retrieved from <https://www.congpeng.org/>

- Poot, J., Alimi, O., Cameron, M. P., & Maré, D. C. (2016). The gravity model of migration: the successful comeback of an ageing superstar in regional science. *Investigaciones Regionales-Journal of Regional Research*(36), 63–86.
- Porteous, O. (2019). High trade costs and their consequences: An estimated dynamic model of african agricultural storage and trade. *American Economic Journal: Applied Economics*, 11(4), 327–366.
- Porteous, O. (2022). Reverse dutch disease with trade costs: Prospects for agriculture in africa's oil-rich economies. *Journal of International Economics*, 138, 103651.
- Redding, S. J. (2016). Goods trade, factor mobility and welfare. *Journal of International Economics*, 101, 148–167.
- Sahr, K. (2022). User documentation for discrete global grid generation software. *Southern Oregon Univ., Ashland, OR, USA, Tech. Rep. Dggrid version, 7.5*.
- Sahr, K., White, D., & Kimerling, A. J. (2003). Geodesic discrete global grid systems. *Cartography and Geographic Information Science*, 30(2), 121–134.
- Stekhoven, D. J., & Bühlmann, P. (2012). Missforest: non-parametric missing value imputation for mixed-type data. *Bioinformatics*, 28(1), 112–118.
- Teravaninthorn, S., & Raballand, G. (2009). *Transport prices and costs in africa: A review of the international corridors* (No. 6610). The World Bank Group. Retrieved from <https://ideas.repec.org/b/wbk/wbpubs/6610.html>
- Wang, H., Li, J., Chen, Q.-Y., & Ni, D. (2011). Logistic modeling of the equilibrium speed–density relationship. *Transportation Research Part A: Policy and Practice*, 45(6), 554–566.
- Wolfram, C. (2021, April). *Efficiency of road networks*. Blog post. Retrieved from <https://christopherwolfram.com/projects/efficiency-of-road-networks/> (Accessed on 27th March 2024)
- Zipf, G. K. (1946). The $p_1^*p_2/d$ hypothesis: on the intercity movement of persons. *American Sociological Review*, 11(6), 677–686.

Appendix

Figure A1: Average Network Speed and WorldPop Population Estimate

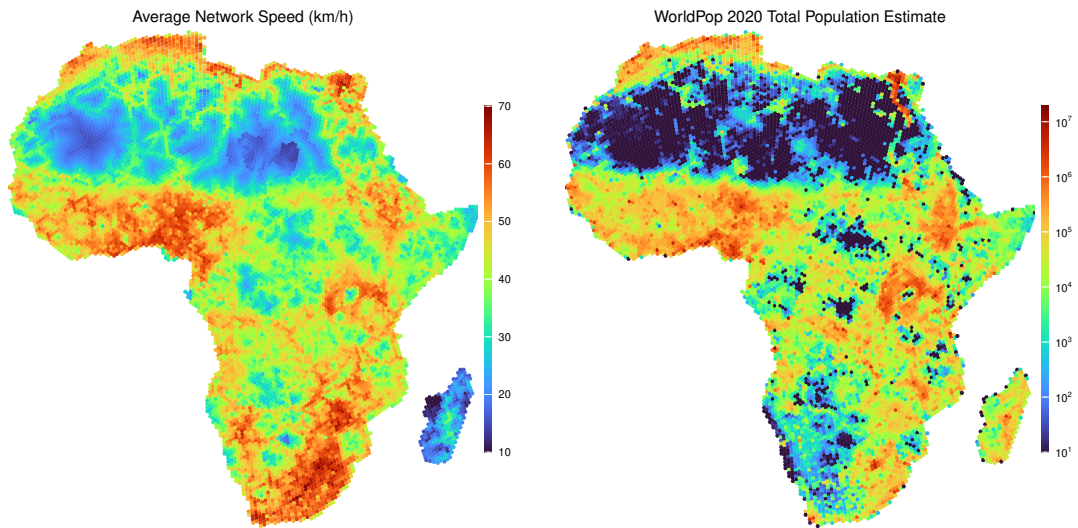


Figure A2: Gridded GDP and International Wealth Index

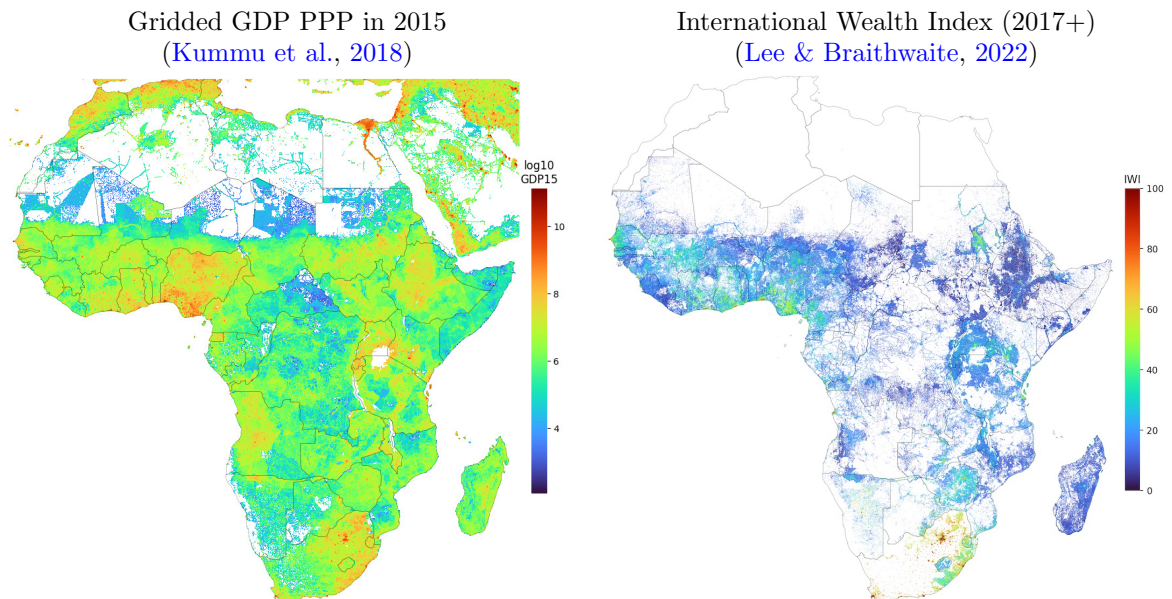
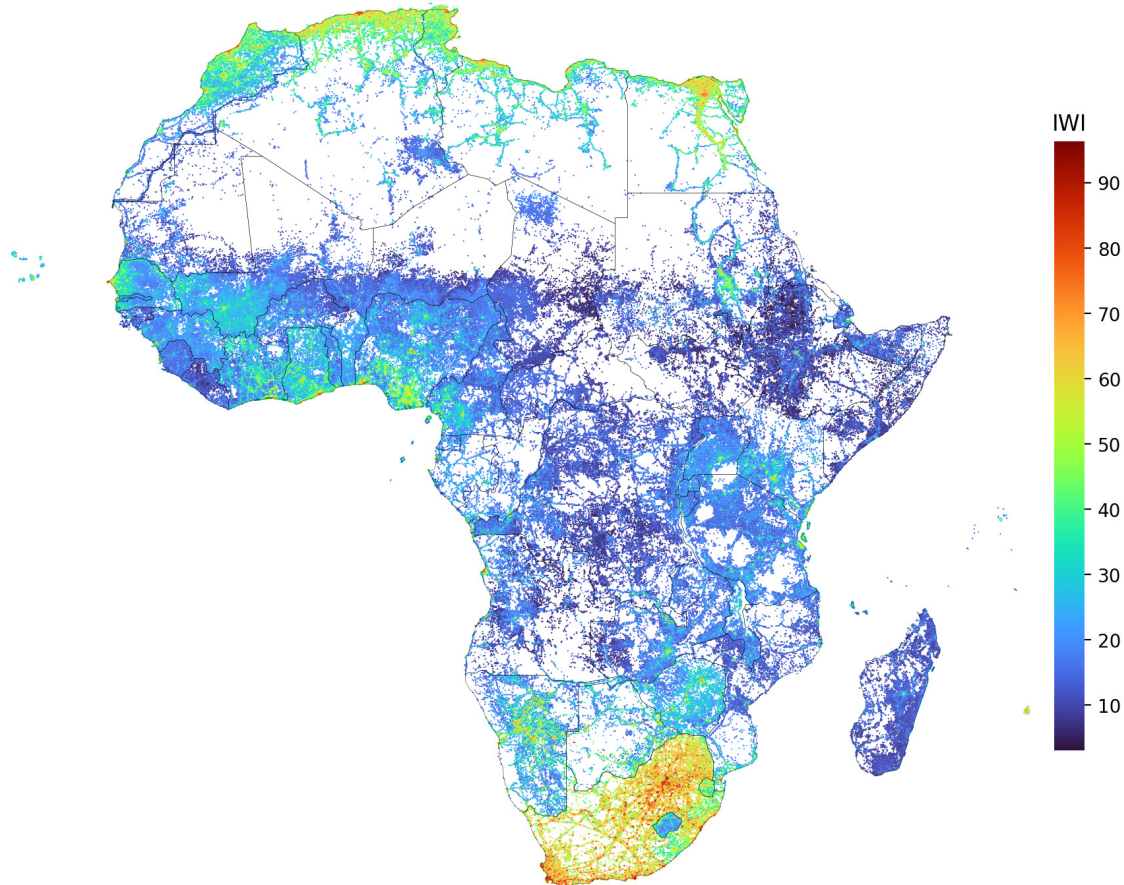


Figure A3: Imputed International Wealth Index using Database of [Krantz \(2023\)](#)

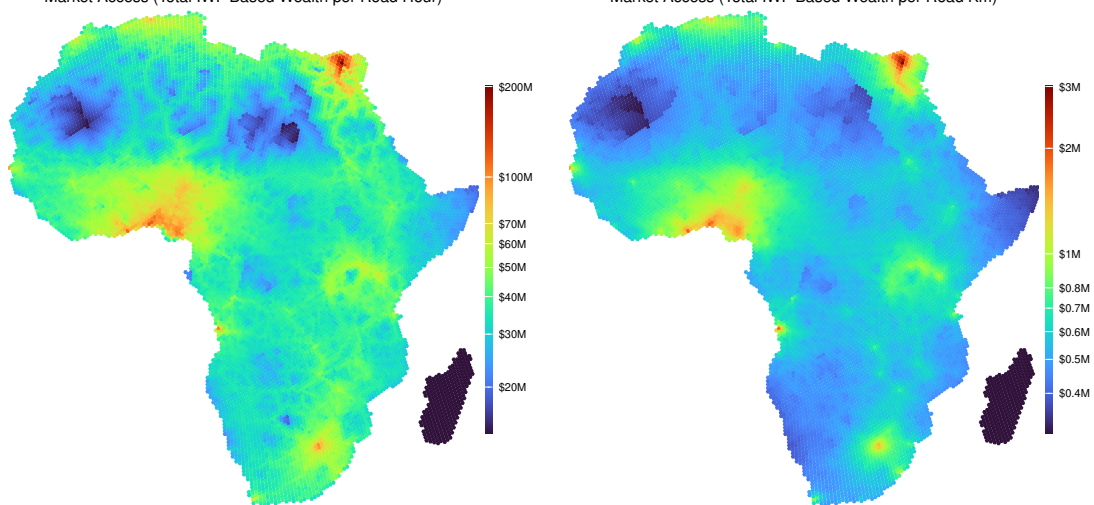
Predicted International Wealth Index: Imputed With MissForest, R-Squared = 0.970



Notes: The high R^2 is not surprising as the estimates of [Lee & Braithwaite \(2022\)](#) also utilize many features from OSM in their methodology and Random Forests is very flexible. A concern with the imputation is that the relationship between infrastructure and wealth may be different south of the Sahara. [Lee & Braithwaite \(2022\)](#) mention the absence of (recent) DHS surveys in North Africa as an obstacle to extending their methodology to them. Their success in estimating cross-country models for all of SSA, including South Africa, however suggests that these models - approximated by *MissForest* - should also provide acceptable predictions in North Africa.

Figure A4: Market Access Maps using Total IWI-Based Wealth

$\theta = 1$ ([Peng & Chen, 2021](#)), $\text{cor}(\text{MA}, \text{Wealth}) = 0.389-0.406$



$\theta = 3.8$ ([Jedwab & Storeygard, 2022](#)), $\text{cor}(\text{MA}, \text{Wealth}) = 0.876-0.966$

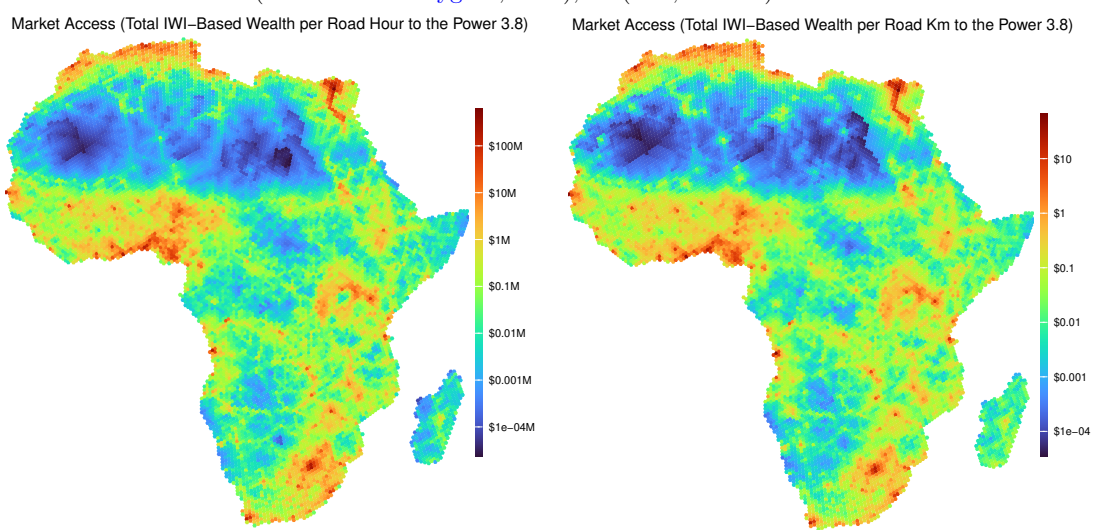


Figure A5: Market Access Maps using GDP in 2015 USD PPP: With Frictions

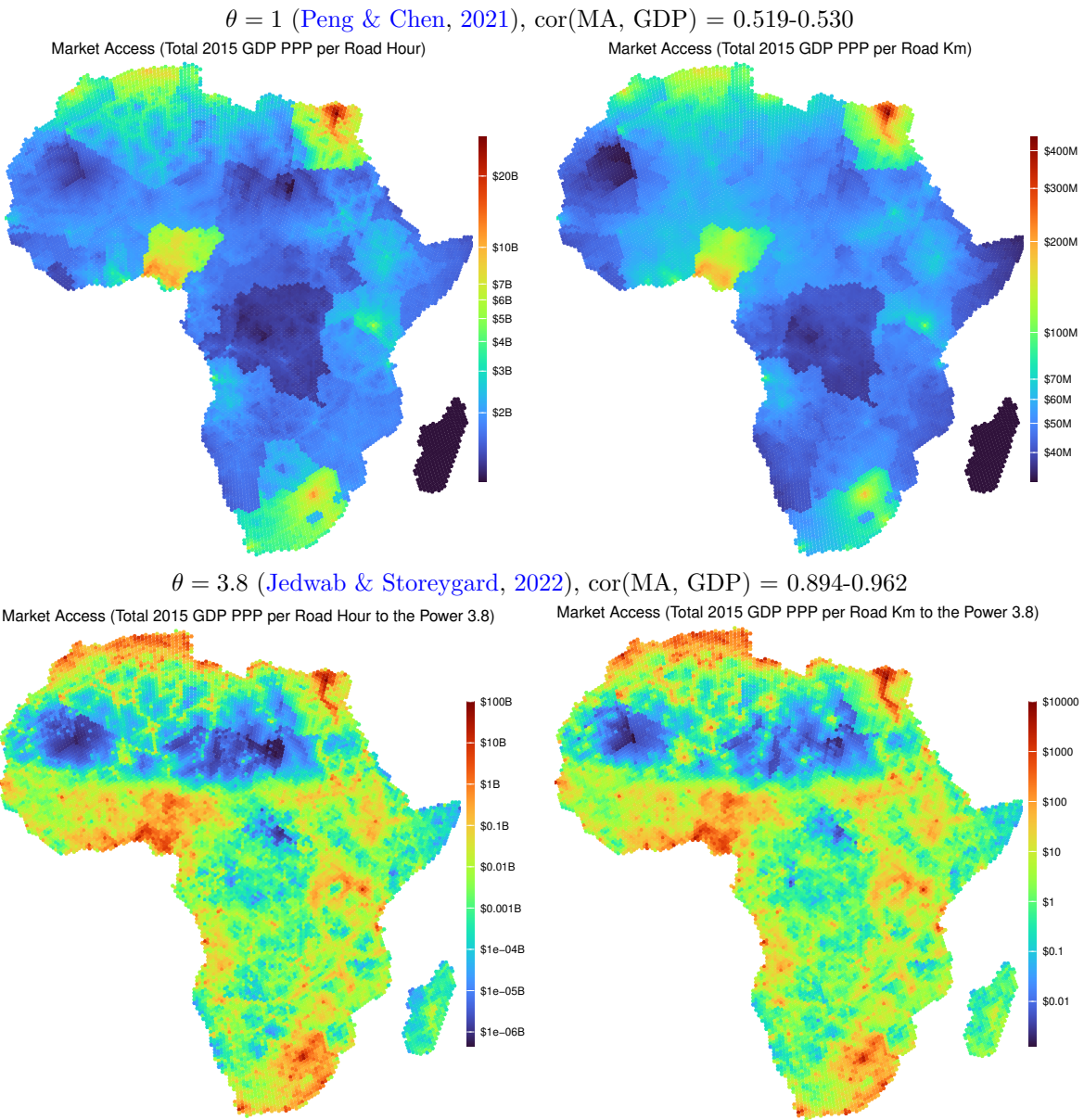


Figure A6: Market Access Maps using Total IWI-Based Wealth: With Frictions

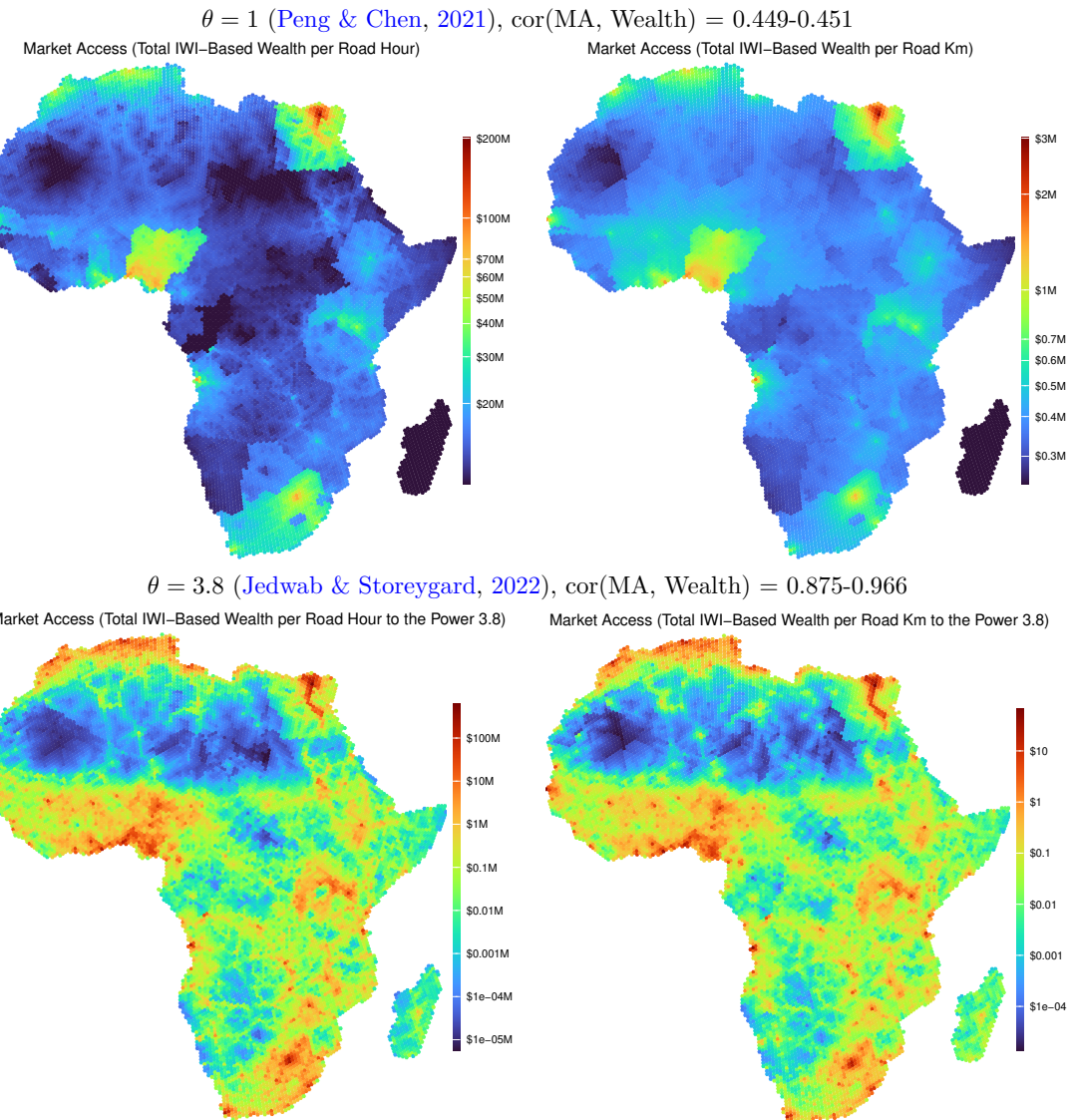
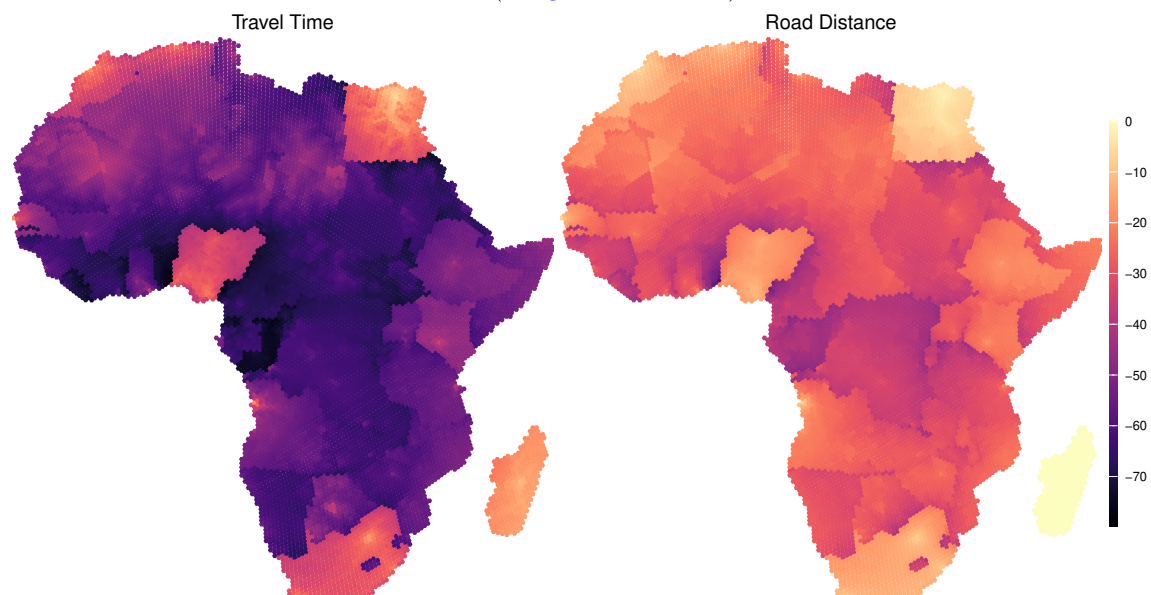


Figure A7: Market Access Loss (%) from Border Frictions using Total IWI-Based Wealth

$\theta = 1$ (Peng & Chen, 2021)



$\theta = 3.8$ (Jedwab & Storeygard, 2022)

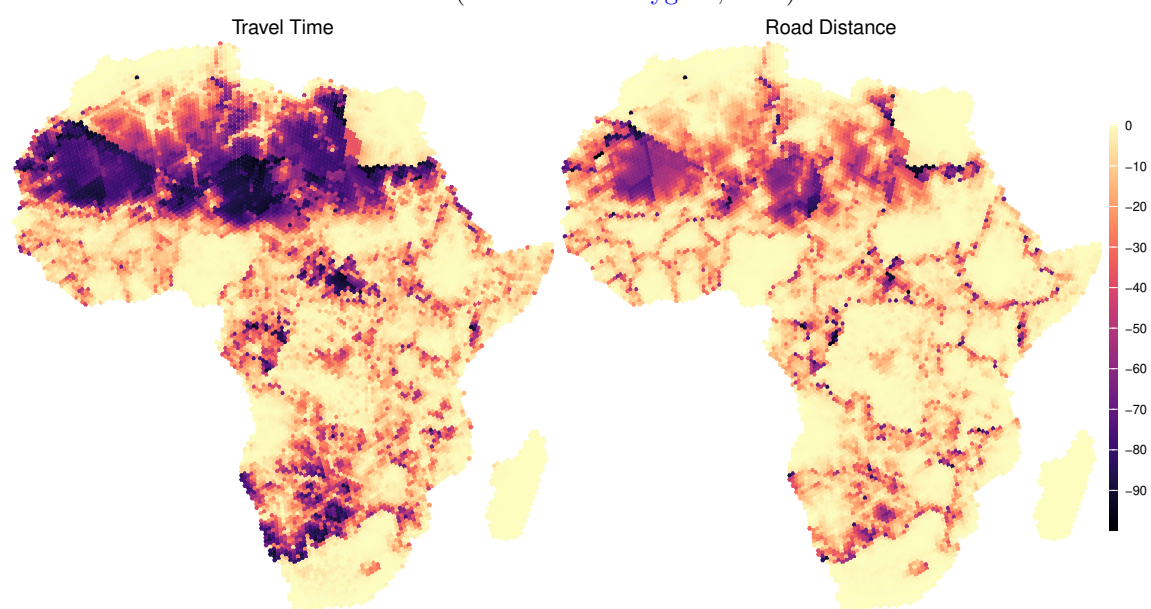


Figure A8: Optimized Full Network Graph: Duration Weighted Edges

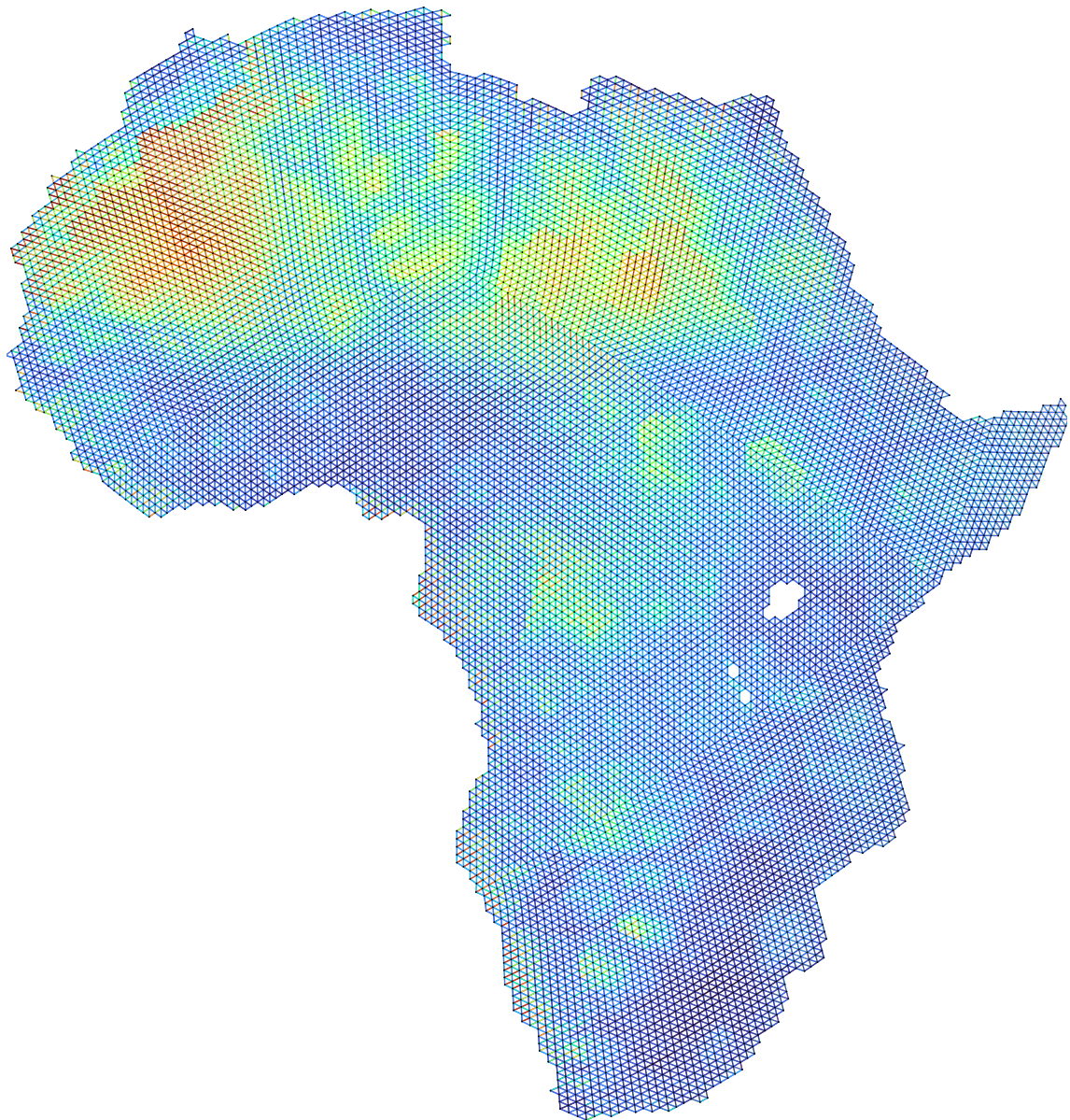


Figure A9: Discretized Trans-African Network Plus Original Routes

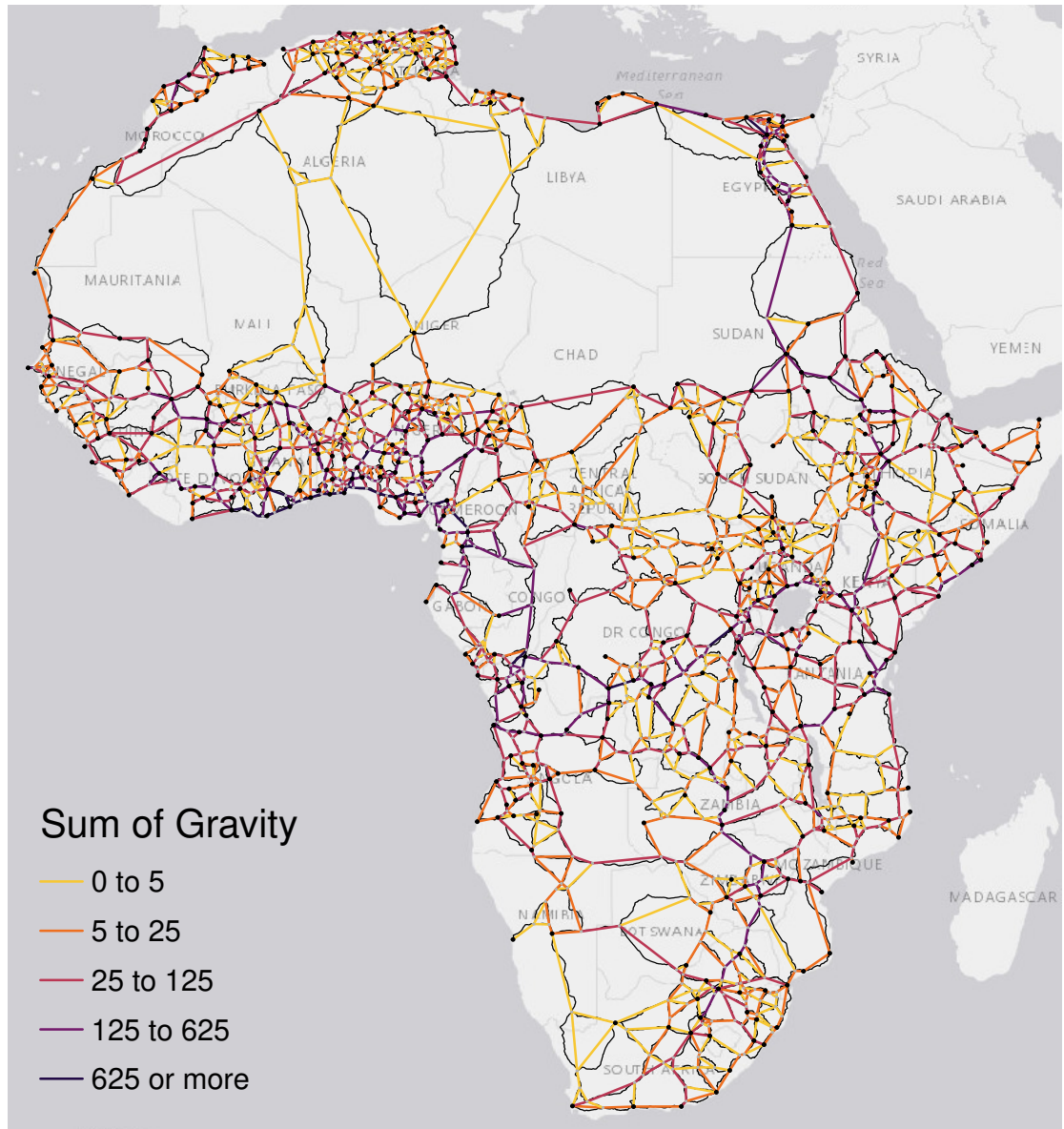


Figure A10: Discretized Trans-African Network and New Links for US Route Efficiency

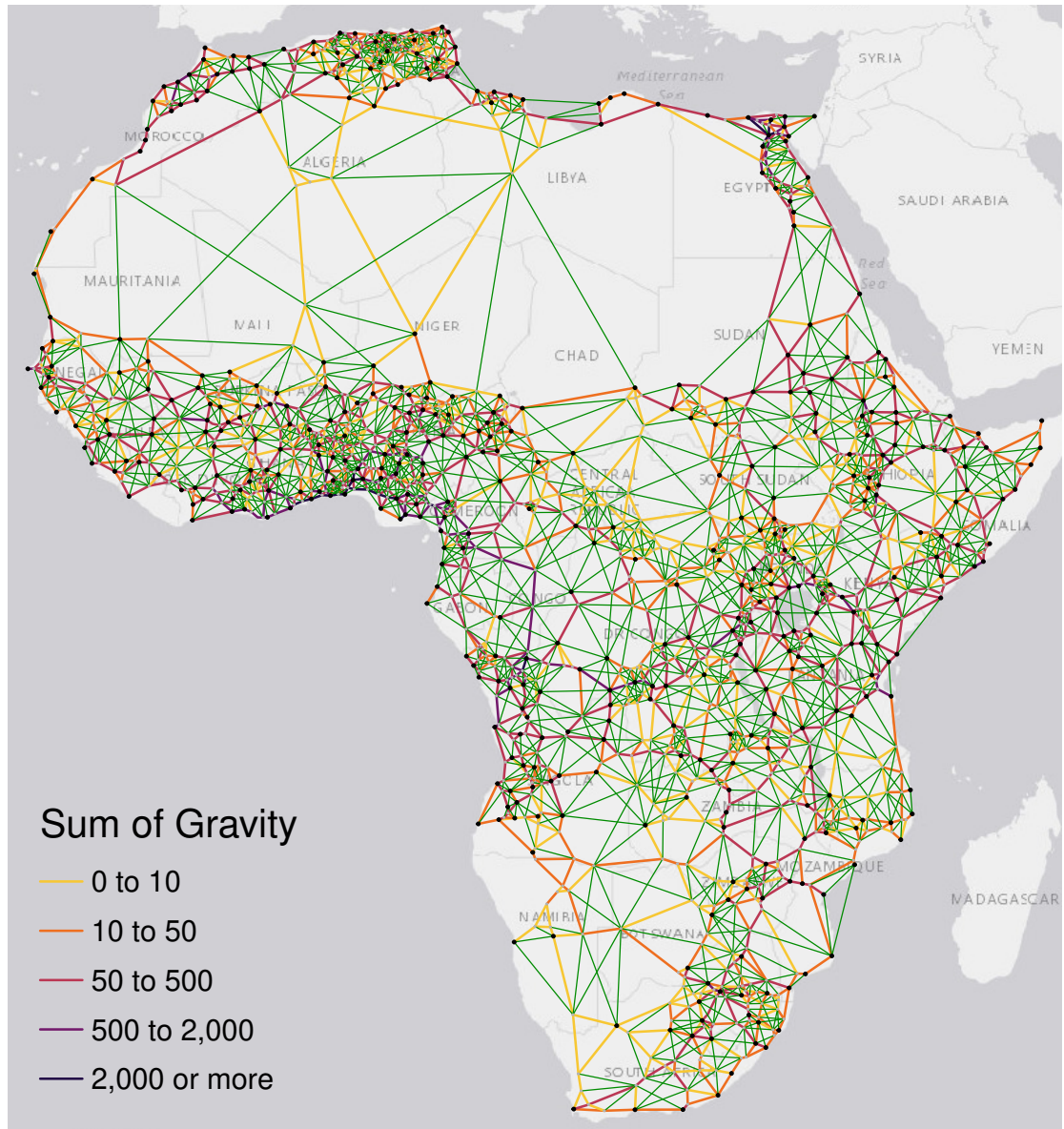


Figure A11: Local Road Distance Reduction: $\min(\kappa_{ik}^r) = 0.85$

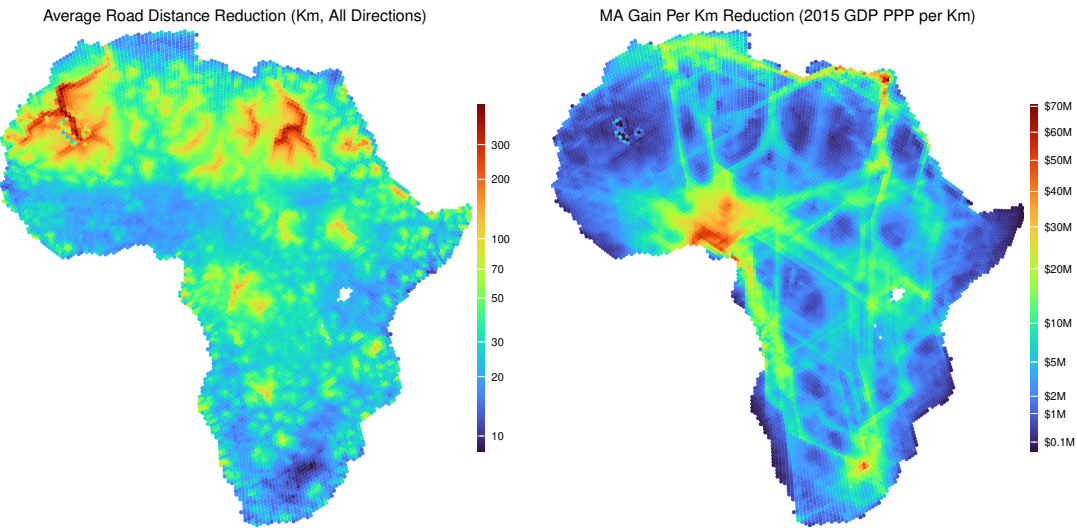


Figure A12: Estimated Network Building Cost per Kilometer

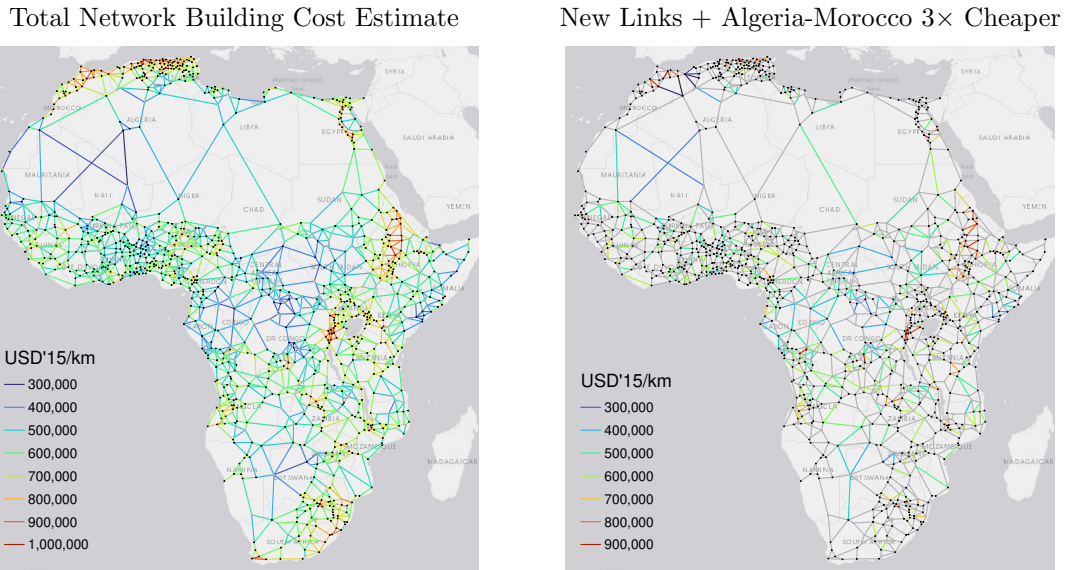


Figure A13: Nightlights vs. IWI to Measure City Productivity

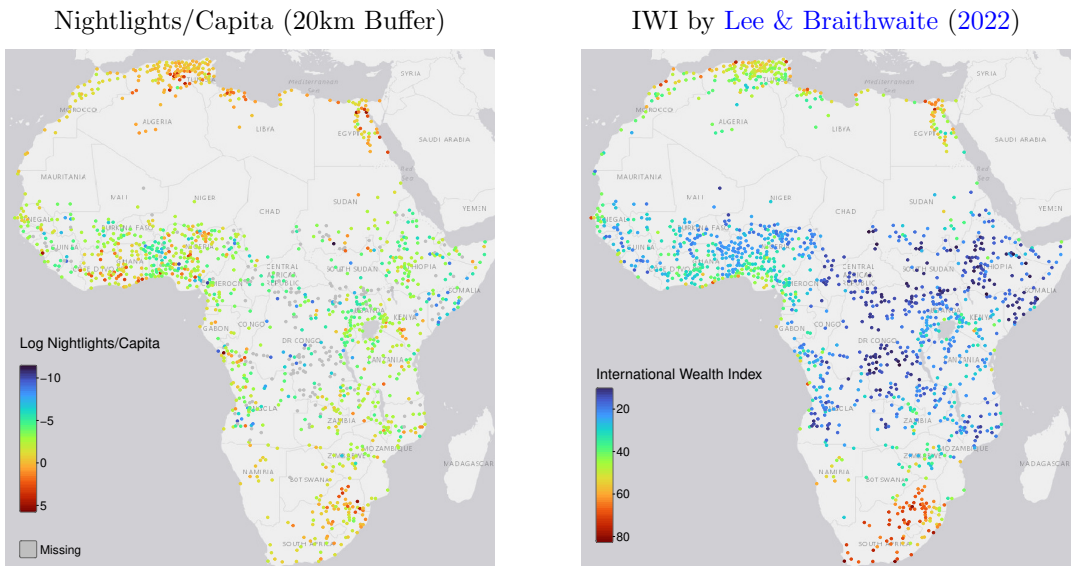


Figure A14: Optimal \$50B Investments, Trade, and Welfare by σ

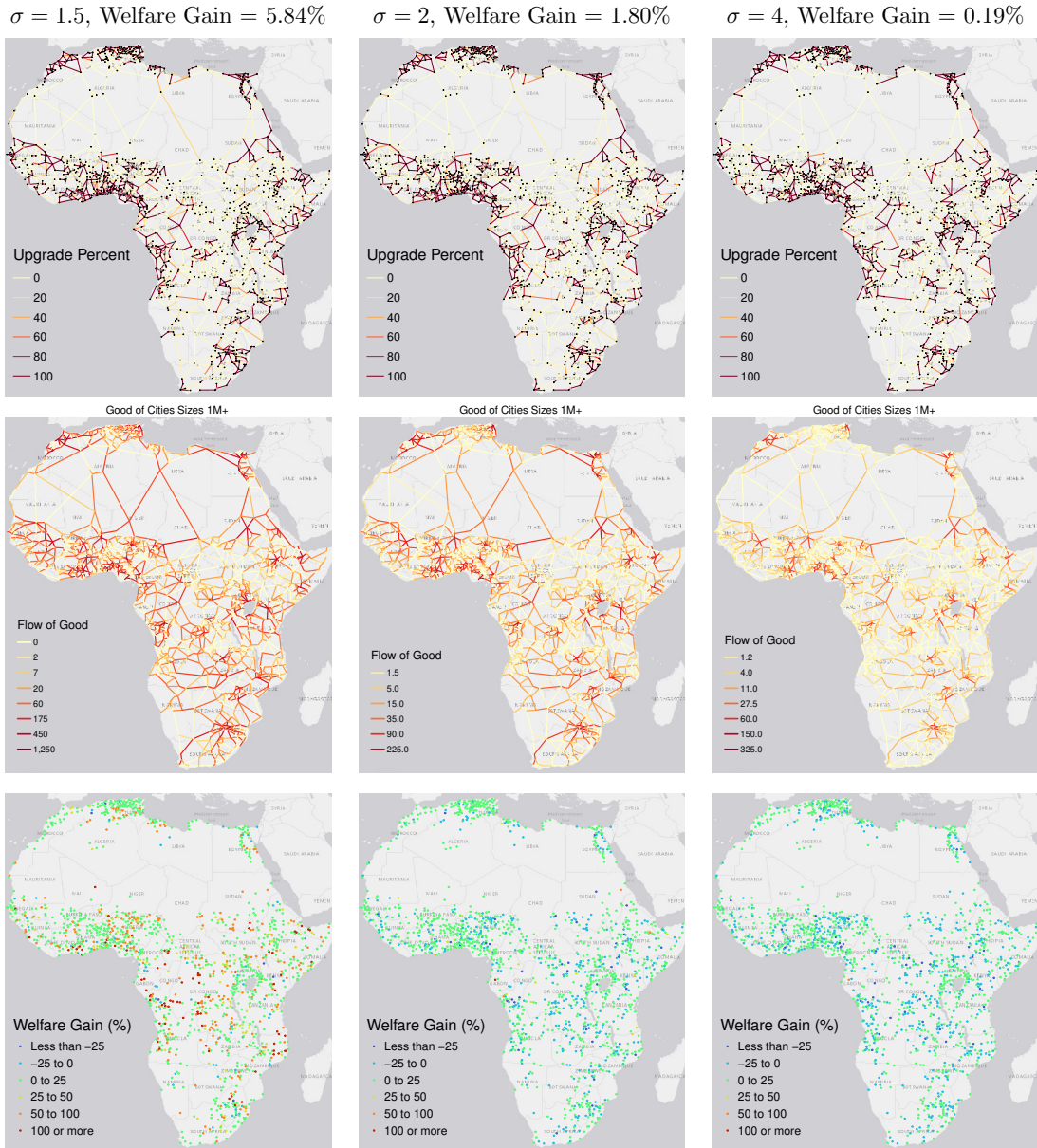


Figure A15: Optimal Infrastructure Allocation Without Imported Goods

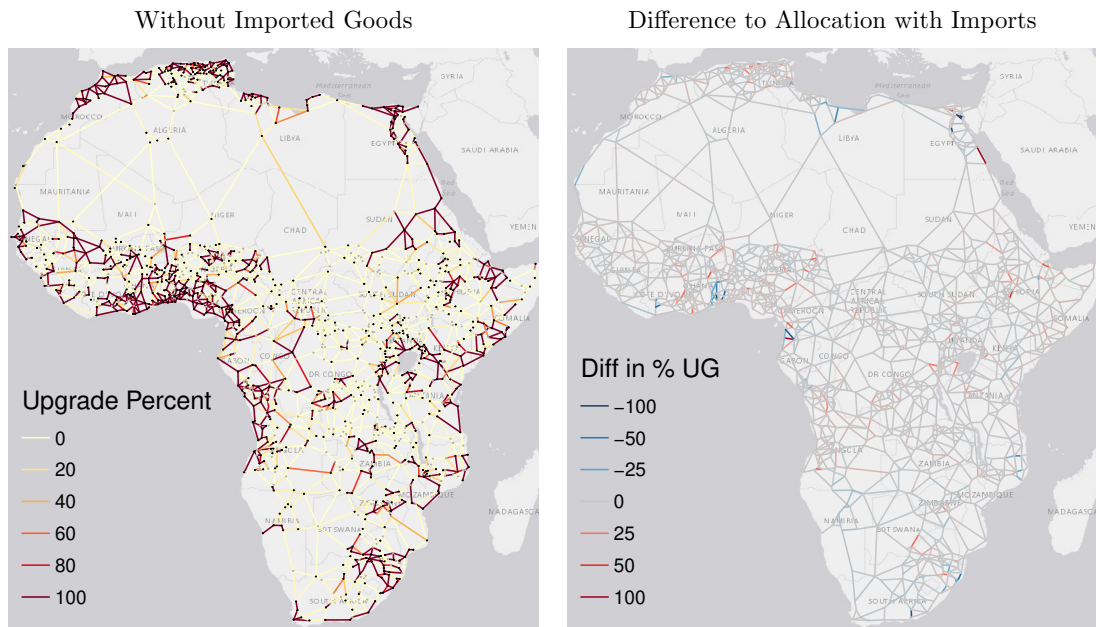


Figure A16: Ratio of Goods Flows under Border Frictions to Frictionless Flows

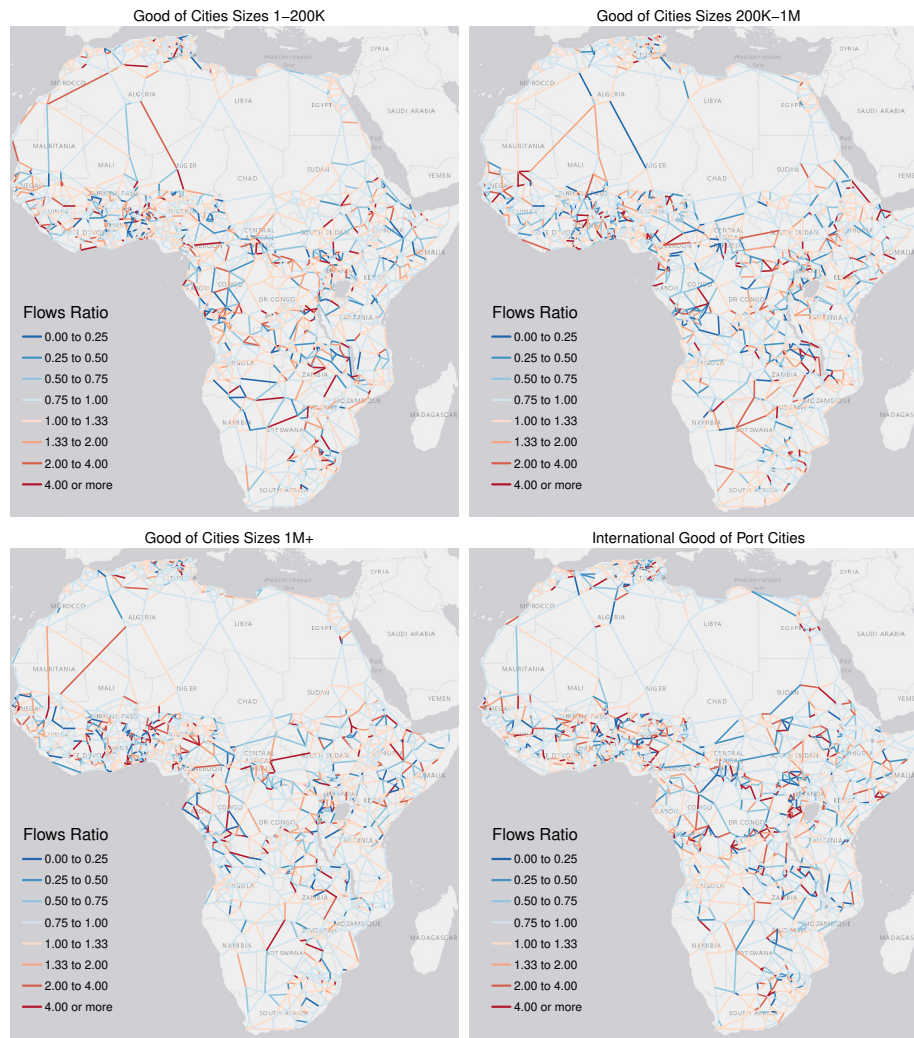


Figure A17: Flow of Goods and Local Consumption under IRS

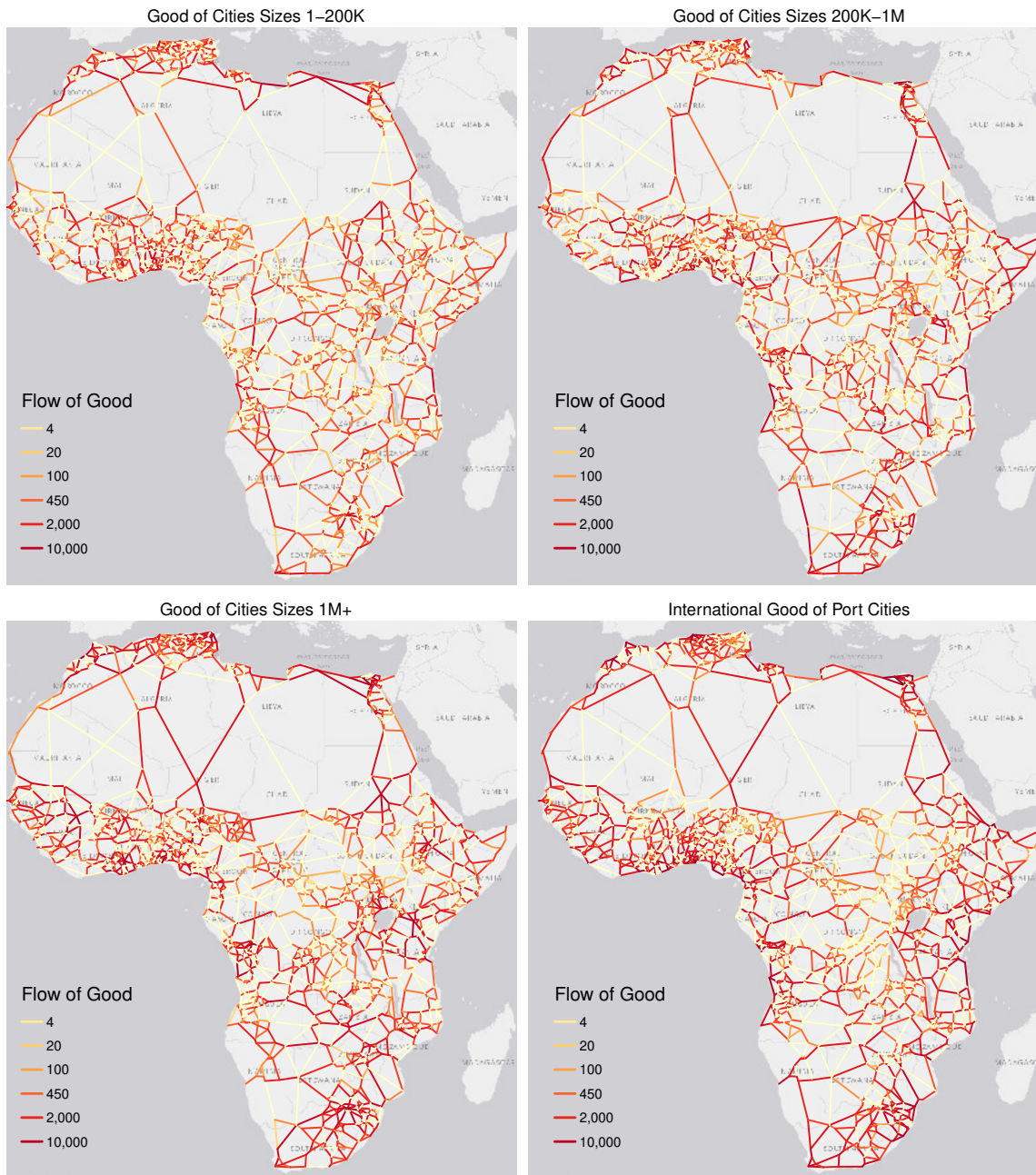


Figure A18: Optimal \$50B Investments, Trade, and Welfare under IRS by σ

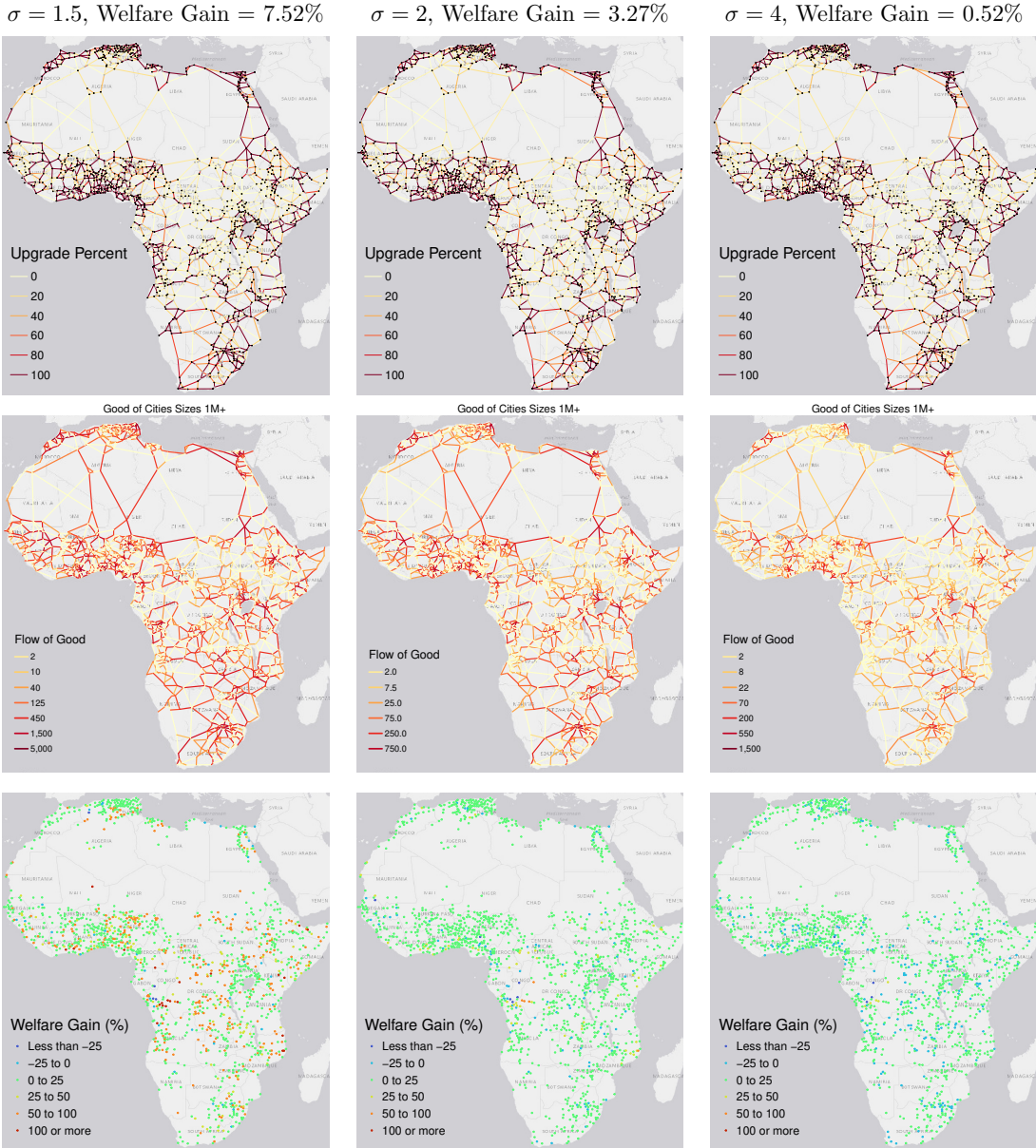


Figure A19: Optimal Infrastructure Allocation Without Imported Goods: IRS Case

Without Imported Goods

Difference to Allocation with Imports

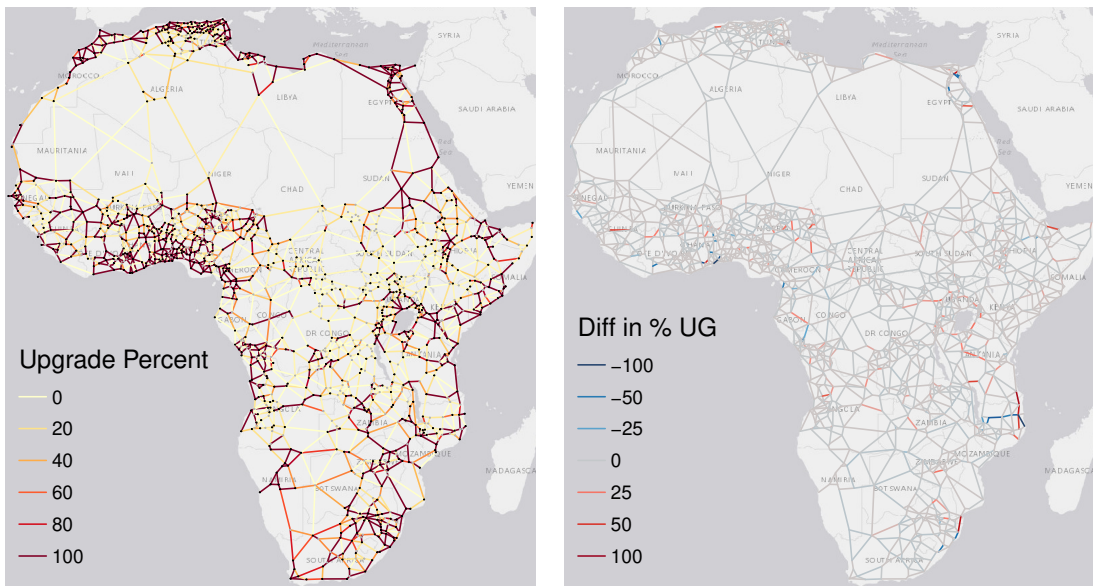


Figure A20: Ratio of Goods Flows under Border Frictions to Frictionless Flows: IRS Case

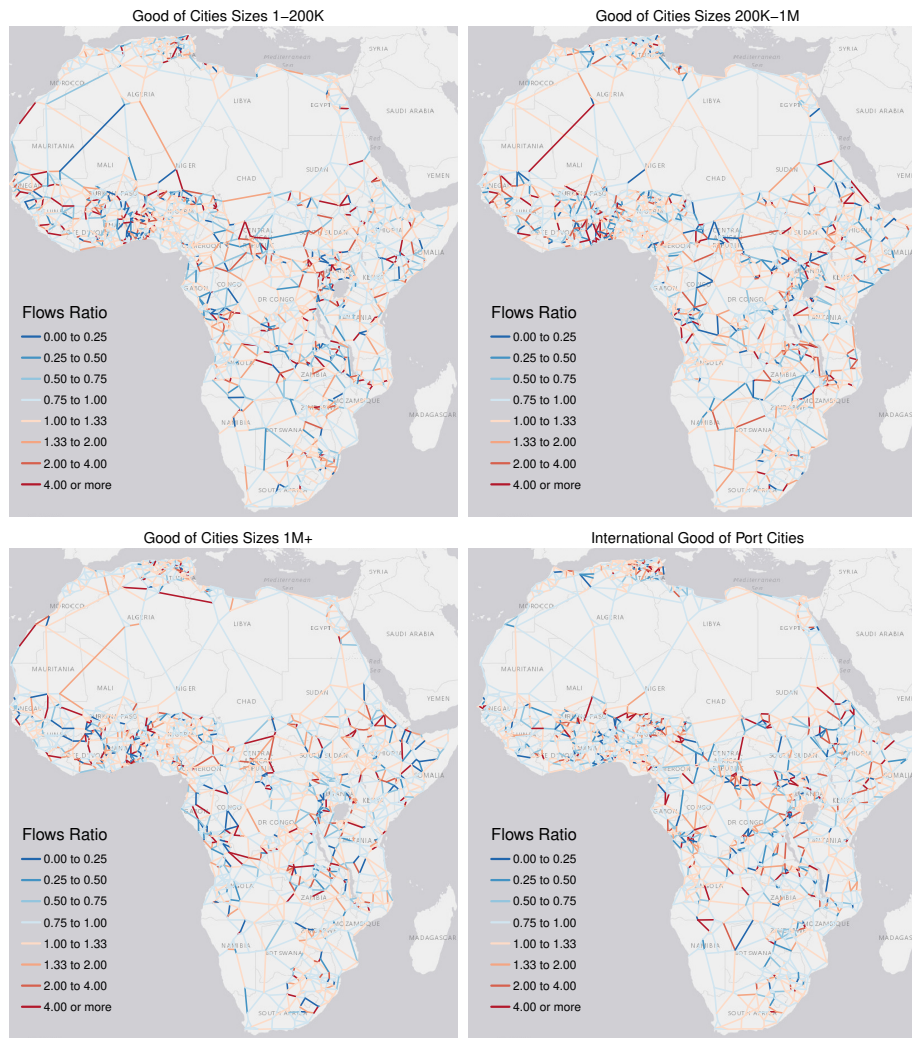


Figure A21: Trans-African Network Connecting Large Cities: Parameterization with Real Roads

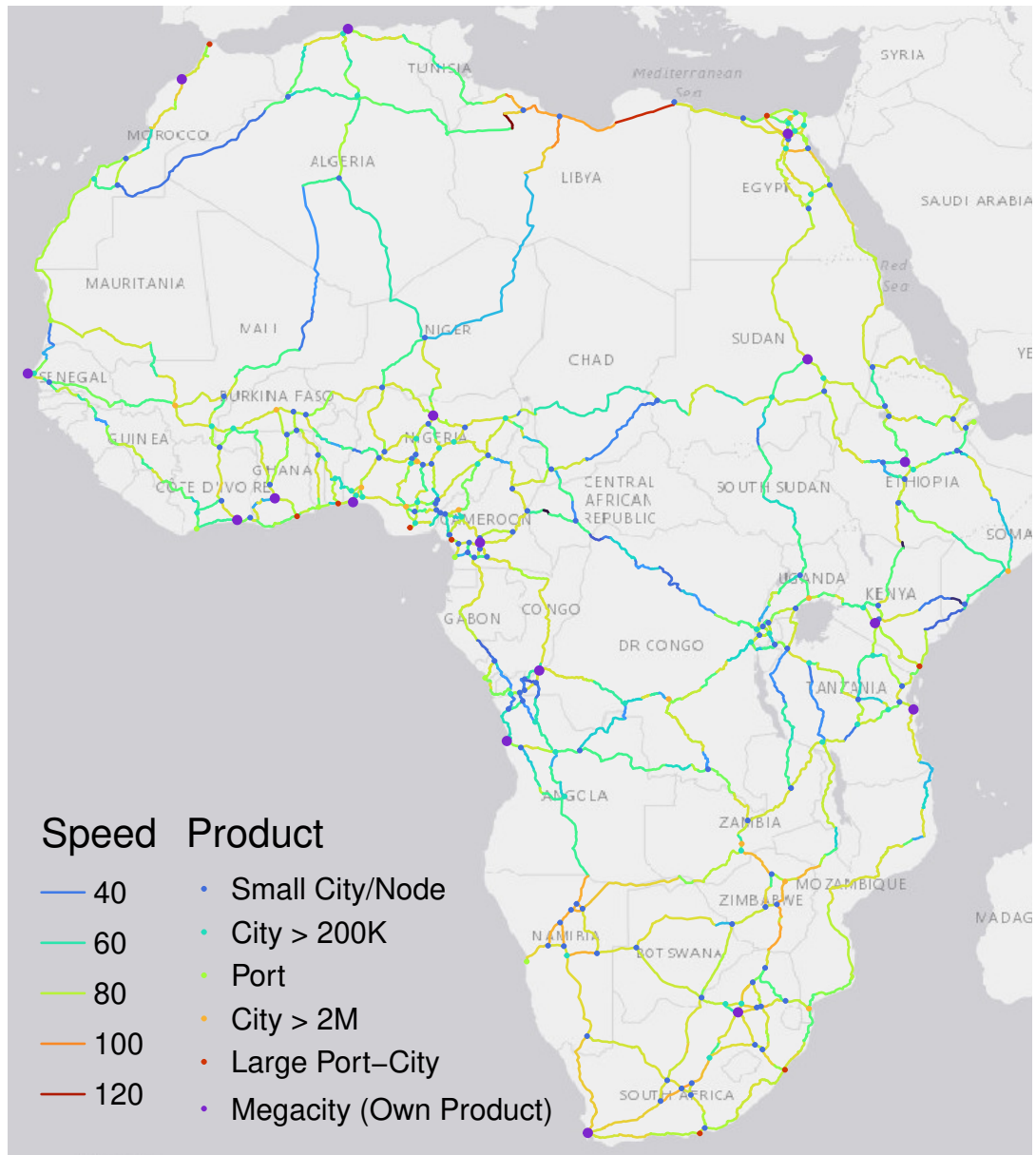


Figure A22: Flow of Goods Through Trans-African Network Connecting Large Cities

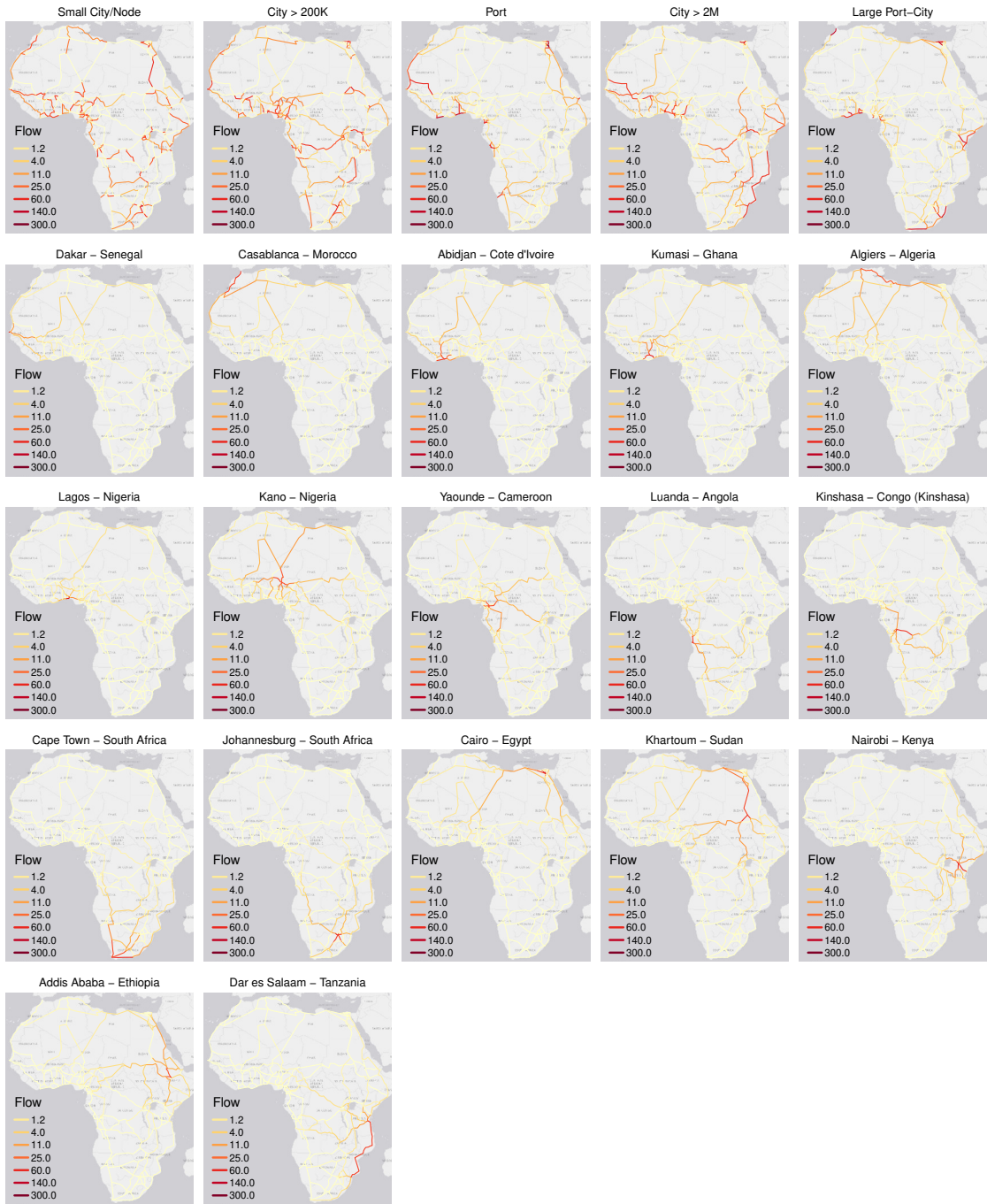
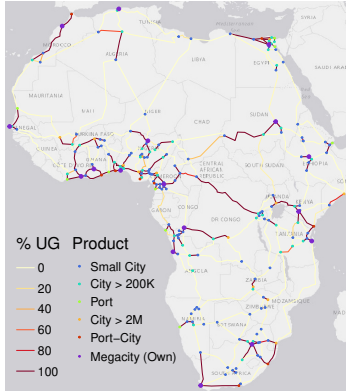
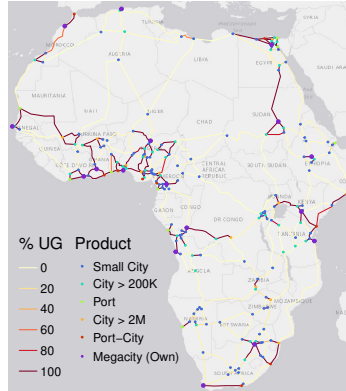


Figure A23: Optimal \$10B Trans-African Investments and Trade by σ

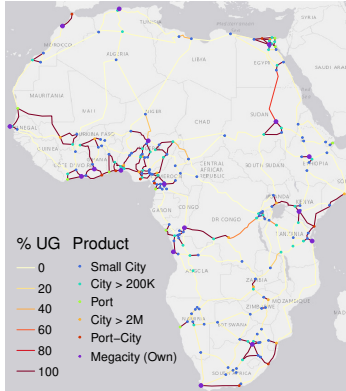
$\sigma = 2$, Welfare Gain = 0.5%



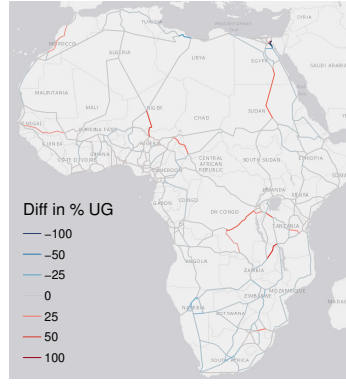
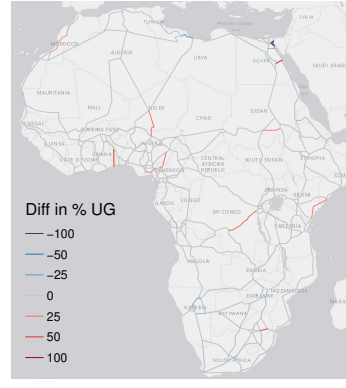
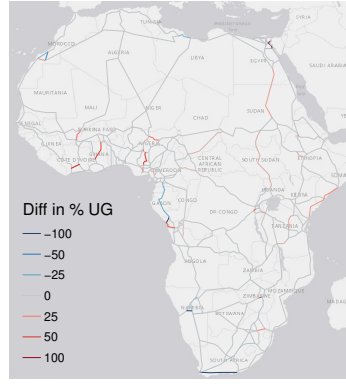
$\sigma = 3.8$, Welfare Gain = 0.04%



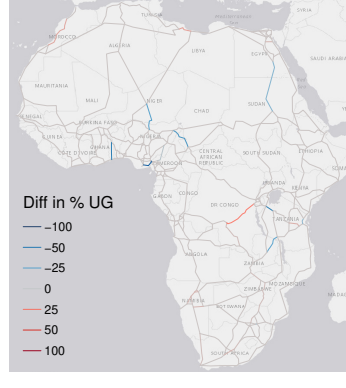
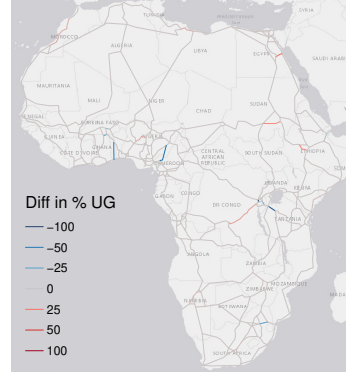
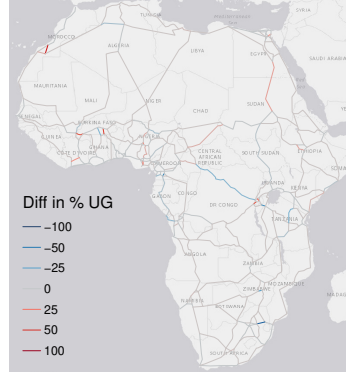
$\sigma = 5$, Welfare Gain = 0.02%



No Imported Goods (Difference)



With Border Frictions (Difference)



Flow of Goods (With Imported Goods, No Frictions) - Selected Megacities

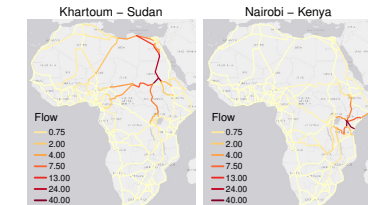
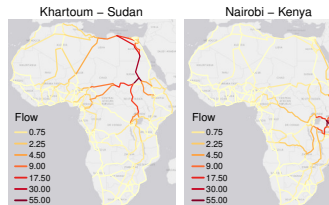
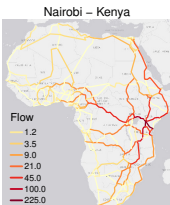
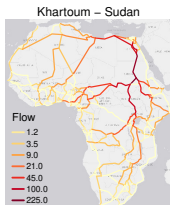
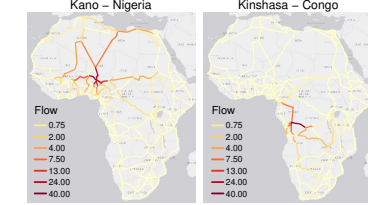
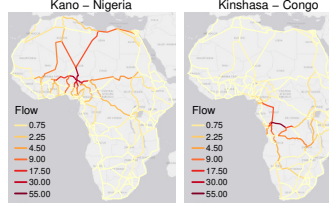
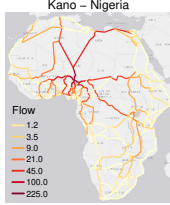
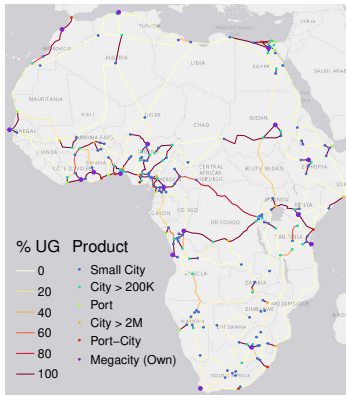
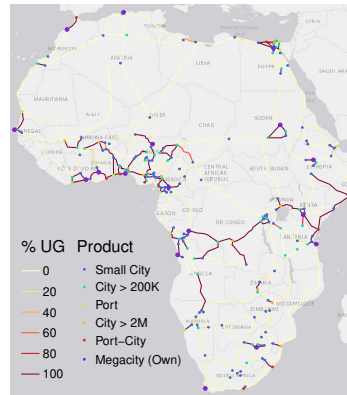


Figure A24: Optimal \$10B Trans-African Investments by σ with Inequality Aversion ($\rho = 2$)

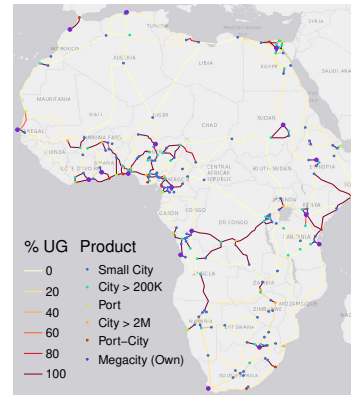
$\sigma = 2$, Welfare Gain = 0.48%



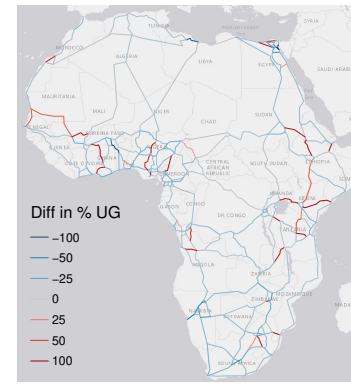
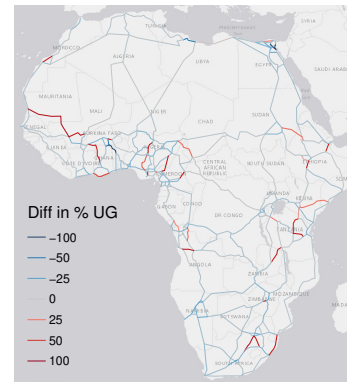
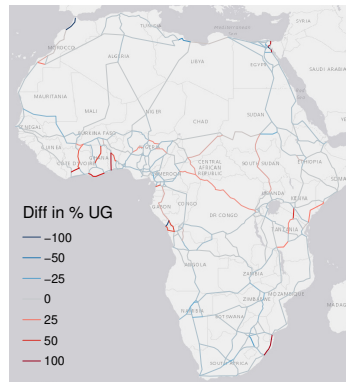
$\sigma = 3.8$, Welfare Gain = 0.038%



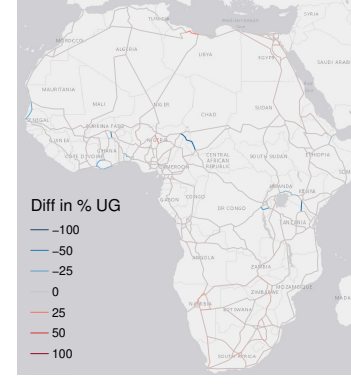
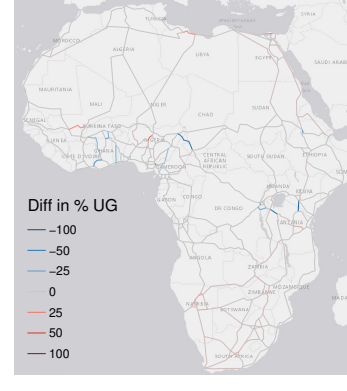
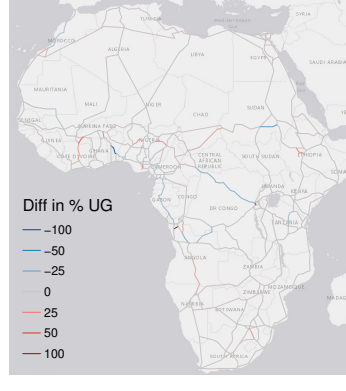
$\sigma = 5$, Welfare Gain = 0.019%



No Imported Goods (Difference)



With Border Frictions (Difference)



Flow of Goods (With Imported Goods, No Frictions) - Selected Megacities

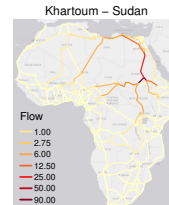
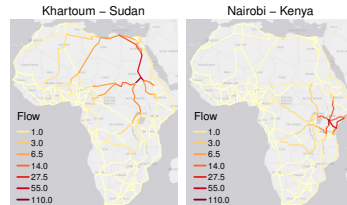
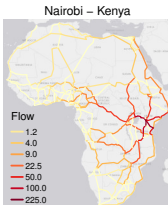
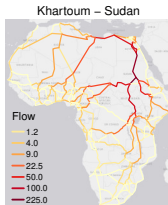
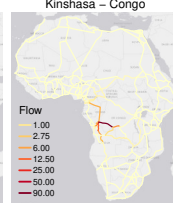
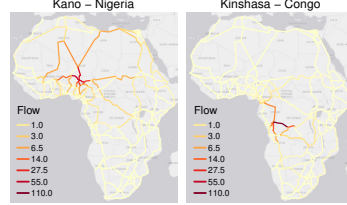
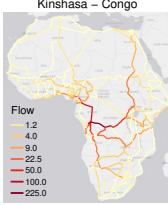
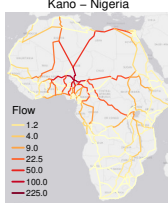


Figure A25: Flow of Goods Through Trans-African Network Connecting Large Cities: IRS Case

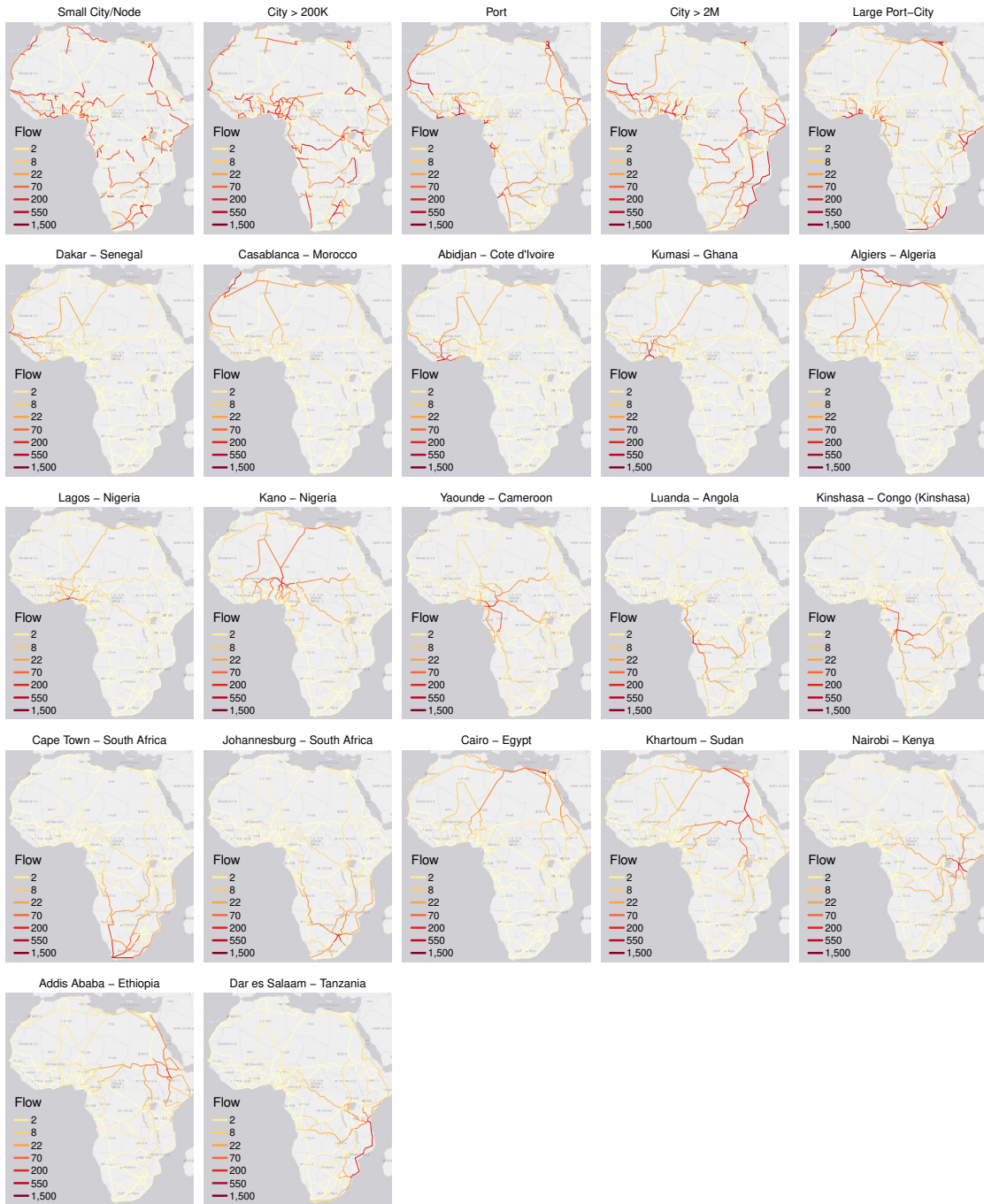


Figure A26: Optimal Trans-African Network Investments under Increasing Returns

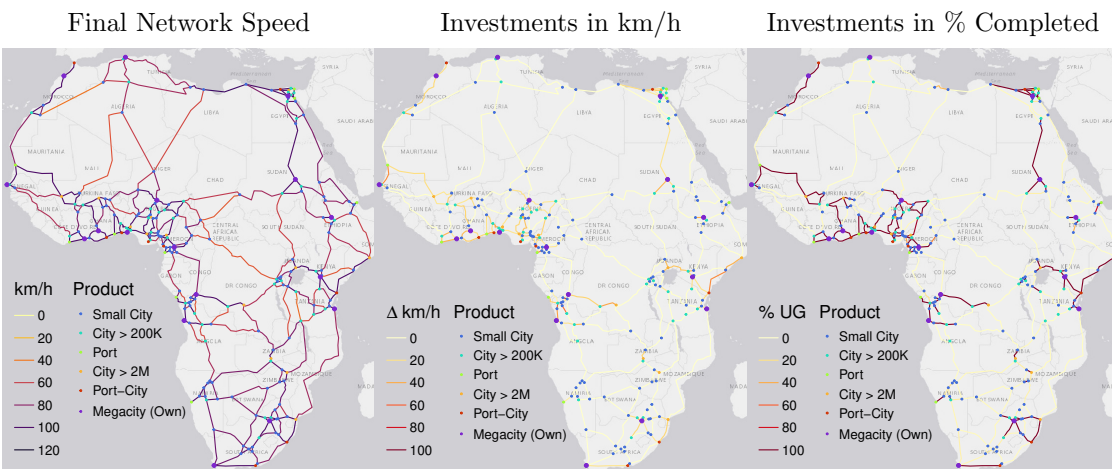
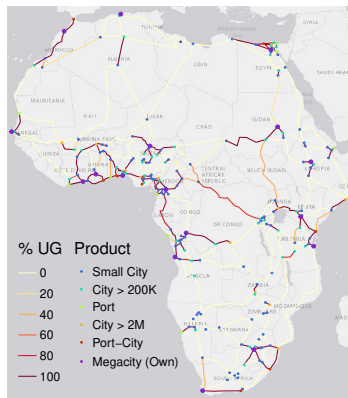
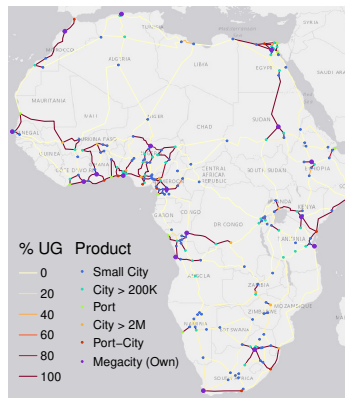


Figure A27: Optimal \$10B Trans-African Investments and Trade by σ : IRS Case

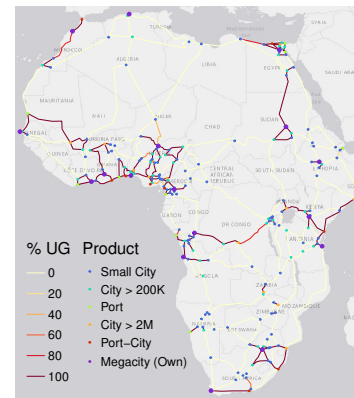
$\sigma = 2$, Welfare Gain = 1.42%



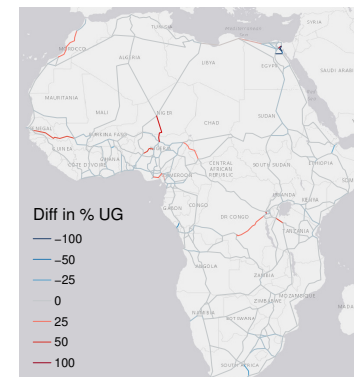
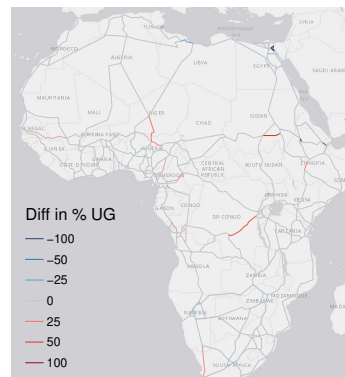
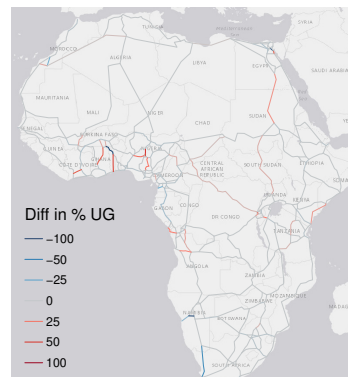
$\sigma = 3.8$, Welfare Gain = 0.16%



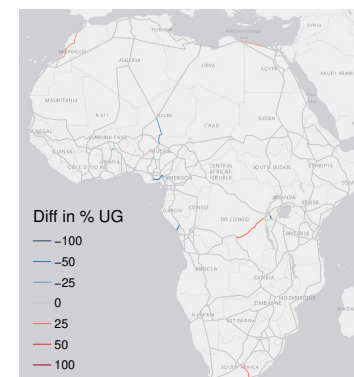
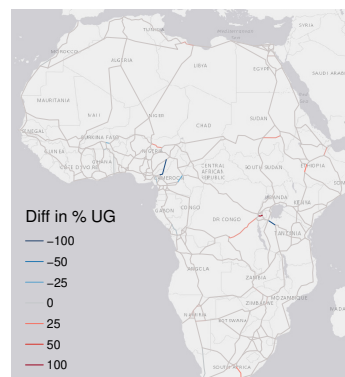
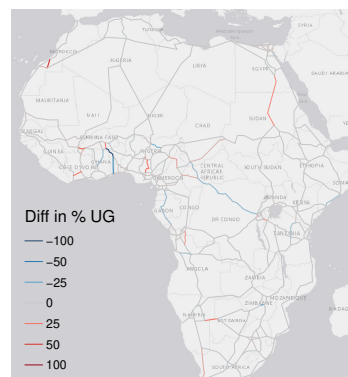
$\sigma = 5$, Welfare Gain = 0.08%



No Imported Goods (Difference)



With Border Frictions (Difference)



Flow of Goods (With Imported Goods, No Frictions) - Selected Megacities

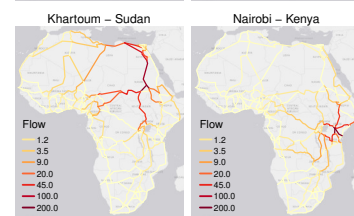
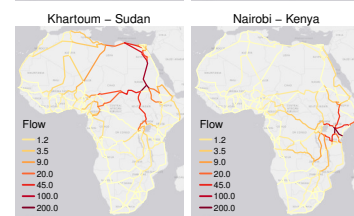
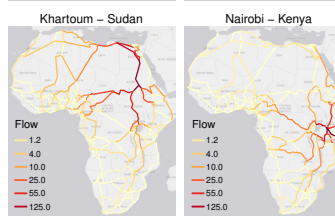
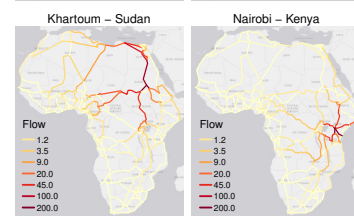
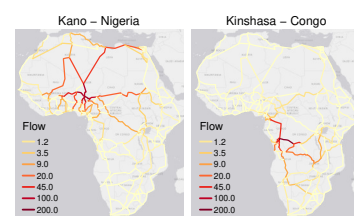
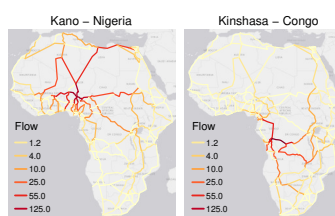
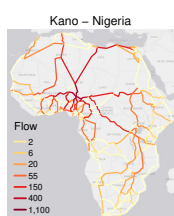
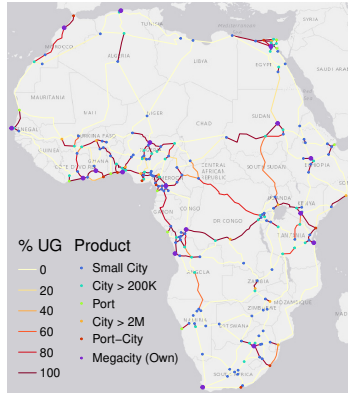
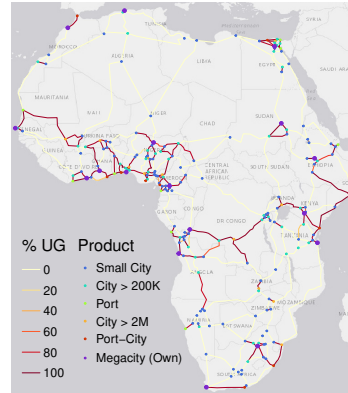


Figure A28: Optimal \$10B Trans-African Investments by σ with Inequality Aversion ($\rho = 2$): IRS Case

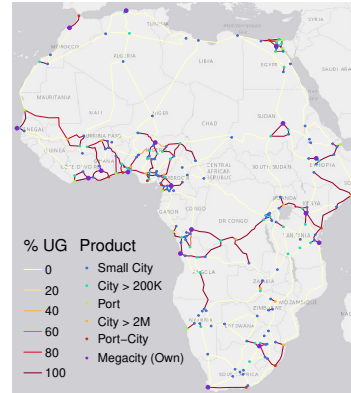
$\sigma = 2$, Welfare Gain = 1.38%



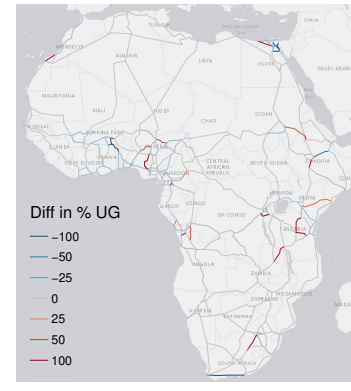
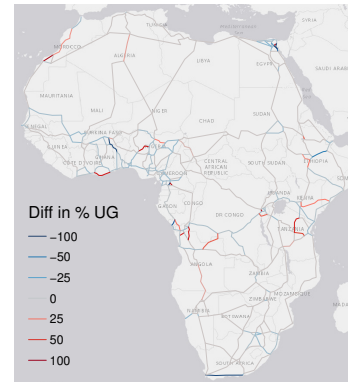
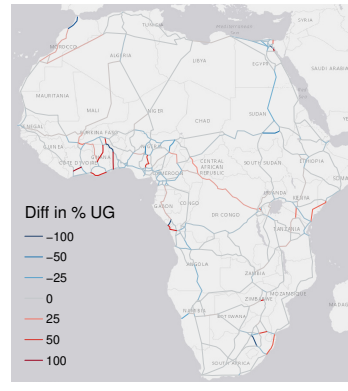
$\sigma = 3.8$, Welfare Gain = 0.1%



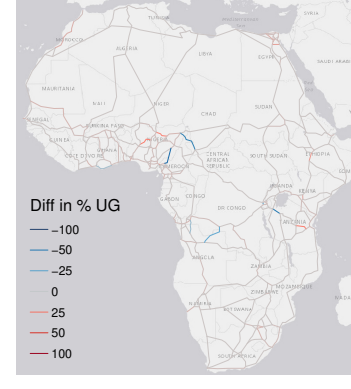
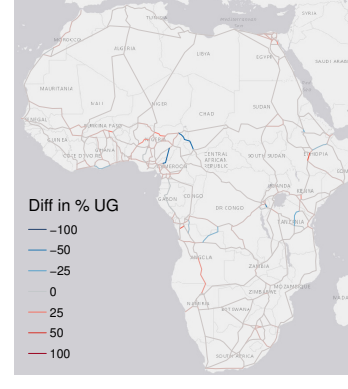
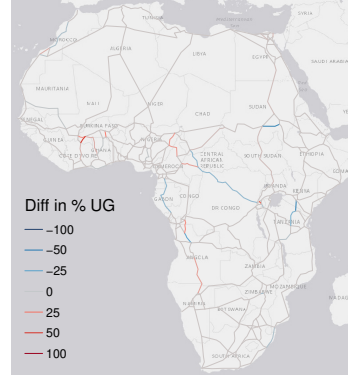
$\sigma = 5$, Welfare Gain = 0.01%



No Imported Goods (Difference)



With Border Frictions (Difference)



Flow of Goods (With Imported Goods, No Frictions) - Selected Megacities

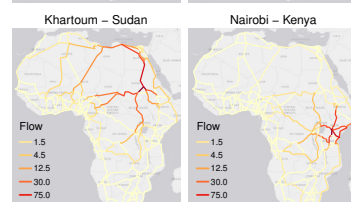
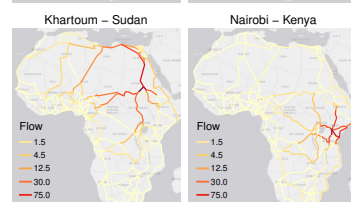
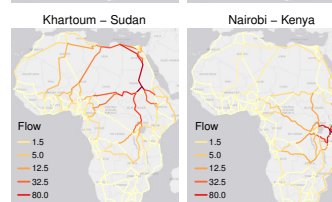
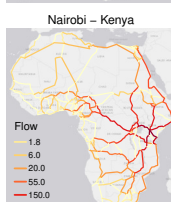
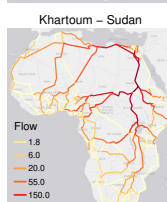
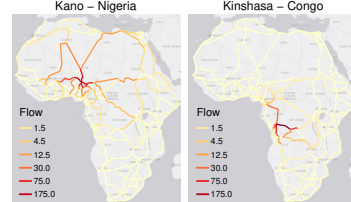
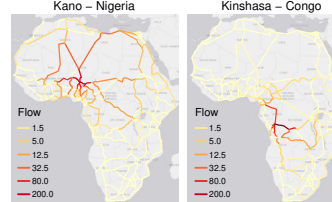
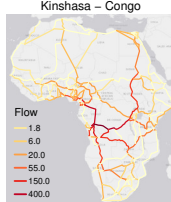
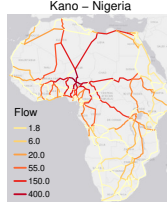


Figure A29: Flow of Goods Through Trans-African Network: Fastest and Shortest Routes

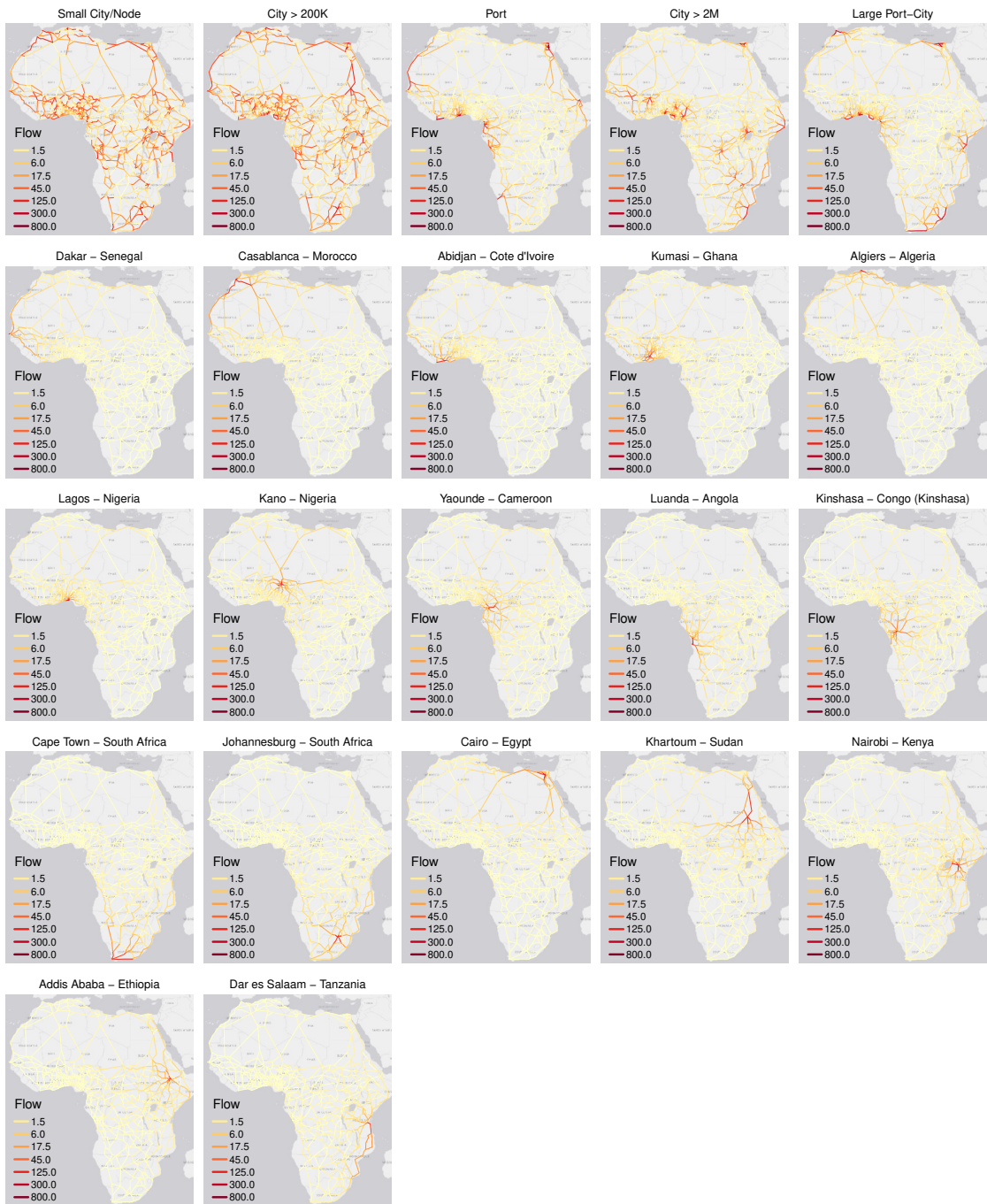


Figure A30: Optimal \$10B and \$20B Trans-African Investments by σ - Infrastructure

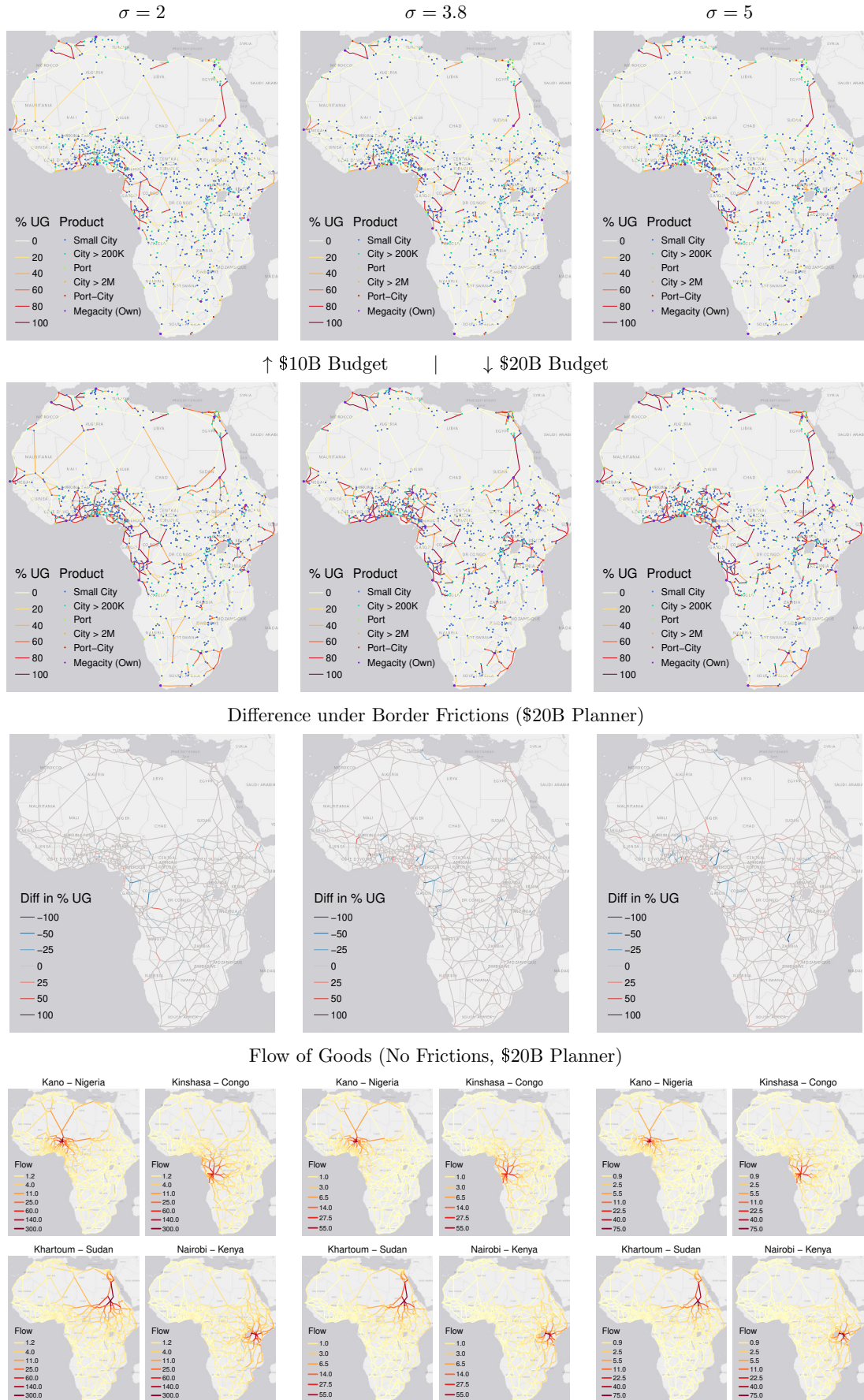


Figure A31: Welfare gains by σ : Standard and Frictions Scenarios

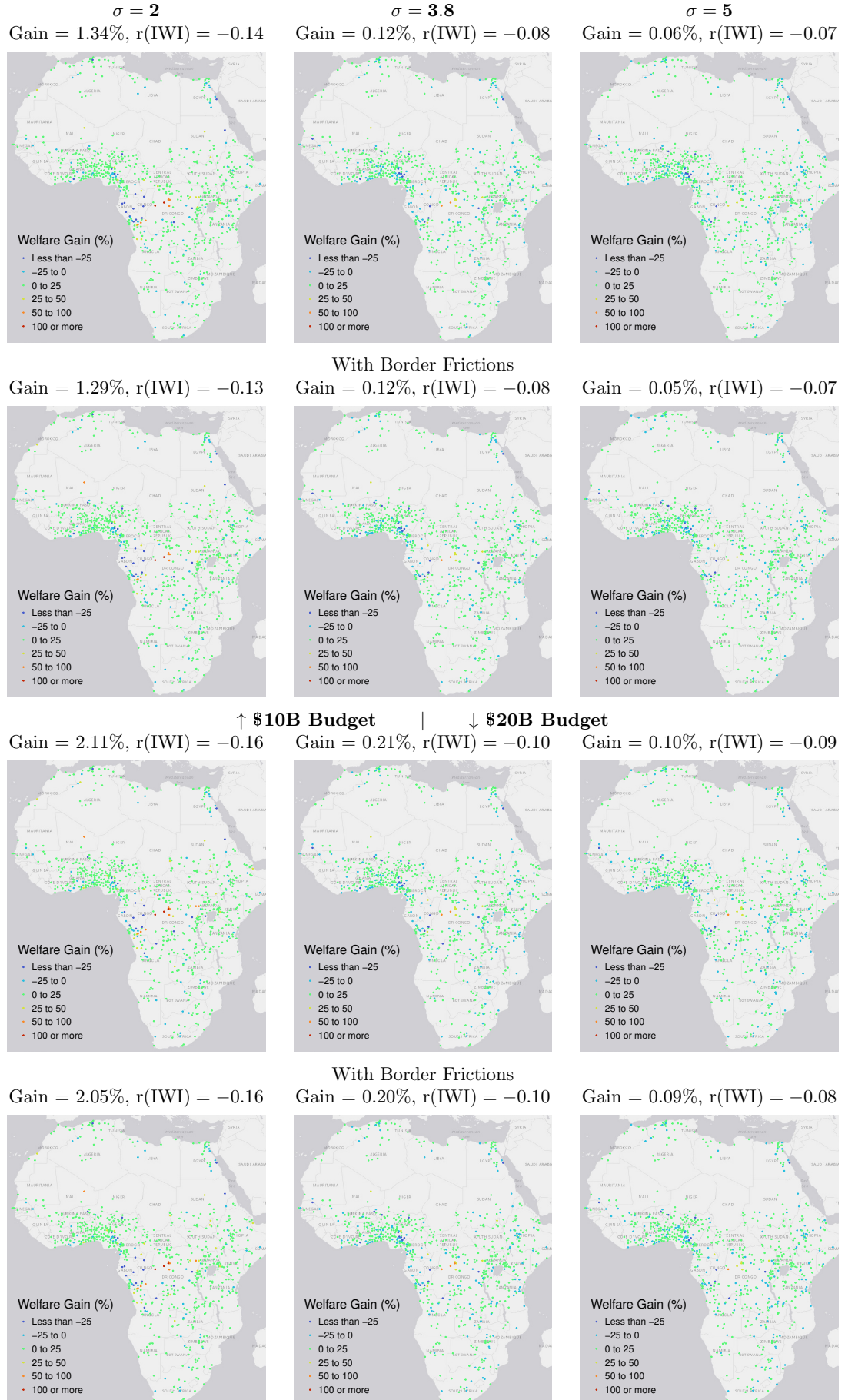


Figure A32: Optimal \$10B Trans-African Investments & Welfare with Inequality Aversion by σ

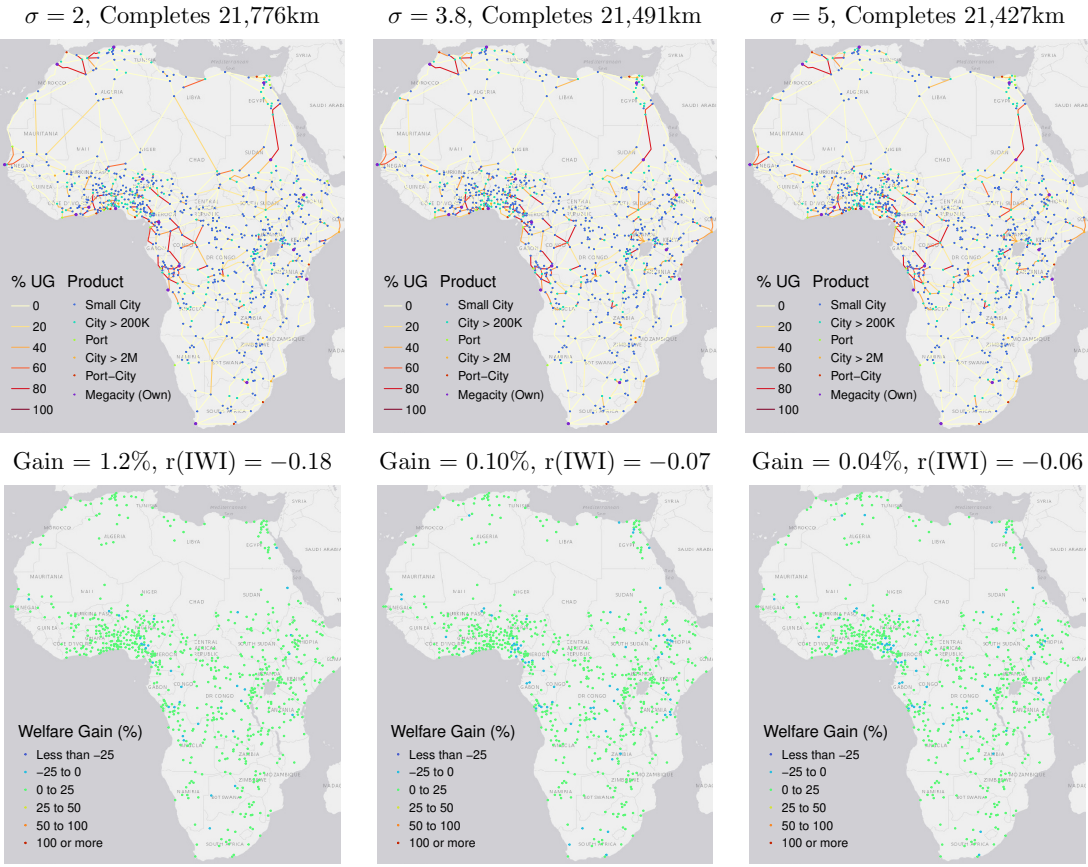


Figure A33: Optimal \$10B Trans-African Investments & Welfare with Increasing Returns by σ

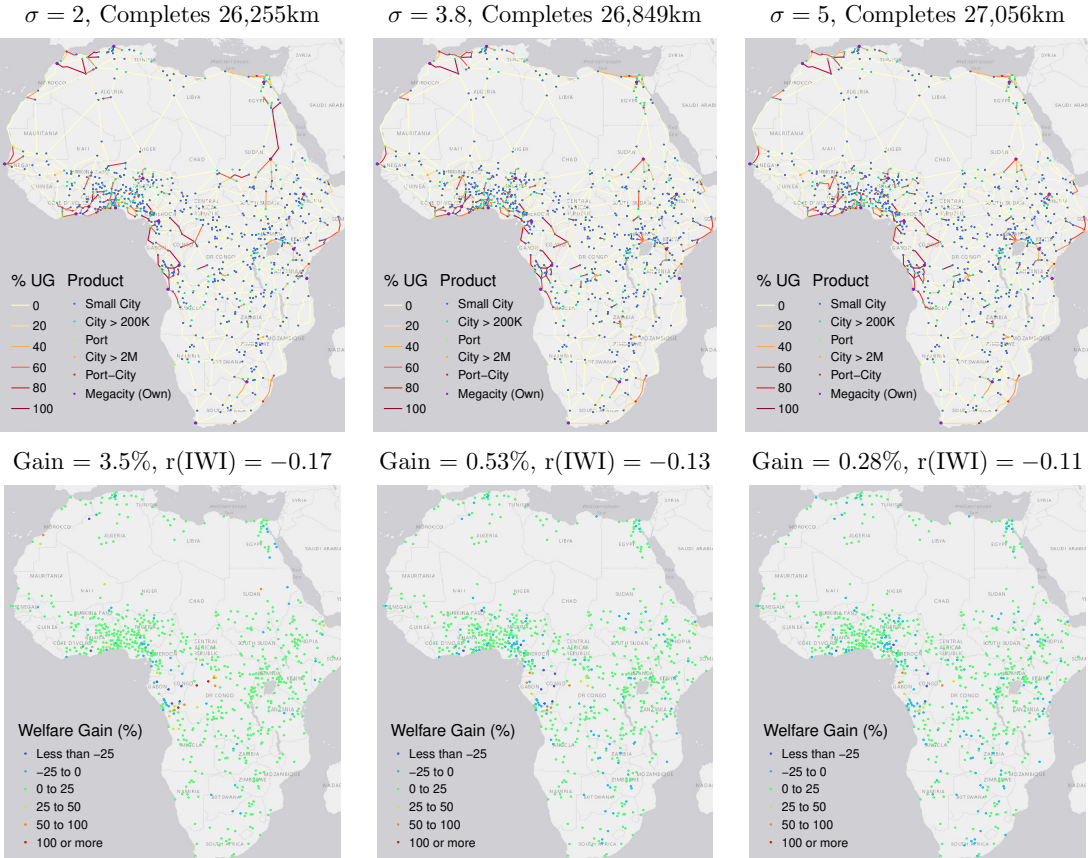


Figure A34: Optimal \$20B Trans-African Network Investments on Large Network with $\sigma = 1.5$

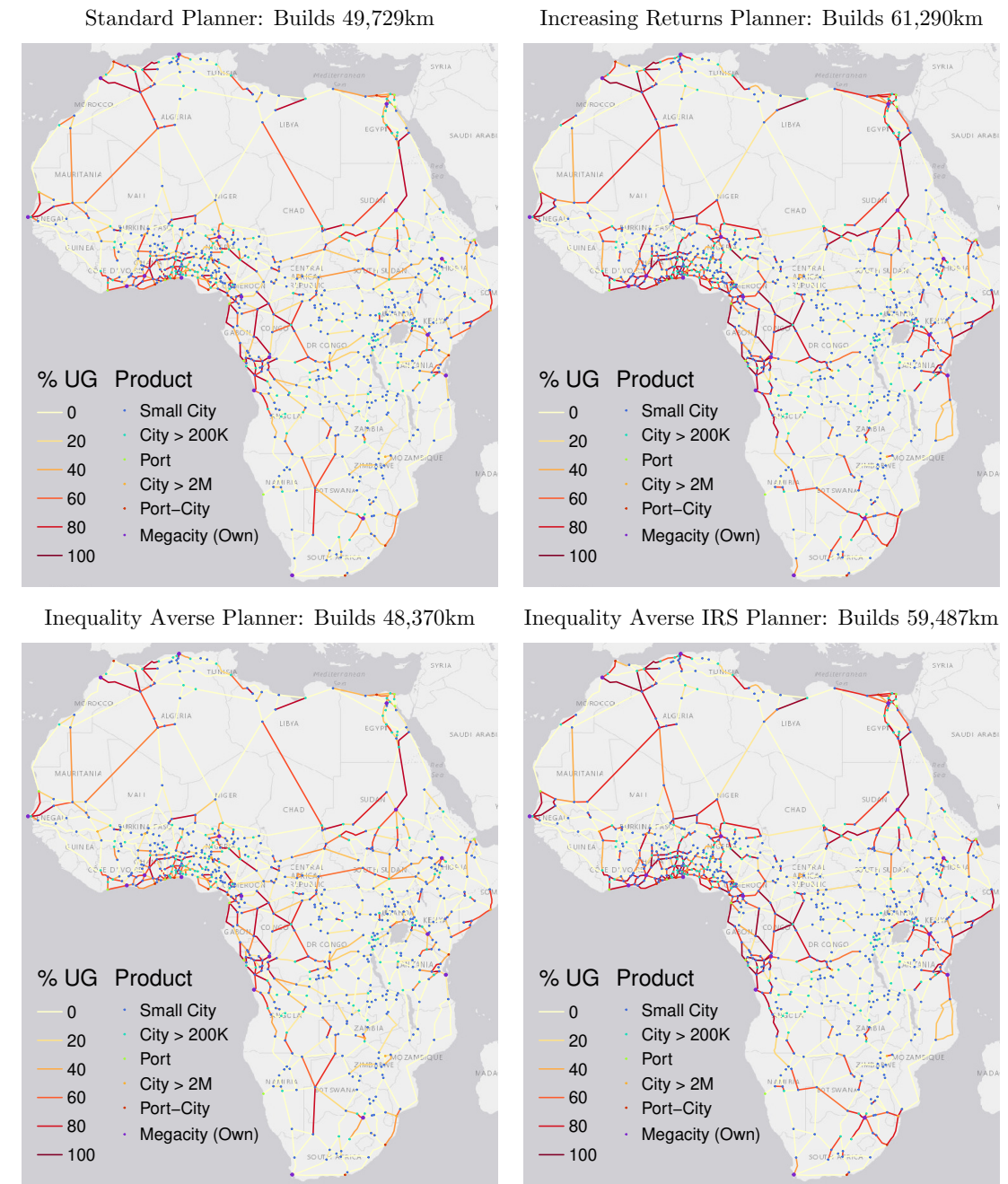


Figure A35: Optimal \$20B Trans-African Flows & Welfare on Large Network with $\sigma = 1.5$

